University of Southampton

Faculty of Engineering & Physical Sciences

Fluid Structure Interactions Group

Suitability of a linseed oil epoxy resin for composite applications.

by

Marcos Antonio Gimenes Benega

ORCID ID orcid.org/0000-0003-4954-7384

Thesis for the degree Doctor of Philosophy

April 2019

University of Southampton

Abstract

Faculty of Engineering & Physical Sciences

Fluid Structure Interactions Group

Thesis for the degree of Doctor of Philosophy

Suitability of a linseed oil epoxy resin for composite applications.

by

Marcos Antonio Gimenes Benega

Vegetable oils are a great sustainable source for the production of resins. When these oils are epoxidized, their viscosities are greatly increased which prevents their use in the production of composites, especially via resin transfer moulding and infusion. This work studies aspects of the synthesis, curing and properties of cured epoxy resins derived from linseed oil. Two versions of the resin are used; the first comprising the epoxidized triglycerides of linseed oil (ELO), the second a low-viscosity version (TELO) obtained from the transesterification of ELO in methanol. The synthesis is initially carried out with heterogeneous catalysts such as TS-1 and Ti-SiO_2. These catalysts show great activity towards epoxidation of fatty acid methyl esters (FAMEs), yet the epoxidation and transesterification of triglycerides was limited; a homogeneous synthesis is then used in larger batches.

Two curing approaches are used for ELO and TELO. The first consisted of blending them with conventional epoxy resin (DGEBA) cured by conventional and phenalkamide hardeners. The phenalkamide was chosen after a comparison of five different commercial phenalkamide and phenalkamine hardeners. The second curing procedure was done using a blend of ELO and TELO with a commercial UV-curable resin derived from linseed oil.

FT-IR and gel fraction tests show that all samples reached a high degree of curing. The use of TELO greatly reduces the viscosity of the blends but there are also reductions in elastic modulus, tensile strength and glass transition temperature. The long fatty acid chains in ELO and TELO have a plasticizing effect. The glycerol fragment connecting the fatty acid in ELO is essential for a high crosslinking density. The use of linseed oil derived epoxy resins in composite structures is limited. The conventional epoxy systems still have better properties yet to be achieved by bio-based ones.

Table of Contents

List of Tables

List of Figures

List of Figures

List of Figures

Research Thesis: Declaration of Authorship

Print name:	Marcos Antonio Gimenes Benega

Title of thesis:	Suitability of a linseed oil epoxy resin for composite applications.

I declare that this thesis and the work presented in it are my own and has been generated by me as the result of my own original research.

I confirm that:

1. This work was done wholly or mainly while in candidature for a research degree at this University;
2. Where any part of this thesis has previously been submitted for a degree or any other qualification at this University or any other institution, this has been clearly stated;
3. Where I have consulted the published work of others, this is always clearly attributed;
4. Where I have quoted from the work of others, the source is always given. With the exception of such quotations, this thesis is entirely my own work;
5. I have acknowledged all main sources of help;
6. Where the thesis is based on work done by myself jointly with others, I have made clear exactly what was done by others and what I have contributed myself;
7. Parts of this work have been published as:

Benega, M.A.G., Raja, R., Blake, J.I.R., 2017. A preliminary evaluation of bio-based epoxy resin hardeners for maritime application. Procedia Eng. 200, 186–192. https://doi.org/10.1016/j.proeng.2017.07.027

Signature:		Date:	

Acknowledgements

I would initially like to thank the Brazilian National Council for Scientific and Technological Development (CNPq) for funding the project. I would further like to thank my supervisors Professor James I. R. Blake and Professor Robert Raja to show my appreciation for their trust in my work, guidance, feedback and advice.

I could not be more grateful to my parents, Solange Hugenschimidt Gimenes Benega and Antonio Benega. Their unconditional love and support are the basis of everything I am and will be. I wish to thank my fiancé Isaac Miles Gustafsson-Wood for helping me stand my ground. I could not do it without him.

I would like to thank the University of Southampton, the Faculty of Engineering and Physical Sciences and the Graduate Office, especially Jennifer Knight who was my first contact with the university from overseas.

I would like to thank Dr Luci Diva Brocardo Machado from the Nuclear and Energy Institute for access, assistance and the experienced shared in thermal analysis.

I am grateful for the many people I was able to meet, their influence throughout this process helped carry on. Especially Fernando Peleias for suggesting me do the PhD abroad, Nu Rhahida Arini, my first good friend in the office, and my colleagues from the engineering and the chemistry groups. I would also like to extend thanks to Polliana Brant, my first Brasilian friend in Southampton, the whole Brazilian student community in the university, and my high school friends from Brazil, Fabricio Brasioli and Welton Vinicius Rufino.

I would like to dedicate this work to my grandfather José Gimenes-Arana *in memoriam*.

Definitions and Abbreviations

ELO	Epoxidized linseed oil.
EVO	Epoxidized vegetable oil.
TELO	Transesterified epoxidized linseed oil.
FAMEs	Fatty acid methyl esters.
EFAMEs	Epoxidized fatty acid methyl esters.
DGEBA	Bisphenol A diglycidyl ether
UV-L	Commercial UV-curable epoxidized linseed oil
FRP	Fibre reinforced polymer.
T_g	Glass transition temperature.
FT-IR	Fourier-transform infrared spectroscopy.
^{1}H-NMR	Proton nuclear magnetic resonance.
TGA	Thermogravimetric analysis.
DSC	Differential scanning calorimetry.
RTM	Resin transfer moulding.

Chapter 1 Introduction

Environmental and health concerns are motivating society to search for a sustainable lifestyle, reducing environmental impact and carbon footprint. According to the report entitled *Our Common Future*, published by the United Nations [1], sustainable development is achieved when the necessities of present human activities are cared for but allowing future generations to meet their own needs. The dependency on the petro-chemical industry is not sustainable; the crude oil reserves are being depleted. Synthetic materials do not go back to being crude oil and very little is recycled. A study from Geyer *et al* [2] has shown that 6300 Mt of plastic waste was generated by 2015, from that only 9 % was recycled, 12 % incinerated and the rest was disposed of in landfills or accumulated in nature. Although incineration is sometimes treated as recycling because the heat can be used to produce energy, toxic and global warming gases are generated in the process [3]. Anastas and Warner [4] introduced in 1998 "The twelve principles of green chemistry". These are principles that guide the development of less hazardous chemicals and materials. In order to ensure that such materials meet the sustainability criteria, a life cycle assessment (LCA) must be carried out. LCA is a technique that studies the environmental behaviour of products, quantifying and assessing their impact. Unlike other also useful methodologies, that usually analyse emissions and waste generated in the production of the materials, a LCA evaluates the whole life cycle of the materials and all the harm it could cause to the environment [5].

Plastics can be produced from natural materials using a sustainable approach (see Figure 1). During the growt0 of vegetationh, carbon is captured from the atmosphere via photosynthesis, resulting in materials such as vegetable oils, starch and cellulose [6]. The plastics are synthesized from these sources and used in an array of different industries and applications. These materials do not necessarily need to be biodegradable to be sustainable. Instead of being disposed of in landfills, which would require a long time for decomposition, they can be incinerated as biomass. The carbon emitted in the process is derived from crops and will eventually be recaptured by vegetation. Hence, carbon that is underground in the form of crude oil and gas is not added to the atmosphere.

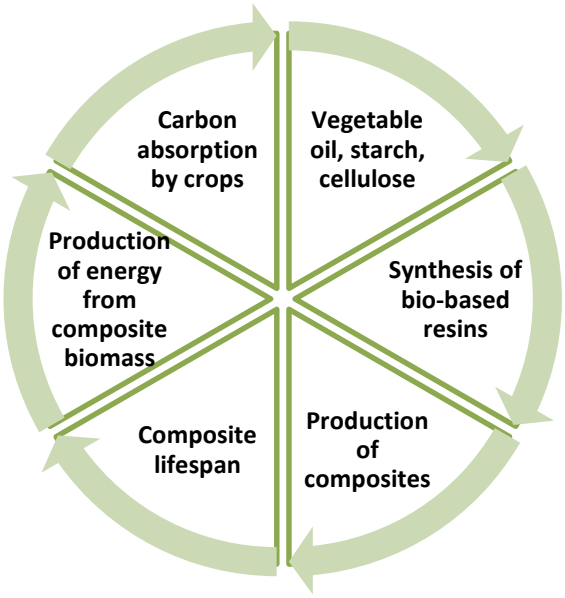

Figure 1 Sustainable lifecycle of bio-based composites.

Though looking for plastic alternatives is important, it is essential to understand that plastics have been an important part of society [7]. Composites, for instance, or more specifically fibre-reinforced polymers (FRP), are materials that can be developed with an array of desirable properties, such as strength and stiffness, abrasion, impact and corrosion resistance. Further to that they are light materials with very low densities [8], [9]. The World Corrosion Organization [10] estimates that around USD 2.2 trillion are spent with corrosion issues. This inherent resistance to corrosion, as well as to salt and chemicals, makes composites attractive to maritime applications, which is harsh environment for materials to withstand [11].

FRPs are already an established technology in fields such as automotive, maritime, civil structures, aerospace and sports equipment [12], [13]. It is estimated that by 2020 the market of composites will be worth over USD 115 billion [14]. The main drivers of the growth are the increasing demand of the composites in wind turbines for energy generation, aerospace and transportation. According to Boeing [15], 50 %of the weight in the aircraft model 787 Dreamliner is from composite structures.

FRPs are formed from at least two phases, a continuous phase, called a matrix, and the other dispersed, such as the fibres, which is surrounded by the matrix, shown in Figure 2. Fibres are the main component in a FRP, responsible for carrying the loads; while the matrix performs as an interface dispersing the loads among the fibres, as well as protecting them from external damage, elevated temperatures and moisture [16]–[18]. Both phases have different shapes and chemical compositions, but when joined together they create a new material whose characteristics are different from the isolated ones [8], [17]–[20].

Although polyesters and vinyl esters are the most used types of matrices in FRP [18], the ester groups in their polymeric chains are susceptible to neutral hydrolysis in aqueous environment [21]. Epoxy resins usually do not have ester groups in their chains, therefore better mechanical and chemical properties are achieved, such as stiffness and resistance to solvents [18]. Further, the epoxide group in the resin is versatile towards different chemical reactions thus allowing different types of curing procedures. Cure shrinkage is much lower than other resin types, which reduce residual internal stresses in the materials [22]. A comparison of a few commercial thermosetting resins for infusion application is presented in Appendix B.

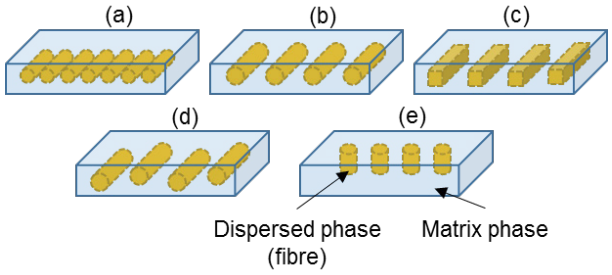

Figure 2 Representation of fibre (dispersed phase) configuration in a matrix, at different: (a) concentration, (b) size, (c) shape, (d) distribution and (e) orientation [8].

The consolidation of fibre and matrix is permanent, the binding of the two components is very effective and their separation for recycling is difficult. In general, two ways are sought for recycling FRP materials. Firstly, the mechanical path consists in breaking the material into smaller pieces that can be incorporated as a filler in other composite materials. Shredding, grinding, washing and drying are used in the process [9]. Secondly, the thermal path is done by pyrolysis, in which the FRP is decomposed by heat in a closed system free from oxygen. This system, however costly, can recuperate different gases and oils that can be used in other applications [9]. When FRPs are not recycled, they can be sent to landfills or incinerated, the latter might be used to generate energy [23], [24] but air pollutants and hazardous ash are generated [23].

Composites behaviour vary according to their proportions, geometry, distribution, and interaction of their constituents. That leads to the tailored development of materials with a combination of properties, which in some cases, are better than the properties found in metal alloys, ceramics or polymers [8], [17]. Composites are used in a wide range of products. They can be manufactured aiming at properties, which are specific for the function they will provide. They feature a high stiffness/weight ratio, high resistance to corrosion and a large range of design possibilities, being easily adaptable to different forms of application [13], [25].

Wood itself can be considered a natural composite where cellulose fibres are dispersed in a lignin matrix [26]. Other bio-based materials are made from agricultural and forestry renewable

feedstock, from the crops themselves to the by-products their processing might generate [27]. These substrates from vegetable sources have different compositions depending on the conditions of the place they were cultivated, as well as irrigation and fertilization [28]–[32].

In this sense, vegetable oils, lipids and fats are brought to attention. They are composed by triglycerides, from which a large proportion can be unsaturated (double bonds) fatty acids, as shown in Figure 3. It is important to note that not all the types of oils are highly unsaturated, which results in a lower epoxide content [33]. Triglycerides are bigger molecules than the monomers used in epoxy and other thermosetting resins, thus they are much more free to adopt different spatial arrangements which can result in rubbery materials.

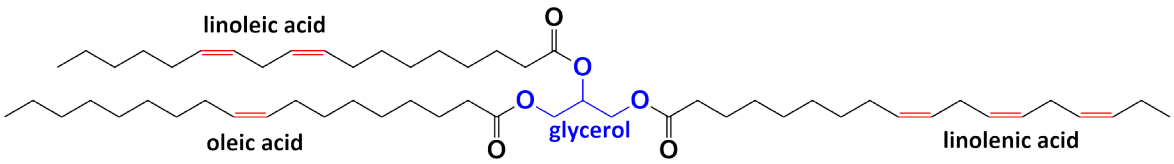

Figure 3 Structure of a triglyceride molecule, the glycerol moiety connects different fatty acids [34].

Vegetable oils are available in high purity and thus, can be used in various organic synthesis[35]. The double bonds in the structure allow vegetable oils from various sources to be transformed into epoxy resins. These bonds are found in triglycerides and the derivative fatty acids but they are not very reactive for use as resins. Therefore, functional groups that are more reactive need to be introduced to the structure (such as epoxides, amines and hydroxyl).

Further to that, the number of double bonds in each fatty acid or triglyceride is important for the development of polymers, specifically high performance ones such as epoxy resins. Polymers are divided into thermoplastic and thermosetting categories. Thermoplastic polymers comprise long chains of monomers that have two connecting groups (functional groups) that allow chain growth during the polymerization reaction. Thermosetting materials on the other hand, have at least one monomer with more than two connecting groups. This feature allows the growing chains to crosslink with other chains creating networks held together by covalent bonds [8], [22].

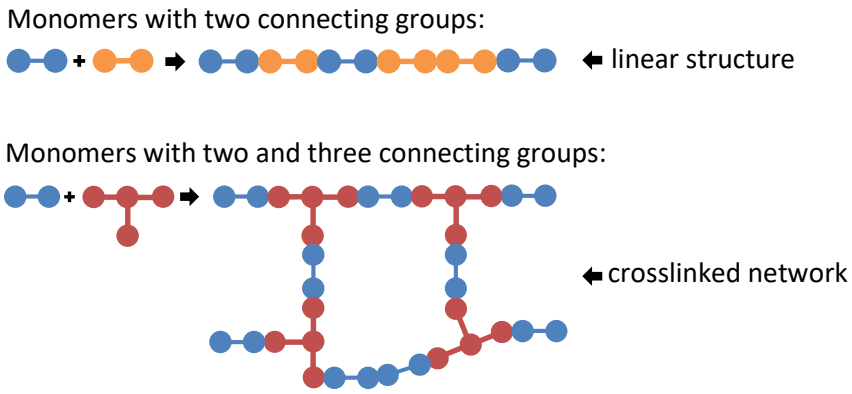

Figure 4 Formation of thermoplastic and thermosetting material from bi- and tri-functional monomers [22].

Linseed oil is often chosen as the precursor of epoxidized oils due to the high number of double bonds within its molecules. According to Dubois *et al* [33], linseed oil is composed of 55 % of linolenic acid (3 double bonds). Next to linseed, perilla oil contains 55 % and chia oil 61.3 %. Though these other oils have high levels of linolenic acid as well, they are not available in the market in large scales such as linseed.

The conversion is possible through several methods already reported in the literature [36], [37]. Products obtained in the oxidation of the double bonds are high-value commercial intermediaries in organic and petrochemical synthesis, since they have great reactivity [38]. In addition, vegetable oils are also amongst the cheapest and most available renewable sources, their use in bio-composites bring great advantages due to their low toxicity. It is estimated that more than 197 million metric tons of vegetable oil from different sources will be consumed in the years of 2018 and 2019, as shown in Figure 5.

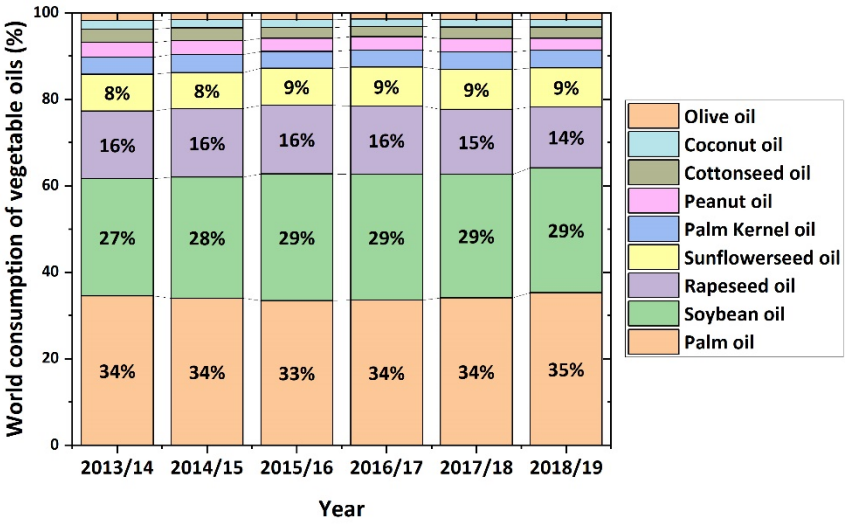

Figure 5 World consumption of vegetable oils [39].

Vegetable oils become highly viscous when epoxidized, see Table 1. It can be a huge drawback for their utilisation in composite manufacturing, especially when the infusion process is used. Some epoxidized oils present a lower viscosity than of a conventional epoxy resin. Still the gain in viscosity they have after epoxidation cannot be neglected. Epoxidized linseed oil is at least twice as viscous as a conventional epoxy resin. This behaviour makes epoxidized linseed oil unfeasible for infusion application. The epoxide groups that are added to the double bonds in the triglyceride molecules increase the intermolecular forces which causes the increase in viscosity.

Table 1 Viscosity of epoxidized soybean and linseed oils [40].

Degree of epoxidation	**Soybean (cP, 20 °C)**	**Linseed (cP, 20 °C)**
No epoxidation	94	88
1/3	140	131
2/3	280	346
Fully epoxidized	543	990

Vacuum bagging and resin transfer moulding (RTM) require a high vacuum so the resin can flow through the fibres, wetting them; hence infusion resins must have very low viscosity [13], between 50 - 1000 cP [41]. A representation of vacuum bagging is given in Figure 6. In the process a mould or support is used, which in turn will give the shape of the composite. The fibres are laid-up, covered by a peel-ply cloth, a breather cloth and finally the vacuum bag. The vacuum is applied to one end of the system. It causes the bag to constrict all the layers together and suck the resins through the fibres.

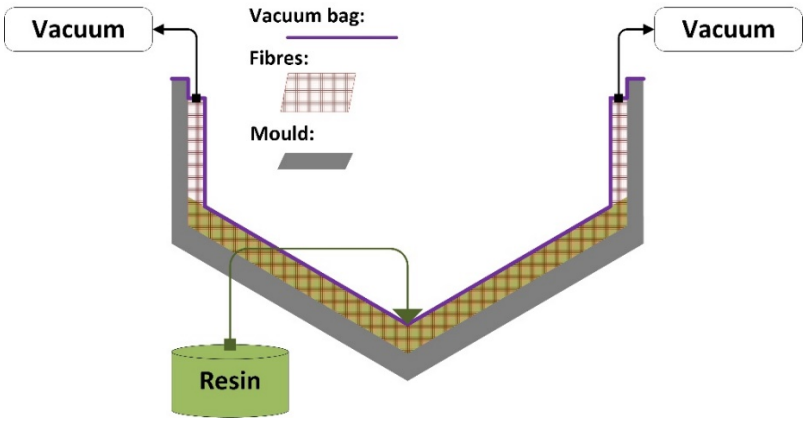

Figure 6 Composite production by infusion [41].

Better composite materials are obtained with vacuum assisted infusion systems. The process removes air bubbles, reduces voids and helps consolidate each layer [42]. Further, maritime composite structures demand great material performance. These materials have to be cheap, light, tough and durable. Nevertheless, being fire, water and chemicals resistant.

Although conventional epoxy resins are well established for composite structures, the behaviour of bio-based resins used in maritime structures has not been extensively studied. Epoxidized vegetable oils have been used and evaluated as plasticizers [43], [44]. Investigations were also carried out towards understanding the water uptake behaviour of resins derived from vegetable oils [45], [46]. These works focus on epoxidized triglycerides and not in the much less viscous epoxidized FAMEs. The absence of this knowledge in the current state of the art is the gap this thesis will fill.

The thesis demonstrates that the glycerol moiety plays a major part in the behaviour of resins derived from vegetable oils. Its presence increases the material's strength and stiffness but it is susceptible to water hydrolysis in high moisture environments. The absence of glycerol greatly reduces the viscosity. The crosslinking given by the epoxide groups is not enough to yield a material whose characteristics are comparable to the conventional epoxy systems. Further, the internal and unbiased epoxide groups in the epoxidized oils and FAMEs require high energy to be cured, such as cationic or UV initiated.

1.1 Aim and objectives

A UV-curable epoxy resin derived from linseed oil is available on the market. Despite having a very high bio-based content (95 % of epoxidized linseed oil), its viscosity is high and hinders its use in composite production processes where low viscosity is required, such as vacuum bagging and RTM. Furthermore, these production processes use moulds and bags that can block UV-light from reaching the resin and providing curing. As an alternative, bio-based curing agents such as dicarboxylic acids and anhydrides have been employed. They often require high temperature curing and yield low glass transition temperature polymers. Amines and amides are, in turn, a very reactive type of hardener in the market, therefore bio-based phenalkamines and phenalkamides can offer a sustainable alternative for curing.

The aim of this project is to synthesize and evaluate a low viscosity epoxy resin derived from linseed oil, suitable for cure by a bio-based hardener or UV-light, reaching the highest bio-based content possible and a performance comparable to conventional epoxy systems.

The project pathway is depicted in Figure 7. The synthesis of the resin was studied by the epoxidation and transesterification of linseed, camelina and soybean oils over heterogeneous catalysts. The fatty acid methyl esters (FAMEs) were initially obtained by the homogeneous transesterification of each oil. Then the FAMEs were heterogeneously epoxidized.

To produce enough material for testing specimens, the project is focussed on the homogenous transesterification of a commercially available epoxidized linseed oil (ELO). From that the low-viscosity transesterified and epoxidized linseed oil (TELO) was obtained. Testing specimens were made by curing ELO and TELO either via UV-light or via hardeners. For the UV-curing, blends of ELO and TELO were prepared with a UV-curable epoxy resin derived from linseed oil (UV-L). For the curing with hardeners, a benchmarking was carried with five different hardeners derived from cashew nut shell liquid (CNSL). The chosen hardener (LITE 3060) was used in blends of ELO, TELO, conventional hardener and conventional epoxy resin.

All blends and specimens were evaluated before and after curing. Liquid samples were assessed by FT-IR and viscosity measurements. The solid samples were submitted to hygrothermal ageing, FT-IR, mechanical and chemical tests.

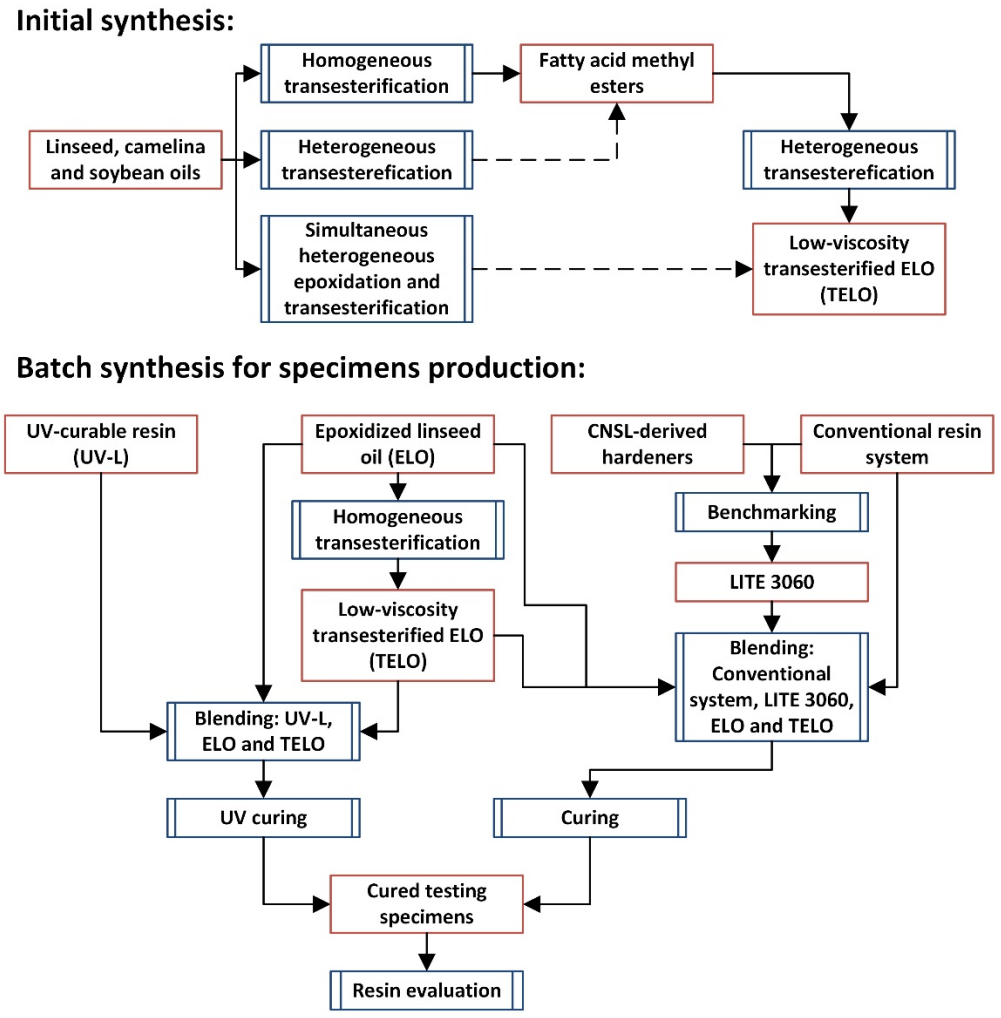

Figure 7 Thesis outline chart.

1.2 Thesis structure

After this introduction and background, chapter 2 analyses the literature around the synthesis and evaluation of epoxy resin derived from vegetable oils, as well as the curing of epoxy resins by CNSL-derived hardeners and UV-light. Chapter 3 presents the results in the synthesis of the bio-based resins used in this project. Chapter 4 covers the results from the screening of phenalkamine and phenalkamide hardeners applied to a conventional epoxy system. Chapter 5 shows the results from the tests carried out with blends of conventional and bio-based epoxy with conventional and CNSL-based hardeners. Chapter 6 presents the data from tests performed in samples made with UV-curable bio-based epoxy resin and the low-viscosity alternative. Chapter 7 concludes this thesis and suggests possible future works.

Chapter 2 Epoxy resins based on vegetable oils

2.1 Epoxidation of vegetable oils

The epoxidation of a vegetable oil is the reaction of its carbon-carbon double bonds (olefin) with an active oxygen, usually from a peroxide or peroxy acid. The addition of oxygen, converting the double bond into a three-membered ring containing oxygen, called epoxide or oxirane ring, shown in Figure 8. The electrophilic oxygen from the peroxy acid reacts with the nucleophilic double bond, see Figure 9 [36], [37], [44], [47].

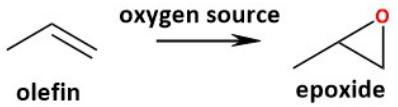

Figure 8 Epoxidation of olefins to from epoxides.

Although vegetable oils are biodegradable, the cured resins derived from them should not be. When applied to composites, the resin must be able to keep its integrity throughout the structure lifespan, especially in high performance applications such as marine vessels, composite bridges and wind turbines. Therefore, the most important sustainability claim is the fact that a fully biobased composite could be incinerated as biomass in the end of its lifespan.

The oils used in the production of epoxy resins have to be composed by fatty acids that have a high number of insaturations. The double bonds will be oxidized to epoxide groups, the higher the amount of epoxide groups the higher the cross-linking density will be and consequently better (stronger and stiffer) materials can be obtained [35]. Epoxides obtained from vegetable oils are preferably produced in an industrial scale with performic acid generated *in situ*, from the reaction of hydrogen peroxide and formic acid [36], [48]. The mechanism for the reaction was first proposed by Prilezhaev in 1909 [49], as shown in Figure 9. The performic acid generated has a high degree of polarization, which results in an electrophilic oxygen that can be added to the unsaturations of the vegetables oils. A transition state is formed, oxygen and proton quickly transition. This mechanism is also called butterfly transition state.

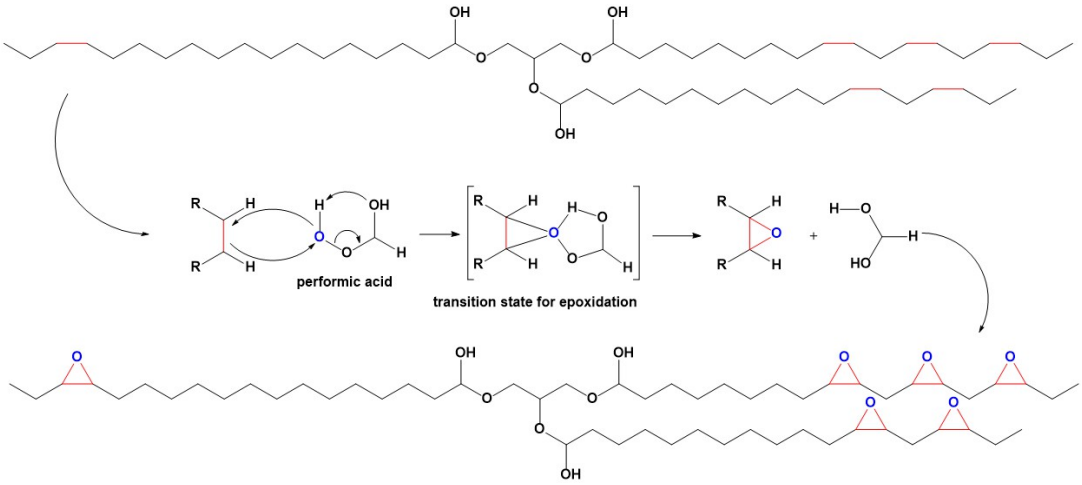

Figure 9 Prilezhaev mechanism for the epoxidation of olefins [49], [50].

Several different processes were developed throughout the years for this synthesis, though in the most conventional method hazardous chemicals such as strong acids and concentrated hydrogen peroxide are employed. Other oxidants can be employed, e.g. m-chloroperoxybenzoic acid (m-CPBA) is very often used [51]–[53].

2.1.1 Chemical treatment

Chemical treatments are the conventional way of epoxidizing vegetable oils and their derivatives, carboxylic acids and hydrogen peroxide are used in this process [37], [48], [54]. Results published by Dinda *et al* [55] concluded that peracetic acid is a better oxygen carrier than formic acid for the reaction (Figure 9) because the higher acidity of formic acid acts in the epoxide ring-opening and decreases the selectivity. Sulphuric acid is the best amongst the inorganic acid catalysts tested (phosphoric acid, nitric acid, and hydrochloric acid), much likely due to high purity (98 %). The other acids used were less concentrated, the water in the acids cause epoxide ring-opening [56]. The study also concluded that reactions carried out in temperatures above 60°C and with greater acid concentration increased the speed of reaction, but also increased ring opening from epoxide to glycol molecules. Epoxide groups can react with weak nucleophiles like water in the presence of acid catalysts forming glycols [50], shown in Figure 10.

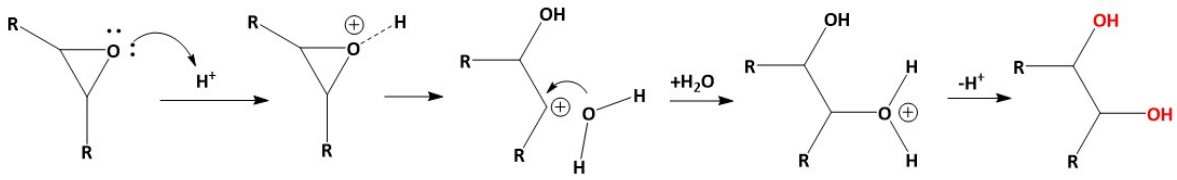

Figure 10 Acid catalysed epoxide ring opening [50].

Further to that, the lower amount of water coming from highly concentrated sulphuric acid and glacial acetic acid might have influenced the higher selectivity obtained. The best results were

achieved after 4 h of reaction at 60 °C with a double bond conversion of 91.2 % and 77 % selectivity towards epoxide groups [55].

Other works were published using different sources of fatty acids, such as cottonseed oil, jatropha oil (belonging to the family of the castor oil plant), sunflower oil, corn oil and mahua oil. They also pointed to sulphuric acid as the best catalyst, in conjunction with temperatures around 60 °C as the best conditions for converting fatty acids into epoxides [57]–[59]. Mungroo *et al* [60] presented similar results regarding the behaviour of performic and peracetic acids but using an Acidic Ion Exchange Resin (AIER) as a catalyst.

2.1.2 Enzymatic method

Enzymes are biological catalysts; they can be employed in several reactions and are able to carry reactions out in milder conditions. Enzymatic processes are a great alternative to chemical treatment and unwanted reactions can be avoided, such as the opening of the epoxy ring. The primary limitation presented by enzymes is their own denaturation caused by reaction parameters, commonly temperature and concentration of hydrogen peroxide. Additionally, due to the fact that the reaction is exothermic, it requires precise temperature control [36], [37], [54], [61].

Orellana-Coke *et al* [62] published satisfactory results where linoleic acid was completely epoxidized by Lipase B, *Candida antarctica*. Excess of hydrogen peroxide was necessary in order to achieve good yields in reactions carried out at 50 °C for 24 h, but on the other hand, the increase of hydrogen peroxide led to a decreased enzymatic activity caused by denaturation. Further work from Törnvall *et al* [61] showed that a precise control of temperature and hydrogen peroxide addition rate promoted reactions without the same type of enzyme denaturation, but these reactions must be carried out at 20 °C for 48 h.

Sun *et al* [63] published results of tests on the epoxidation of *Sapindus mukorossi* oil concluding that the best parameters for the epoxidation of vegetable oils with Lipase B, *Candida antarctica* were 50 °C for 7 h with a ratio of hydrogen peroxide relative to the amount of double bonds in the oil of 4:1 (H_2O_2 : C=C). Other sources of vegetable oil were studied and published by Klaas *et al* [64], [65]. Yields over 80% were reached on the epoxidation of free fatty acids derived from rapeseed, soybean, sunflower and linseed oils. These free fatty acids were able to react with hydrogen peroxide (peroxy fatty acid) over Lipase to form peroxy acids thus auto-oxidating into epoxides, as shown in Figure 11. The high yields were achieved especially because the free fatty acids were much weaker than the usual carboxylic acids used in the Prilezhaev reaction. Weaker acids reduce the epoxy ring opening and enhance selectivity towards epoxides.

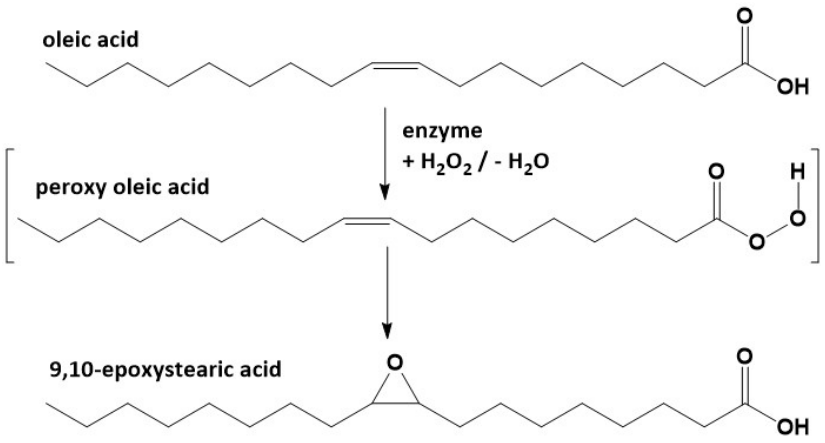

Figure 11 Auto epoxidation of fatty acids [64].

2.1.3 Acidic Ion Exchange resin

Acidic ion exchange resins can be used for the synthesis of peracids from carboxylic acids and hydrogen peroxide for the epoxidation of vegetable oils. It is suggested that the reactions carried out using this method reach high yields because the triglyceride molecules from the oil sources are larger than the pores in the resin. The acid catalysed formation of the peracids happen within the pores of the resin, then the peracids leave the pores and react with the double bonds in the triglyceride molecules. The bulky triglycerides in turn are not able to access the acid sites inside the pores. This way, the acid catalysed epoxide ring opening do not occur and the high yields are achieved [37], [54], [66], [67].

Results published by Mungroo *et al* [60] showed that the resin (Amberlite IR 120-H) can be reused and that the loss of activity is negligible. The conversion of the double bonds into epoxide rings was around 90% for a reaction with canola oil at 65 °C for 5 h. Goud *et al* [68] published similar results using karanja oil. Followed by Dinda *et al* [69] with studies on the epoxidation of cottonseed oil. All these works found their best results in the reactions carried out at around 65 °C. Over this temperature, the selectivity towards epoxides was diminished.

Sinandinovic-Fiser *et al* [70] studied the kinetics of the epoxidation of soybean oil using peracetic acid generated *in situ* over two different strong ion exchange resins (Amberlite IR-120 and Dowex 50X). There were no significant differences between the performances of the resins because both have strong sulfonated acid sites. However better results were obtained for reactions carried out at 75 °C for 7 h, with yields around 80 %. The formation of peracetic acid generated in the ion exchange resin's surface was elected to be the rate-determining step of the reaction. A work from Aguilera *et al* [71] investigated the effect of microwave heating in the epoxidation of cottonseed oil and oleic acid over Amberlite IR-120 with percarboxylic acid formed

in situ. The microwaves were able to accelerate the formation of peracetic acid that happen in the aqueous phase thus speeding up the overall reaction.

2.1.4 Alkene epoxidation over Titanium (Ti)

Heterogeneous catalysts with titanium Ti(IV)/SiO_2 were first developed by Shell for the epoxidation of propylene. Later, scientists of SnamProgetti (Eniricerche) discovered the titano-silicate (TS-1), seen in Figure 12, which was more stable in epoxidation reactions. This catalyst was not inhibited by water. Soluble Ti(IV) compounds and Ti(IV)/SiO_2 are sensitive to deactivation by ligands, such as water, which is a strong coordinating ligand. This behaviour does not allow reactions to be carried out in milder conditions [72], [73]. TS-1 enabled the reaction with diluted hydrogen peroxide, unlike the highly concentrated hydrogen peroxide the conventional Ti(IV)/SiO2 required, greater than 95 % [53], [72].

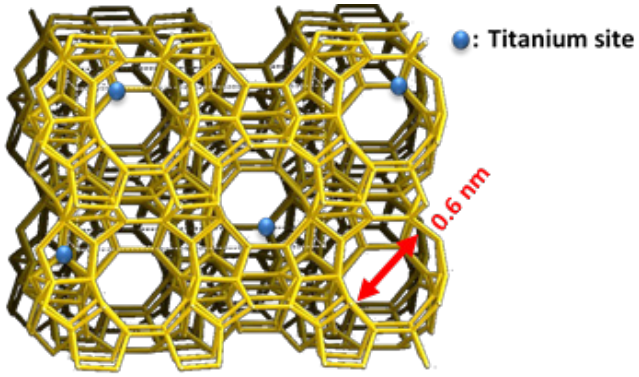

Figure 12 Titano-silicate (TS-1) catalyst structure and pore size.

Earlier it was found by Kollar [74] and Sheldon *et al* [75] that other transition metals such as molybdenum - Mo(VI), tungsten - W(VI) and vanadium - V(V) would also be able to catalyse the epoxidation propylene, especially Mo. Later, it was demonstrated by Sheldon *et al* [73] that the attempts to produce heterogeneous catalysts by combining these metals with silica were not successful, as these combinations resulted in rapid leaching of the metal ion. Which means that the metal was able to escape the framework, therefore reducing the activity of the catalyst. From a green chemistry approach [4], some metals should be avoided because of their toxicity.

In the mechanism, the metal ion works as a Lewis acid by withdrawing electrons from the alkylperoxo moiety and therefore making both peroxidic oxygens more electrophilic. The metal must be in its highest oxidation state; otherwise, there could be a heterolytic decomposition of the ROO- ligand group, seen in Figure 13. Altogether, an effective catalyst must be a weak oxidant and strong Lewis acid [73], [76]. These criteria are met by soluble Mo(VI) but, as mentioned before, Mo(VI) would not be suitable as there were leaching problems in its use [76]. In a more

recent study by Bigi *et al* [77], Mo-MCM-41 was used in the epoxidation of alkenes. They managed to reach yields over 90% for the epoxidation of cyclohexene and cyclooctene using tert-Butyl hydroperoxide (TBHP) as oxidant. Molybdenum leaching was detected in the catalyst preparation and after reactions were carried out.

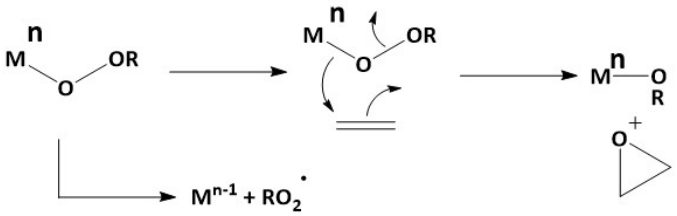

Figure 13 Decomposition of alkylperoxo group [73].

A comprehensive study from van der Wall *et al* [78] compared the epoxidation of 1-octene in a milder condition, using H_2O_2 (30 wt% aqueous) as oxidant over four different titanium containing catalysts. The best yields were obtained in reaction carried out at 60 °C (TS-1: 93 %, Ti-MCM-41: 79 %, Ti-beta: 41 % and Ti, Al-beta: 12 %). Further, the activity of Ti-beta was tested in five different solvents at 40 °C for four hours (Acetonitrile: 98 %, t-butanol: 36 %, 2-propanol: 24 %, ethanol: 7 % and methanol: only glycols).

Given the unique features that the use of Ti(IV) brings to the epoxidation of olefins, extensive work has been developed in the understanding of the mechanisms involved during the reaction [38], [79]–[85]. The reaction begins with the assumed breakage of the bond between titanium, oxygen and silicon (Ti-O-Si) caused by hydrogen peroxide to form Ti-OOH and Si-OH, shown in Figure 14.

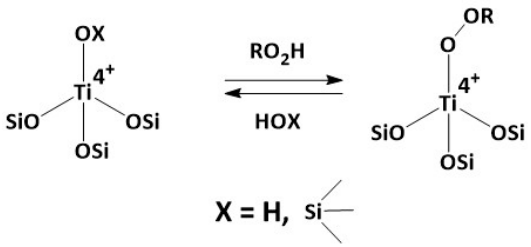

Figure 14 Isomorphously substituted titanium activation [73].

It is believed that a molecule of alcohol or water (solvent) can be co-adsorbed and form an intermediate ring of 5 members [86], [87]. Though theoretical studies suggested that there is no adsorption of alcohol or water [88], [89]. More recently, it was suggested that after the adsorption of the hydrogen peroxide to the titanium atom, as shown in Figure 14, the olefin approaches and consequently with the oxygen transfer there is the formation of a water molecule [84].

2.1.4.1 Epoxidation of oils and fatty acids over titanium heterogeneous catalysts.

Several drawbacks in the Prilezhaev process (Figure 9) have led researchers to look for an easier and yet more sustainable approach for the epoxidation of vegetable oils and their derivatives. For instance, the yields towards epoxide groups are low as the acids present in the reaction catalyse the epoxide ring opening. Further, dangerous chemicals are used in the process such as highly concentrated hydrogen peroxide and strong acids [90]. Vegetable oil molecules and their fatty acid derivatives are bulky and thus, the size of catalyst pores hinder their diffusion. Guidotti *et al* [90] studied the epoxidation of fatty acid methyl esters (FAMEs) on three different titanium-grafted silicalites using TBHP (ter-Butyl hydroperoxide) as an oxidant. Reactions were carried out over 24 h at 90 °C; the catalysts used were Ti-MCM-41 and two types of Ti-SiO_2, one containing an ordered array of mesopores and the other featuring an amorphous structure. In the study, they have reached conversion of 98 %, 76 % and 95 % and selectivities of 85 %, 94 % and 96 % in respect to the catalysts listed order.

Later, Campanella *et al* [91] reported their findings on the epoxidation of soybean oil and its derivatives over amorphous Ti-SiO_2 with tert-butanol and organic H_2O_2 (in 1-phenyletanol). They obtained a yield of 87.75 % as the best result for a reaction carried out at 90 °C for 54 h. The best molar ratio of H_2O_2:double bonds was 1.1:1.

Guidotti *et al* [92] studied different titanium based solid catalysts (Ti-MCM-41, two types of Ti-SiO_2 and TiO_2-SiO_2) on FAMEs derived from different sources, such as high-oleic sunflower oil, castor oil, sunflower oil and coriander oil. Ti-MCM-41 showed the best yields for all the substrates. Nonetheless, the most interesting result was the fact that the composition of the mixture of FAMEs in the different oils played an important role (high-oleic sunflower > coriander > castor > soybean). Although the average percentage of unsaturated FAMEs was similar (92 ± 7 %), the amount and nature of the unsaturated fatty acids was different, as shown in Figure 13.

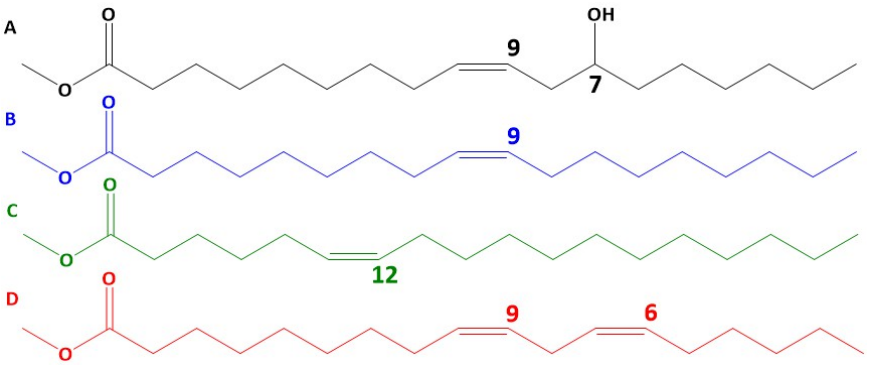

Figure 15 Structure of unsaturated fatty acids: A) methyl ricinoleate B) methyl oleate, C) methyl petroselinate and D) methyl linoleate [92].

Starting by the opposite extreme from the ester group, methyl oleate has a double bond on carbon nine, methyl petroselinate on carbon twelve and methyl ricinoleate on carbon nine followed by a hydroxyl on carbon seven. Supposing they have very similar conformation, the functional groups in their chains played the major role on their diffusion through the catalyst pores [92].

Wilde *et al* [93] screened the epoxidation of methyl oleate with more concentrated H_2O_2 (72 wt.%) over different solid catalysts (industrial TS-1, Ti-MCM-41, TiO_x-SiO_2, TiO_x-SiO_2, WO_x-Al_2O_3, MoO_x-Al_2O_3 and MoO_x-SiO_2) where TS-1 was the only one that presented conversion and selectivity over 80 %, Ti-MCM-41 exhibited leaching. Further, they evaluated different solvents finding out that, in accordance with the work of van der Waal [78], the best solvent was acetonitrile (conversion: 93 % and selectivity: 87 %). The epoxidation of commercial biodiesel, consisting of predominantly 72 wt. % of methyl oleate was performed over T

S-1, using the same concentrated H_2O_2. The activity was compared to a TS-1 synthesized with stacked morphology in a epoxidation carried out at 50 °C for 24 h. The reaction with industrial TS-1 reached high conversion and selectivity (around 80 %). Whereas TS-1 with stacked morphology exhibited a conversion around 55 % and selectivity around 70 % [93].

In a following work, Wilde *et al* [94] published the results for the epoxidation of commercial biodiesel (72 wt. % methyl oleate and 19 wt. % methyl linoleate) carried out with nanosized TS-1 (stacked morphology) and microporous/mesoporous (10 - 40 nm) TS-1 obtained from desilication and recrystallization. Both compared to industrial TS-1. They used less concentrated H_2O_2 (35 wt. %) at 50 °C for 24 h. The conversion of biodiesel per titanium atoms in the catalyst was two times higher for TS-1 desilicated with NaOH and recrystallized, though all selectivities were around 80 %.

2.1.4.2 Payne oxidation

As discussed previously, the epoxidation of fatty acid methyl esters has been studied and much thought was given to the mechanisms involved. Unlike the first results obtained in the epoxidation of propylene with the use of titanium containing solid catalysts, where high conversions were obtained in methanol and ethanol, the epoxidation of bulkier olefins such as fatty acids was not successful in these solvents. Holleben *et al* [95] studied the effects of different nitriles for the epoxidation of cyclohexene and limonene with hydrogen peroxide (30 wt. %) for 24 h at room temperature. The nitriles were not used as solvents, and on the contrary, they used methanol and a mixture of dichloromethane and water as solvents. The best results were obtained with trichloroacetonitrile, must likely due to the high electron withdrawing effect caused by the three chlorine atoms in the structure, increasing the reactivity of a peroxycarboximidic acid intermediate created, which will be discussed further.

Guidotti *et al* [96] studied the epoxidation of cyclohexene over titanium containing catalysts (Ti/SiO_2, Ti-MCM-41 and Ti-MCM-48) with hydrogen peroxide (30 wt. %) as oxidant at 85 °C for 3 h. Although they obtained high selectivities (> 98 %), the highest conversion was 44 % for Ti-MCM-48. They attributed the high selectivity to the slightly alkaline character of acetonitrile that hinders acid catalysed epoxide ring opening.

In a later work by Guidotti *et al* [97], the activity of Ti-MCM-41, Ti-MCM-48 and Ti-aerosil was tested in the epoxidation of methyl oleate. Hydrogen peroxide (50 wt. %) was used as an oxidant at 85 °C in an inert atmosphere for four hours. Ti-MCM-41 performed slightly better than the others (conversion = 52 % and selectivity = 83 %) and was further tested at different hydrogen peroxide and catalyst concentrations. It reached up to 96 % conversion and 95 % selectivity.

Wilde *et al* [93] studied the effects of different solvents in the epoxidation of commercial biodiesel (72 wt. % methyl oleate) at 50 °C for 24 h. Amongst ethylacetate, acetone, acetonitrile, acetonitrile/methanol, diglyme, methanol and diisopropylether; acetonitrile exhibited the best performance with a 93 % conversion and 87 % selectivity. In a further work, Wilde *et al* [94] tested different titanium containing catalysts for the epoxidation of commercial biodiesel using similar conditions to the previous work, with acetonitrile as solvent at 50 °C, reaching over 80 % conversion and selectivity.

All these works pointed to acetonitrile as the best solvent for the epoxidation of fatty acids. It is suggested that the reaction follows the Payne oxidation pathway [98]–[100]. In Payne's oxidation, acetonitrile and hydrogen peroxide combine forming in situ a very reactive intermediate peroxycarboximidic acid [94], [95], [97]. As seen in Figure 16.

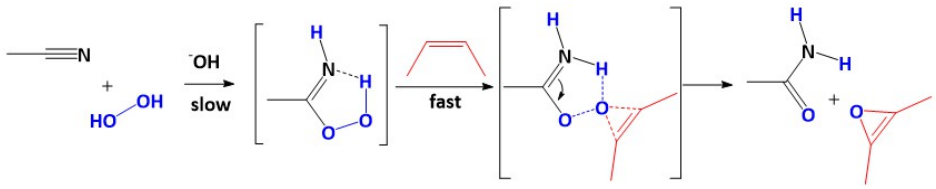

Figure 16 Payne's mechanism for olefin oxidation [98].

The formation of peroxycarboximidic acid happens slowly under mild alkaline conditions (pH 7.5 - 8). Payne *et al* [99] reported that less than 5 % of hydrogen peroxide reacted without the presence of a base in the reaction. Whereas in recent works, no catalysts are being used other than titanium containing ones. Consequently, fatty acids are bulky molecules and thus might not be able to approach active sites in the catalyst pores, due to size limitations, the formation of a small and much more mobile intermediate molecule might enable the fatty acids to be reached by the peroxycarboximidic acid and the epoxidation can take place.

2.2 Epoxy resin hardeners derived from cashew nut shell liquid

Hardeners are used for crosslinking epoxy resins, acting as catalysts or reacting with the epoxy rings, thereby providing cross-links in the resin structure. There are already commercially available curing agents from sustainable sources. These new materials are mainly derived from starch, cellulose and triglycerides, but they do not have aromatic groups in their molecules, which are able to bring greater mechanical properties, as well as heat and fire resistance. The curing agents used are mainly dicarboxylic acids [101], [102] and anhydrides [103]–[106]. Other hardeners based on amines and amides must be exploited for this usage as well. Amines and amides are highly reactive and largely used for curing conventional epoxy resins; yet toxic and volatile, they need to be developed into more sustainable derivatives in the future [107], [108].

In this context, phenalkamines and phenalkamides feature a series of benefits that make them interesting. They are obtained from cardanol, shown in Figure 17, a component present in the cashew nut shell liquid (CNSL), which is considered a by-product in the cashew nut industry [109]. It is possible to find 20 to 25 % of a cashew nut weight in CNSL [107], [108], [110]–[112]. In a phenalkamine/phenalkamide structure (Figure 17), there is an aromatic ring present, responsible for chemical and fire resistance; a long aliphatic chain, capable of bringing a hydrophobic character to the resin and increase the water resistance. Further, a phenolic hydroxyl that increases the reactivity at low temperatures and consequently facilitates curing. Finally a chain with amines or amide, which brings high mechanical properties to the resin by improving the crosslinking density [107], [110], [113], [114].

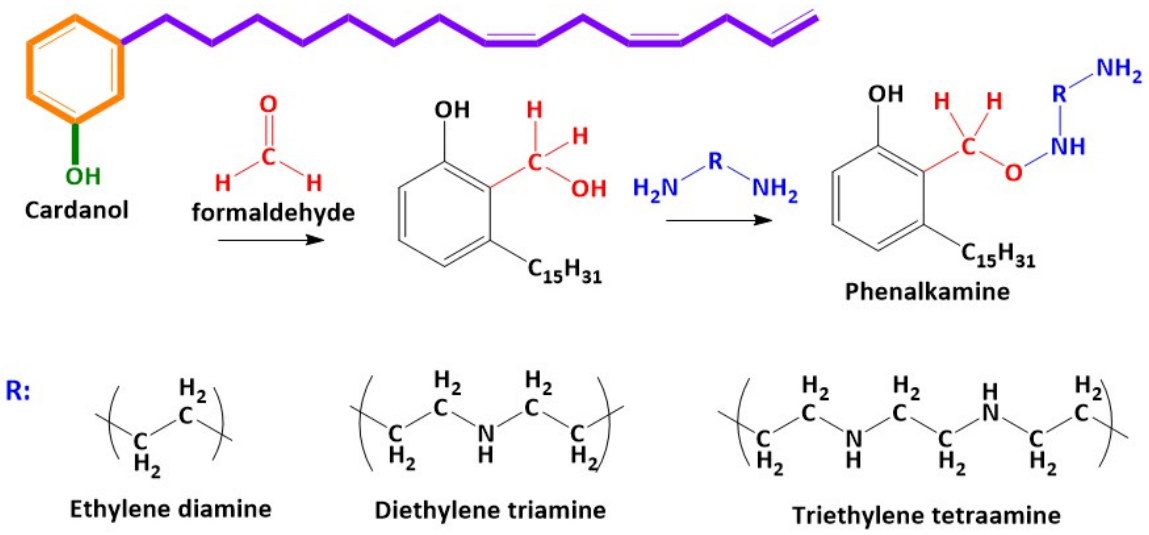

Figure 17 Structure of a phenalkamine derived from cardanol [115]–[117].

Dai *et al.* [110] studied the temperature sensitivity in the curing of a conventional epoxidic coating system cured by commercial phenalkamines. Thin specimens (around 200 µm) were fully cured at 5 °C and 24 °C. Further, the moisture uptake of the systems were compared to systems cured with conventional curing agents in salty water, at 25ºC and 65ºC for three weeks. The systems containing phenalkamines absorbed at least 50% less water than the system with polyamide and around 35% less than systems containing cycloaliphatic and Mannich base curing agents.

Ghosh *et al* [118] investigated the effect of temperature and moisture sensitivity in epoxy coatings cured by a phenalkamine and conventional counterpart hardener. To mimic seasonal conditions (25 ± 2 °C, 50 ± 5 % relative humidity and 10 ± 2 °C, 90 ± 5 % relative humidity) they cured 150 µm thick layers and exposed them to water, humidity and corrosion resistance tests. The phenalkamine hardener performed slightly worse in the tests and the T_g value was about 40 % lower.

Rao and Pathak [119] developed blends of epoxy/phenalkamine and epoxy/benzoxazine and studied their interaction in different proportions for the application in pre-impregnated fibres (prepregs). Copolymers were prepared and initially cured at room temperature, followed by DSC analysis at different stages: 100 °C for 30 min, 140 °C for 1 h, 180 °C for 1 h or 200 °C for 4 h. The peak curing point for the blends was at 253.7 ± 4.6 °C, which was the result of the benzoxazine ring opening. T_g was reduced with higher amounts of epoxy/phenalkamine in the blend, given by the long side chain from cardanol, which increases flexibility and consequently reduces the glassy structure of the cured resin. The char yield was increased with the higher amounts of benzoxazine in the sample, which reflects the higher thermal resistance given by aromatic rings. Although, in this specific case, the phenalkamine hardener reduced the thermal resistance. Other bio-based

hardeners such as dicarboxylic acids and anhydrides do not naturally feature aromatic rings [101], [106], [120].

Pathak and Rao [117] evaluated the adhesive properties of phenalkamines synthesized with three different amines (ethylene diamine (A), diethylene triamine (B) and triethylene tretramine (C)). These phenalkamines were used for curing a conventional epoxy system (DGEBA - bisphenol-A diglycidyl ether). Different epoxy to phenalkamine ratios where tested (1:1, 1:2 and 1:3). The adhesive properties were tested in copper, aluminium and brass, and once again, the results depended on the amines used in the phenalkamine synthesis. Curing times were different depending on the amine used A>B>C. The phenalkamine synthesized with ethylene diamine has a smaller amine content and therefore is less reactive, requiring a longer time to cure (up to 3h). According to Petrie [18], this extra time allows the resin to penetrate irregularities in the material and increase the surface area between resin and substrate (wetting).

Huang *et al* [121] managed to prepare a phenalkamine hardener with a lighter (Gardner colour from 16 to 7) and more stable colour by replacing the phenolic hydroxyl (-OH) group present in the cardanol backbone by a butoxy ($-O(CH_2)_3CH_3$) group. The viscosity was reduced by 88 %. Phenalkamine/DGEBA epoxy and butoxy-phenalkamine/DGEBA epoxy blends were prepared and initially cured for 3 h at 25 °C followed by 8 h at 80 °C post-cure. T_g temperatures were fairly similar to each other, but the blends performed differently mechanically. The blend phenalkamine/DGEBA showed a 23 % higher tensile strength, the binding strength (lap shear strength) was 54 % lower than the butoxy-phenalkamine/DGEBA epoxy blend. These results are driven by the hydroxyl or butoxy groups in the cardanol backbone. According to Shechter *et al* [122], the hydroxyl groups participate in the curing reaction as a catalyst, speeding it up. The butoxy-phenalkamine blend not only has a lower viscosity and a slower cure but also results in a more flexible material. These characteristic are better for binding, which is seen in the lap-shear strength tests, performed in their work.

Liu *et al* [123] prepared phenalkamines using hexamethylenediamine aiming to create a hardener that could provide flexibility and water resistance. The resulting material was in a solid state and inconvenient for blending. Another two phenalkamine hardeners containing diethylenetriamine (DETA) with nonylphenol or m-cresol were prepared, with viscosities of 13 and 9.4 cP respectively. Solid samples were prepared by mixing a DGEBA epoxy resin with each of the three prepared phenalkamines and another one with DETA only. The samples were cured for 3 h at 25 °C and post-cured for 6 h at 80 °C. The blend made only with hexamethylenediamine exhibited the lowest T_g and tensile strength. The addition of DETA with nonylphenol or m-cresol increased those values. The blend only containing DETA presented the highest T_g and tensile strength. The long

aliphatic chain in the cardanol molecule gives flexibility to final cured products, which in conjunction with the also long-chained hexamethylenediamine, were responsible for the low T_g and tensile strength reported. With the addition of DETA to the phenalkamine, the crosslinking density was increased. T_g and tensile strength were higher when no phenalkamine was applied, given by a high crosslinking density without the plasticizing effect of cardanol's side chain and hexamethylenediamine.

Darroman *et al* [124] used epoxidized cardanol and epoxidized phenalkamine to obtain epoxy blends. According to their study, a phenalkamine counterpart was prepared to avoid the Mannich reaction used in the synthesis of phenalkamines and therefore avoid the use of formaldehyde. They reported that cardanol's aliphatic side chain has an average of 2.97 unsaturations that can be functionalized. In their approach, allylbromide was added to these unsaturations as well as to the phenol group in the cardanol moiety (allylation), followed by the reaction with cysteamine hydrochloride. A scheme of the final product is presented in Figure 18.

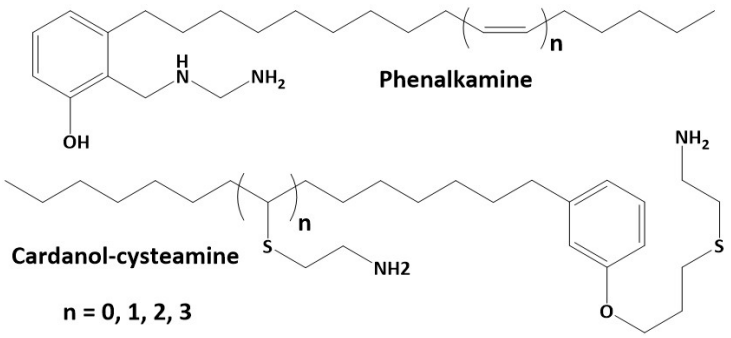

Figure 18 Representation of an epoxidized phenalkamine synthesized by Mannich reaction and the Cardanol-cysteamine counterpart [124].

Epoxidized cardanol was used as the epoxy resin, phenalkamine and the synthesized cardanol-cysteamine were used as hardeners. Several samples were prepared with varying stoichiometric resin to hardener ratios. ^{1}H-NMR analysis showed that the cardanol-cysteamine hardener had a higher AHEW (amine hydrogen equivalent weight) and had a higher degree of crosslinking. The phenalkamine hardener had the amine groups closer to each other, which enabled a tighter crosslinking resulting in a more glassy state. Such behaviour was evidenced by the T_g temperatures, being 19 °C for the cardanol-cysteamine and 30 °C for the phenalkamine with resin/hardener ratios of 1:1 and 1:1.3 respectively. The phenalkamine hardener had a secondary amine, which was less reactive than the primary ones in the cardanol-cysteamine one, thus the highest T_g was found in the given ratio (1:1.3).

Ma *et al* [125] prepared two phenalkamine hardeners with thiourea-DETA groups by the Mannich reaction, one of them had the cardanol's phenolic hydroxyl replaced by 2,3-dihydroxy propyl

ether. A scheme is given in Figure 19. These phenalkamines were used to prepare DGEBA blends that were initially cured for 8 h at 30 °C and post-cured for 4 h at 80 °C. In the same fashion, a third blend was prepared with DETA for tensile tests.

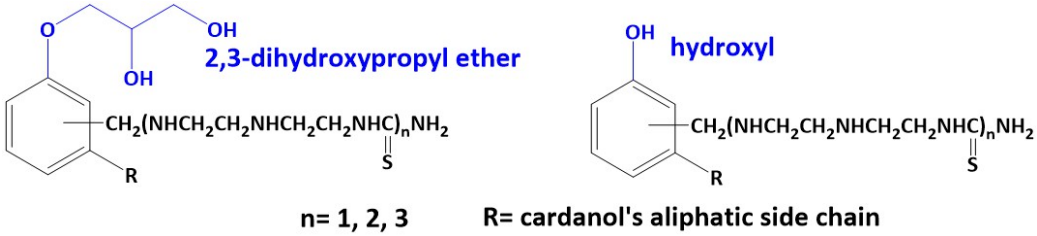

Figure 19 Representation of phenalkamines synthesized with thiourea groups and substituted hydroxyl.

Although hardeners with high AHEW were achieved with thiourea groups, the majority of those hydrogens are from secondary amines, which, as reported by Darroman *et al* [124], are less reactive. Hence when the phenalkamines are compared to DETA, the tensile strengths are inferior (reduced in 41.80 % and 48.90 % for the hydroxyl-phenalkamine and 2,3-dihydroxypropyl ether-phenalkamine respectively). When thermal characteristics are evaluated, 2,3-dihydroxypropyl ether-phenalkamine showed a T_g of 80.1 °C and hydroxyl phenalkamine of 46.5 °C. Such behaviour was discussed by Shechter *et al* [122], not only the phenolic hydroxyl but also those provided by protic solvents function as catalysts, a scheme is of which presented in Figure 20.

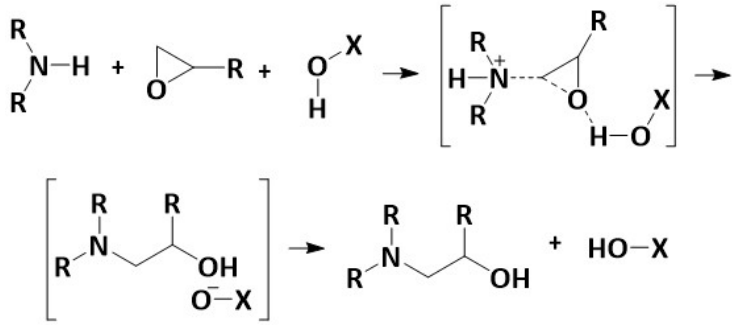

Figure 20 Hydroxyl catalysed epoxy ring opening [122].

DETA has two primary amines; however, when it is used to prepare the phenalkamines with thiourea, all of these amines become secondary and thus less reactive. The addition of 2,3-dihydroxyl ether increases the amount of hydroxyl groups and improves the reactivity and crosslinking density given by 2,3-dihydroxypropyl ether-phenalkamine, which provides a higher T_g while slightly reducing the tensile strength.

Zhang and Xu [126] studied the curing kinetics of several DGEBA/phenalkamine blends. These phenalkamines were synthesized with increasing amounts of secondary amines (1, 2, 3 and 5)

using ethylenediamine, diethylenetriamine, triethylenetetramine and pentaethylenehexamine. The reactivity given by the short-chain amines (diamine and triamine) is higher due to the lower viscosity the phenalkamines synthesized with them have. The activation energy increases as the curing develops and it is attributed to the smaller amounts of tertiary amines in them, which are responsible for catalysing the epoxy ring opening. The activation energy for the long-chain amines is slightly higher in the beginning of the curing reaction; it is smaller due to the higher amounts of tertiary amines in their chains.

Using a different approach, Balgude *et al* [127] prepared cardanol-based hardeners for coating applications by functionalizing the insaturations in the aliphatic chain with maleic anhydride followed by its condensation with DETA, seen in Figure 21.

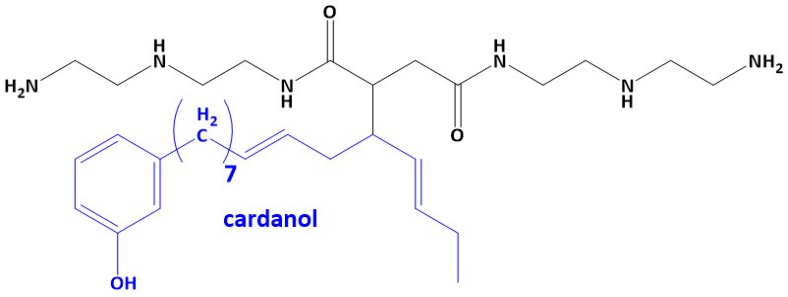

Figure 21 Cardanol based polyamide [127].

The synthesis was made so that the hardeners had different amine values varying around the amine value of a conventional hardener, also tested in the study. T_g followed the amine content giving higher crosslinking densities in the higher amine values. In the same fashion, tensile strength increased. Such behaviour contrasts with what is seen when the phenalkamines are prepared by the Mannich reaction where the amines are added to the phenol group, leaving the long aliphatic chain free, which in turn acts as a plasticizer in the final product, reducing tensile strength.

The plasticizing effect given by phenalkamines was also reported by Sahoo *et al* [128]. Blends of conventional DGEBA epoxy and ELO were prepared. The systems were cured by a commercial phenalkamine (NC558 - Cardolite Corporation). Viscosity tests showed that the DGEBA-phenalkamine blend has a much higher shear-thinning effect than the blends containing ELO, which behave similarly to a Newtonian fluid (viscosity is only dependent on the temperature and not on the shear rates applied [129]). Tensile strength and T_g were reduced and elongation at break increased with higher amounts of ELO. Sahoo *et al* [130] found the same behaviour when comparing the effect of ECO (epoxidized castor oil) and EMR (epoxidized methyl ricinoleate) in DGEBA-phenalkamine blends. EMR is the result of the transesterification of castor oil's triglycerides, resulting in a much less viscous fluid.

2.3 Curing of epoxidized vegetable oils

The position of the epoxide groups in the epoxidized oils make curing and crosslinking more difficult. Internal epoxide groups (di-substituted and electronically unbiased) are less reactive than terminal ones [131]–[133], seen in Figure 22. Similar charges between the two carbons in the triglyceride epoxide groups hinder the approach of amines, which is facilitated when the epoxide group is terminal, as in bisphenol-A diglycidyl ether (DGEBA).

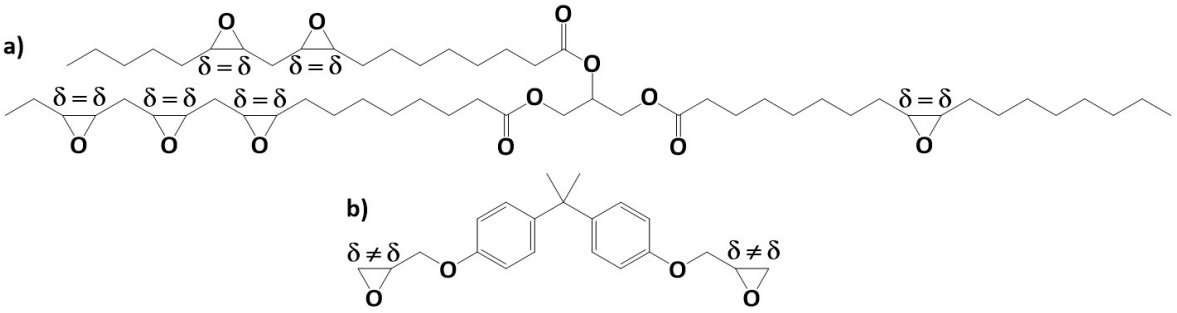

Figure 22 Structure of: (a) Triglyceride with internal epoxide group and (b) DGEBA with terminal epoxide group.

UV-radiation is sometimes used to overcome the lower reactivity of internal epoxide groups. Photoinitiators transform into radicals or ions that initiate the crosslinking reaction [134]–[137]. The most used type of photoinitiators are salts such as aryldiazonium, diaryl iodonium, triarylsulfonium and tetra alkyl phosphonium [138]. A scheme of the photolysis of diphenyliodonium hexafluorophosphate is shown in Figure 23.

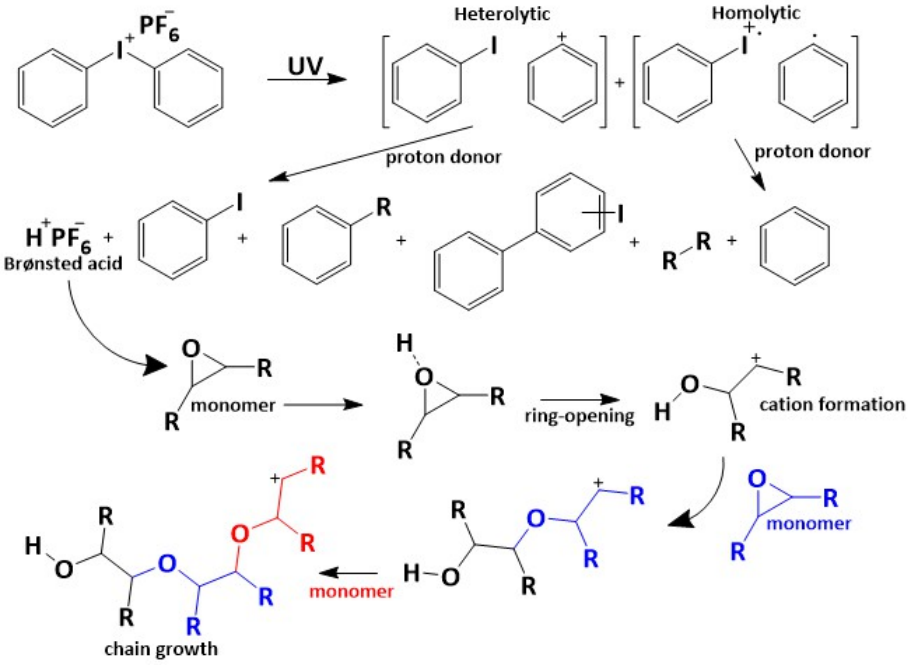

Figure 23 Photoinitiator UV decomposition and cationic polymerization [137].

The UV driven photolysis of the photoinitiator in the presence of a proton donor produces a strong acid that open the epoxy ring and generates a cation. The reaction follows the cation attacking another epoxide in the cation addition polymerization [135], [137]. From the cation formation, the reaction is dependent on temperature and not on the UV source anymore, usually referred as dark polymerization, making it a much slower process [137], [138].

Decker *et al* [136] found that the addition of epoxidized soybean oil to UV-curable epoxy resins increased the hardness, flexibility, chemical and scratch resistance of the blends. Further to that, the reduction in viscosity provided by the epoxidized soybean oil speeded up the crosslinking reaction. Dzielendziak *et al* [46] used UV-curable linseed oil to study its hygrothermal ageing in resin specimens. They showed that water uptake could be reduced in blends containing zeolites due to the reduction in voids created inside the resin during the curing process. Malmstein *et al* [45] compared the properties of epoxidized linseed and castor oils, as well as a conventional epoxy resin in glass-laminated composites. In their work, glass/epoxy and glass/castor composite panels were prepared by vacuum infusion. UV curable glass/linseed was hand laid-up due to the much higher viscosity epoxidized linseed oil has, which hinders its use in vacuum infusion. Castor oil usually has more than 90 % of its composition based on mono unsaturated ricinoleic acid [139]. On the contrary, linseed oil is rich in tri-unsaturated linolenic acid (55 %) and di-unsaturated linoleic acid (16.8 %), with amounts of mono-unsaturated oleic acid (18.4 %) [33]. The fatty acid profiles of linseed oil makes it much more viscous than epoxidized castor oil. Muturi *et al* [40] showed that soybean and linseed oils become highly viscous when epoxidized as opposed to much less viscous vernonia oil. Decker *et al* [136] showed that the propagation of a cationic polymerization is greatly affected by molecular mobility, unlike radical polymerization.

Blends cured by processes different from UV are also sought. Park *et al* [140] used heat sensitive catalysts (N-benzylpyrazinium hexafluoroantimonate and N-benzylquinoxalinium hexafluoroantimonate) to produce heat-curable epoxidized castor oils. The samples were cured at three different temperatures reaching up to 160 °C. Espinosa-Perez *et al* [141] prepared blends of epoxidized canola and soybean oil with a petroleum-based epoxy resin. The systems were cured by either amines or dicarboxylic acids. The epoxidized oils worked as plasticizers reducing T_g temperatures and mechanical properties. Samper *et al* [142] used anhydrides and obtained blends of linseed and soybean epoxidized oils, with BDMA (benzyldimethylamine) as catalyst. In both works, high temperatures were required for curing (160 °C for dicarboxylic acids and ≥ 90 °C for anhydrides) and post-curing (160 °C for anhydrides). España *et at* [104] also reported findings on the cure of epoxidized soybean oil with maleic anhydride; temperatures from 100 °C were necessary for curing.

Kumar *et at* [143] reported an improvement on T_g temperatures and tensile strength of samples prepared with petroleum-based epoxy resin with added epoxidized soybean oil. The blends were cured by methylhexahydrophthalic anhydride and 2-methylimidazole was used as a catalyst, shown in Figure 24.

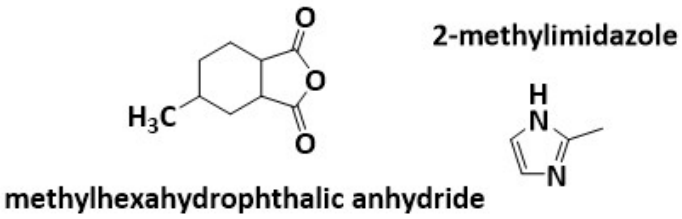

Figure 24 Chemical structure of methylhexahydrophthalic anhydride and 2-methylimidazole

Even with the catalyst addition, temperatures of 130 °C and 150 °C were used to achieve curing. Jian *et al* [144] used dicarboxylic oligomers from poly(butylene succinate) to improve the crystallinity (via X-Ray Diffraction) of epoxidized soybean oil. The higher the molecular weight of the oligomer the lower the curing rate was. The use of DMAP as a catalyst improved the rates. The longer oligomers improved crystallinity and thermal and mechanical properties. The curing process was performed at 160 °C. Zeng *et al* [145] reported that increasing amounts of DMAP (up to 3 wt.%) reduced the curing temperatures down to 172.5 °C. The catalyst was used in blends of epoxidized soybean oil and sebacic acid and other dicarboxylic acids. T_g was found at below 0 °C. Ding *et al* [101] obtained thermoset blends of epoxidized linseed oil and dicarboxylic acids with DMAP (4-dimethylaminopyridine) as a catalyst and high temperature curing (160 °C). Dicarboxylic acid containing up to 36 carbons in the structure were used. Only the ones with less than 12 carbons showed T_g temperatures above 0 °C; 0.4, 3.7 and7.0 °C for 10, 8 and 6 carbons respectively.

The results reported by Zeng *et at* [145] and Ding *et al* [101] show that long dicarboxylic acid chains reduce the T_g temperatures. Contrarily, as presented by Jian et al. [144], when the chains are long enough the molecules are able to rearrange into crystalline structures and increase T_g.

Qi *et al* [146] managed to produce a fully bio-based thermoset resin from epoxidized soybean oil. Tanic acid was used due to the high amount of phenolic hydroxyl groups in it and histidine as a catalyst. Though temperatures between 120 °C and 180 °C were used in the curing process, T_g between 54 ° and 63 °C were achieved.

Most recently Sahoo *et al* [130] used phenalkamines for curing epoxy and ELO blends, also using high post-cure temperatures (120 °C for 2 h and 150 °C for 6 h). However, our study [147] showed that post-curing samples hardened by different phenalkamines and phenalkamides at 10 °C higher

than the glass transition temperature (T_g) can be detrimental to the final elastic modulus, reducing it from 4 % to 24 %.

2.4 Summary

Many studies are being carried out in the search for sustainable materials. These materials are important but unlikely to replace the current conventional resins systems, especially for high-performance resins such as epoxy. Epoxy resins have been in the market since 1946, they are one of the best and most versatile types of resin [18]. The knowledge around epoxy formulations is so great that troubleshooting during manufacture has become easy. Therefore, new materials cannot depend only on the sustainability claim; rather they need to show comparable high-performance properties and reliability. No comprehensive work was dedicated to the synthesis of low viscosity bio-based monomers from vegetable oils for developing epoxy resins.

Chapter 3 Synthesis of low-viscosity epoxy resins derived from vegetable oils

This chapter is divided in two sections that will present the findings in the development of a low viscosity alternative for a commercially available epoxy resin synthesized with linseed oil. The epoxidation of vegetable oils increases their viscosities; therefore, the transesterification of the triglycerides into the smaller fatty acid methyl esters can produce a much less viscous product. Transesterification is used in the biodiesel industry [148]–[150], hence any findings in better transesterification routes might benefit both resin and fuel industries.

3.1 Sustainable epoxidation and transesterification of camelina, soybean and linseed oils.

3.1.1 Introduction

Camelina, soybean and linseed oils were chosen as substrates because of their fatty acid profiles. They differ between their amounts of unsaturations per fatty acid, as shown in Figure 25. The unsaturations will be epoxidized and therefore provide more functional groups for polymer chain growth and crosslinking.

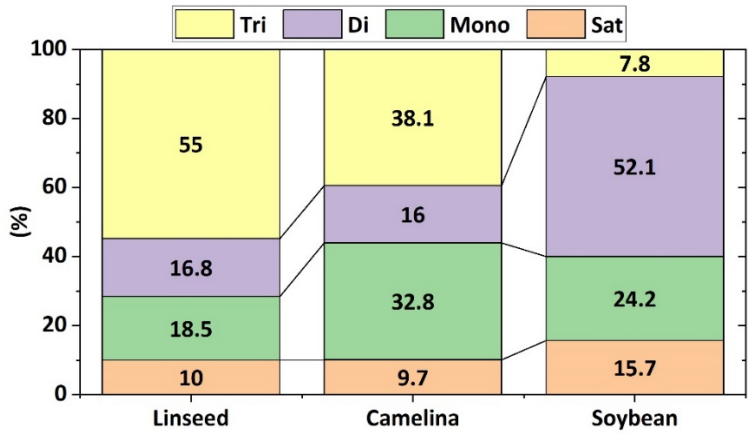

Figure 25 Fatty acid profile of soybean, linseed and camelina oils (saturated, mono-, di-, and tri-unsaturated fatty acids) [33].

The traditional epoxidation of vegetable oil is performed with peracids that are highly dangerous and toxic. Ion exchange resins show high selectivity towards epoxides, yet peracids are still used in the process. The enzymatic method is less harsh but a precise control of the reaction parameters is necessary because enzymes can be denaturated. Solid heterogeneous catalysts

such TS-1 and Ti-SiO_2 were chosen because they can perform epoxidation in much milder conditions. Unlike the methods that require peracids, diluted hydrogen peroxide (30 wt. %) is enough for the reactions. Further to that, the catalyst is able to withstand different reaction temperatures, it is easily filtered off the reaction products and can be regenerated. Acetonitrile was chosen as the solvent in several of the epoxidation reactions, either by itself or with methanol. According to the "12 Principles of Green Chemistry" [4], acetonitrile should be avoided because of its toxicity. Though at this development stage the reactions were based on the work of Wild *et al* [93]. In their work several solvents were tested and acetonitrile showed to be the best one, reaching higher reaction conversion and selectivity.

3.1.2 Experimental

3.1.2.1 Materials

The epoxidation of Soybean (SO), Camelina (CO) and Linseed (LO) oils and mainly their fatty acid methyl esters (FAMEs) were studied. The reactions were carried out using diluted (30 wt. %) hydrogen peroxide as oxidant and TS-1 as catalyst. Samples of the oils were supplied by Inovia UK, samples of Epoxidized Soybean Oil (ESO) and Epoxidized Linseed Oil (ELO) were supplied by Akcros Chemicals. TS-1 was purchased from ACSMaterials (pore size 0.56 - 0.58 nm). Ti-SiO_2 was provided by a colleague (pore size 16 nm) [151], these catalysts were used as obtained.

3.1.2.2 Substrate and products characterization

All the oils, FAMEs and respective epoxidized derivatives were characterized by Nuclear Magnetic Resonance (NMR). NMR is a highly accurate technique used for characterization and quantification of a great variety of compounds. Its use in vegetable oils and their derivatives has proved to be very reliable and easy [47], [120], [152]–[155]. The most important peaks in the spectrum are given on Table 2.

Table 2 Peaks of interest in ^{1}H-NMR spectra of vegetable oils and fatty acid methyl esters.

Peak range (ppm) [120], [153], [154]	**Structure**
1.45-1.60	(-C**H**$_2$-CHOCH-)
1.70-1.85	(-CHOCH-C**H**$_2$-CHOCH)
2.00-2.10	(-C**H**$_2$-CH=CH-)
2.80-2.85	(-CH=CH-C**H**$_2$-CH=CH-)
2.90-2.95	(-C**H**OC**H**-), (-C**H**OC**H**-CH_2-CH=CH-)
3.00	(-C**H**OCH-CH_2-CHOC**H**-)
3.06-3.24	(-CHOC**H**-CH_2-C**H**OCH-)

5.35-5.45	(-C**H**=C**H**-)
5.60-5.65	(-CHOCH-CH_2-C**H**=C**H**-CH_2-CHOCH-)
3.43-3.62	(CHO**H**-CHO**H**-)

By following the peak's variation, it is possible to obtain the conversion and selectivity of the epoxidation peaks. All the peaks of interest in the ^{1}H-NMR spectra obtained from the samples used in this work were integrated. Initially the sum of the intensity of the integrated area of all epoxide signals (A_e) was calculated, as seen in Equation (1). A_{OH} is the integrated area for the glycol groups generated after epoxide opening, $A_{C=C}$ is the integrated area of the unsaturations signal.

$$A_e = 2.90\ to\ 3.24\ ppm \qquad A_{OH} = 3.44\ ppm \qquad A_{C=C} = 5.40\ ppm \tag{1}$$

The reaction conversion (X) is then calculated using Equation (2).

$$X(\%) = \frac{A_e + A_{OH}}{A_e + A_{OH} + A_{C=C}} \times 100 \tag{2}$$

The selectivity towards epoxide groups (S_e) is obtained from Equation (3)

$$S_e(\%) = \frac{A_e}{A_e + A_{OH} + A_{C=C}} \times 100 \tag{3}$$

3.1.2.3 Epoxidation of Fatty Acid Methyl Esters over TS-1

Prior to the epoxidation reaction, the oils were transesterified via an acid catalysed transesterification. Although this process requires 24 h for completion, it becomes easier to separate the final products, as it does not generate soaps in the reaction. For the reaction, 2.5 mL of sulphuric acid was slowly added to 100 mL of methanol. This mixture was added to a round bottom glass containing 40.00 g of the oil samples at 40 °C. The reaction temperature was then raised to 60 °C and it was left to react for 24 h. After completion, the final mixture was washed with chloroform and distilled water until the organic phase reached neutral pH. Chloroform was eliminated in the rotary evaporator and the FAMEs were obtained.

For the epoxidation reaction, 1.0 g of FAMEs derived from each oil (SO, CO and LO), 1.7 g of TS-1 and 70 mL of acetonitrile were added to a 100 mL two-neck round bottom flask equipped with a condenser and rubber stopper. The mixture was placed in an oil bath and the temperature was raised to 50 °C. Then 1 mL of hydrogen peroxide (30 wt. %) was added dropwise. The reaction was carried out for 24 h and samples were taken after 1 h, 3 h, 6 h and 24 h. This procedure was based on the work of Wilde *et al* [93], [94]. Conversion and selectivities were calculated based on NMR spectra, as discussed on item 3.1.2.2.

Three other reactions were carried out with FAMEs derived from linseed oil: Blank (without TS-1), Calcined (with TS-1 used in the previous reaction which was then calcined at 550 °C for 6 h, under air flow) and Reduced TS-1 (70 % reduction in TS-1 amount). These reactions were carried out for 24 h at 50 °C with the collection of only one sample in the end. TS-1 was filtrated off and the remaining liquid phase was treated with hexane to obtain the epoxidized FAMEs in an organic layer. The organic layer was washed with distilled water to eliminate traces of acetonitrile and unreacted hydrogen peroxide. The FAMEs were concentrated in the rotary evaporator. Over 90 % of the product was obtained as Epoxidized FAMEs after the reactions.

3.1.2.4 Epoxidation and transesterification of Linseed oil over TS-1 and Ti-SiO_2

A simultaneous transesterification and epoxidation reaction was attempted based on the parameters used for the epoxidation of the FAMEs. A 50:50 volume ratio mixture of methanol and acetonitrile was used as a solvent. In the reaction, 50 mL of acetonitrile and 50 mL of methanol were added to a 250 mL two-necked round bottom flask containing 1 g of TS-1 and 2 g of linseed oil. The mixture was heated to 5 °C and then 5.5 mL of hydrogen peroxide (30 wt. %) was added dropwise. The reaction was carried out under reflux for 24 h. At the end, TS-1 was filtered off, the mixture was treated with hexane for obtaining an organic layer, which was separated and washed with distilled water. The organic phase was concentrated in a rotary evaporator. The remaining oily product was analysed by NMR spectroscopy. The reaction over Ti-SiO_2 (pore size = 16 nm) was performed in the same fashion.

3.1.3 Results and discussion

3.1.3.1 Epoxidation of fatty acid methyl esters over TS-1

The NMR spectra obtained for the samples of pure FAMEs and after 1h, 3h, 6h and 24h of reactions are shown in Figure 26.

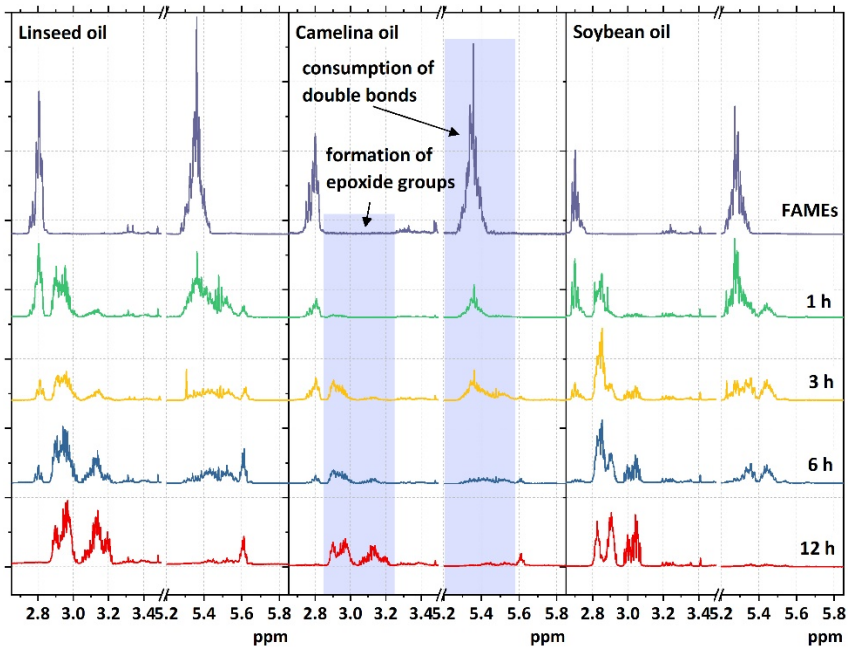

Figure 26 ^{1}H-NMR spectra of the epoxidation reactions of Fatty acid methyl esters derived from linseed, camelina and soybean oils.

From the integration values obtained from the delimited peak areas of each spectrum, it was possible to calculate the conversion and selectivities towards epoxides for the reactions. The results are shown in Figure 27.

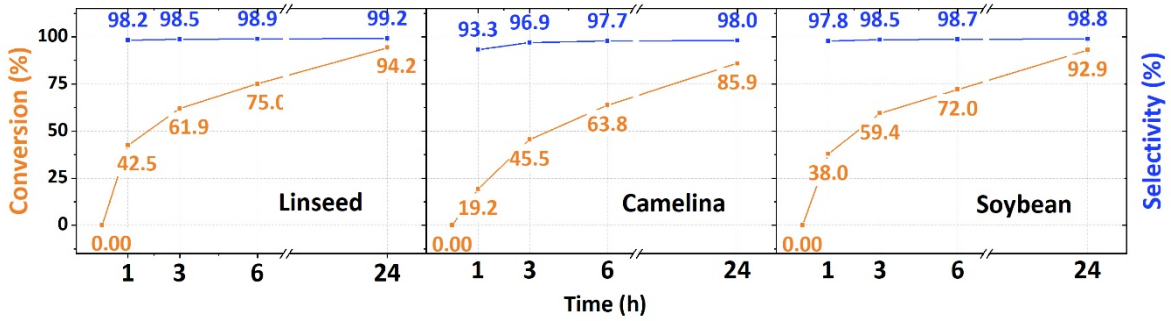

Figure 27 Conversion and selectivity of the epoxidation of fatty acid methyl esters derived from linseed, camelina and soybean oils.

All the samples resulted in high conversion and selectivities where best results were obtained from linseed > soybean > camelina oils. All the oils have similar amounts of unsaturated FAMEs: soybean (84.1 %), camelina (86.9 %) and linseed (90.3 %) [33]. The reaction rates were not related to the total amount but followed the fatty acid profile of each oil, meaning the proportions of mono-, di- and tri-unsaturated fatty acids, given in Figure 25. It was initially supposed that the epoxidation of one of the double bonds could hinder the reaction of the neighbouring ones, but on the contrary, the higher the amount of neighbouring double bonds, the higher the reaction

rate was. It appears that having a double bond readily available for the following oxidation speeds up the reaction.

Although camelina FAMEs have a high amount of tri-unsaturated fatty acids, it also has the highest amount of mono-unsaturated ones. Wilde *et al* [94] also tested a mixture of FAMEs from commercial biodiesel but reached lower yields (80 %), most likely because the biodiesel had around 72 wt. % methyl oleate (mono-) and 19 wt. % methyl linoleate (di-). Further to those reactions, the results for Blank, Calcined catalyst and Reduced amount TS-1 are shown in Figure 28.

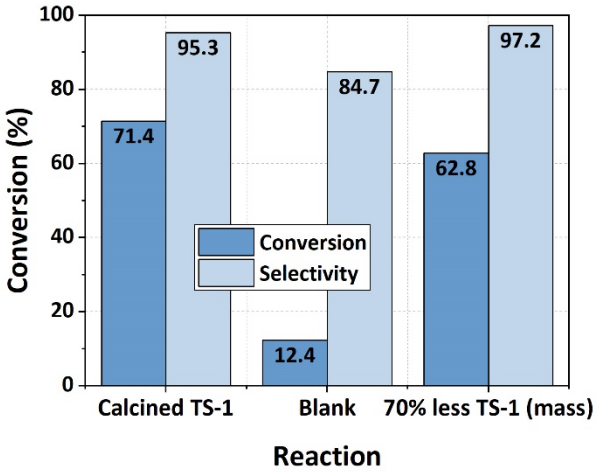

Figure 28 Further epoxidation of Linseed oil FAMEs over TS-1.

The reduction in the amount of TS-1 in the reaction by 70 % brought the conversion down to around 62.8 % showing that catalyst was initially being used in excess. Hence, the selectivity was still high. For the Blank reaction, epoxidation was still possible with a high selectivity, but the conversion was very low. That suggests TS-1 is catalysing the formation of the peroxycarboximidic acid through Payne's oxidation pathway (see 2.1.4.2). The reaction with calcined TS-1 had a lower performance, showing that the catalyst is being deactivated.

3.1.3.2 Epoxidation and transesterification of linseed oil over TS-1 and Ti-SiO_2

Unlike the FAMEs, the whole triglyceride molecules are much bigger and bulkier. In that sense, the simultaneous epoxidation and transesterification reactions were attempted over TS-1 and Ti-SiO_2.

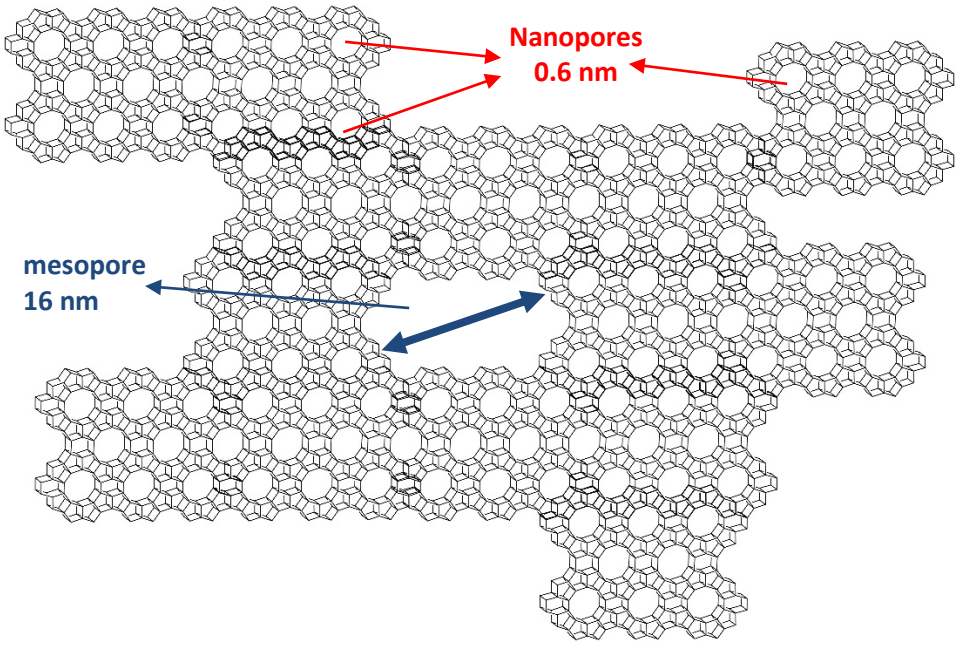

Figure 29 Representation of solid catalyst containing microporisity (TS-1) and mesoporosity (Ti-SiO_2) [156].

The results are shown in Figure 30, which shows that the epoxidation reaction reached a higher yield over Ti-SiO_2.

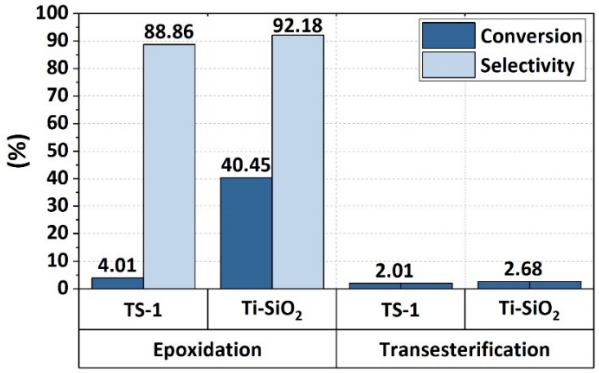

Figure 30 Transesterification and epoxidation of linseed oil over TS-1 and Ti-SiO_2.

Linseed oil molecules are much bigger than its derived FAMEs such as methyl oleate. That would explain why the conversion was ten times higher in Ti-SiO_2 which has a much bigger pore size, enhancing the diffusion of reactants. The suggested Payne's formation of peroxycarboximidic acid is not the only factor for the successful epoxidation, as pore size played an important role as well. Both selectivities were high meaning epoxides being produced are stable. Further, the epoxidation over TS-1 was around three times lower than a blank reaction fully carried out in acetonitrile.

3.1.4 Summary

Epoxidation of FAMEs over TS-1 proved to be efficient and high yields were achieved. The reaction rate indicates dependence on the profile of the fatty acids used in the synthesis. Closer double bonds accelerate the reaction speed instead of hindering it. TS-1 full regeneration was not accomplished; the results lead to the conclusion that it can be achieved, possibly by increasing calcination time. The reaction carried out without catalyst exhibited conversion of double bonds towards epoxides, much likely via Payne's oxidation pathway. The process is very slow and requires a catalyst. Therefore, TS-1 was crucial for the epoxidation. The reduction on the amount of TS-1 was detrimental to the reaction; it is shown that it is important to have an excess of the catalyst.

Transesterification reactions over TS-1 and Ti-SiO_2 were not successful. Acid catalysed transesterification is by itself a slow process, even when strong acids are used (H_2SO_4), therefore acidity might have been the main issue in the transesterification. The epoxidation nonetheless was very pronounced over Ti-SiO_2, which disregards the transesterification failure being caused by lack of diffusion of the bulky triglycerides.

Though the initial plan was to compare the mechanical properties of epoxy resins made from the three different oils (camelina, soybean and linseed), the reaction required an excess of catalyst. Producing enough amounts of epoxidized oils and FAMEs for the preparation of testing specimens was not feasible. In consequence, it was decided to change the focus to linseed oil because it has the highest amount of unsaturations and it is already been used in the market in its UV-curable version.

3.2 Transesterification of epoxidized linseed oil

3.2.1 Introduction

Although very high yields were achieved in the epoxidation of FAMEs over TS-1, the amounts obtained were very small and producing enough material for testing would not be feasible. Further to that, the heterogeneous catalysed transesterification reactions were not successful. Therefore, this section will discuss the homogeneous transesterification of epoxidized linseed oil (ELO) to obtain its epoxidized fatty acid methyl esters (TELO). This particular chosen pathway was described by Holsner [150] and is able to transesterify ELO keeping the epoxide groups.

3.2.2 Experimental

ELO was provided by Valtris Specialty Chemicals (Lankroflex L, EEW 182). Sodium methoxide (95 % reagent grade) was purchased from Sigma-Aldrich. Benzonitrile (anhydrous) was purchased from Sigma-Aldrich and used as internal standard (IS). Hexane and methanol (HPLC grade) were purchased from Fisher Scientific.

3.2.2.1 ^{1}H-NMR characterization

^{1}H-NMR has been successfully used for characterizing epoxidized vegetable oils as well as detecting traces of oxidized oil in biodiesel, due to its high accuracy [153]–[155], [157]–[159]. In this work, a Bruker AVII400 FT-NMR spectrometer (400 MHz) was used. For the procedure, benzonitrile (Sigma-Aldrich ≥ 99%) was used as internal standard (IS) and D chloroform (Euriso top 99.80% D) as a solvent.

3.2.2.2 Transesterification of epoxidized linseed oil

For a batch of TELO, 450 g of the ELO was placed in a 1000 mL glass round bottom flask with a magnetic stirrer, 150 mL of methanol was added and then 4.5 g of sodium methoxide. The reaction quickly started with a visible colour change. The flask was placed in an oil bath at 50 °C and the reaction was carried out for 3 h under reflux and stirring. The resulting mixture was placed in a separation funnel and left to cool down. Distilled water and hexane (100 mL each) were added to the mixture and the funnel was manually agitated. The emulsion-like mixture was separated by centrifuging for 15 minutes at 8500 RPM. The organic layer was separated and dried in a rotary evaporator. The yield was obtained by ^{1}H-NMR spectra, shown in Figure 31. All peaks referring to glycerol completely disappearing in the process.

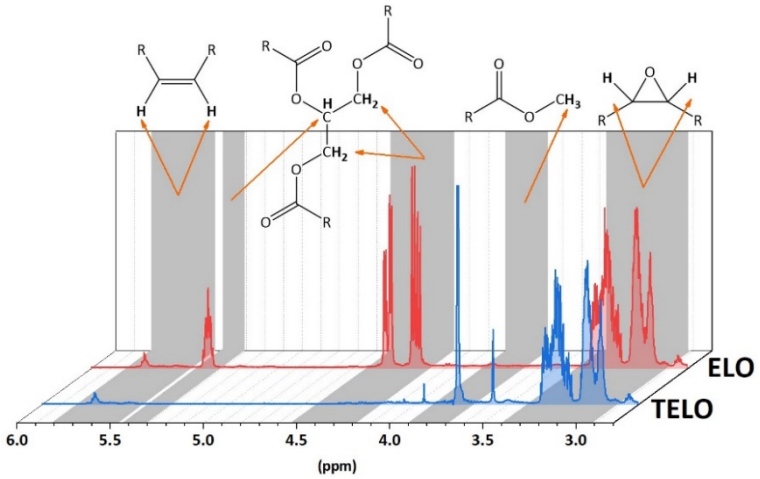

Figure 31 ^{1}H-NMR spectra of ELO and TELO.

3.2.3 Results and discussion

Epoxy resins can be characterized by their Epoxy Equivalent Weight (EEW). It determines the amount of resin (g) containing one gram-equivalent of epoxide groups [160], or per mol (g/mol) [161]. From EEW it is possible to estimate the amount of epoxy hardener (AEW - Amine Equivalent Weight) required for a stoichiometric or near-stoichiometric cure of the epoxy system [162], [163]. EEW values are usually provided by the suppliers; however, the value changes for ELO when it is transesterified to TELO, as the molecular weight changes. Based on several works [153], [155], [160], [164] a methodology to determine the EEW of the epoxidized oil and its transesterified version was developed using ^{1}H NMR. Spectra are shown in Figure 31.

With known amounts of ELO or TELO and internal standard (IS), as well as using the integrated area under each correspondent peak in the ^{1}H-NMR spectra, it was possible to determine EEW for ELO and TELO. For EEW calculations, a known amount of IS was added to every sample, which was detected on the ^{1}H-NMR spectrum recorded. The area under the peak regions for IS and epoxide groups in the spectra were obtained. The integrated peak areas ($A_{epoxide,\ IS}$) represent signals from a number of protons (n_H) in each molecule or functional group, as seen in Figure 32.

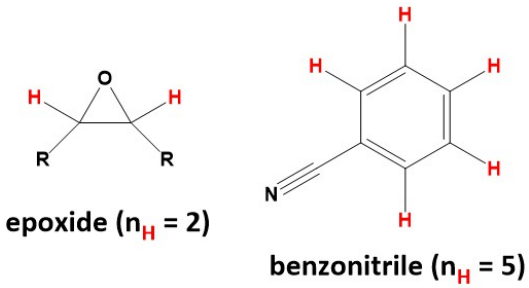

Figure 32 Number of protons (H) present in the epoxide groups of ELO and TELO and in the IS.

Hence, the peak intensity per proton (i) is obtained from Equation (4).

$$i_{epoxide,IS} = \frac{A_{epoxide,IS}}{n_{H_{epoxide,IS}}} \quad (4)$$

Further the number of moles of IS (n_{IS}) is obtained with the known mass of IS (m_{IS}) and its molecular weight (M_w) in Equation (5).

$$n_{IS} = \frac{m_{IS}\,(g)}{Mw_{IS}\,(g/mol)} \quad (5)$$

The number of moles of IS (n_{IS}) yields its respective peak intensity (i_{IS}). The number of epoxide groups ($n_{epoxide}$) is calculated using the ratio between the peak intensity generated by the epoxide groups and IS, given in Equation (6).

$$n_{epoxide} = n_{IS}\,(mol) \times \left(\frac{i_{epoxide}}{i_{IS}}\right) \quad (6)$$

It is important to note that n_{IS} stands for the number of IS molecules and $n_{epoxide}$ is the number of epoxide groups in the whole ELO/TELO sample, meaning each triglyceride can have several epoxide groups. Finally, using the sample mass ($m_{ELO,\,TELO}$), it is possible to obtain the EEW values using Equation 4:

$$EEW_{ELO,TELO}\,(g/mol) = \frac{m_{ELO,TELO}\,(g)}{n_{epoxide}} \quad (7)$$

In such a manner, $EEW_{ELO,\,TELO}$ represents the masses of ELO or TELO (g) containing 1 mol of epoxide groups.

Because of the transesterification reaction of ELO, no peak related to glycerol groups were found in TELO, seen in Figure 31. The EEW value given by the supplier for ELO was 182 g/mol and the value calculated from the ^{1}H-NMR was 172.22 g/mol. For TELO the calculated EEW was 215.16 g/mol. The epoxidized FAMEs were successfully obtained from ELO. The ^{1}H-NMR method used for determining the EEW value for ELO resulted in a similar value to the one given by the supplier. The EEW value for the epoxidized FAMEs is different because they have a different molecular weight from the triglycerides in ELO.

3.2.4 Summary

ELO was transesterified to TELO keeping its epoxide content. ^{1}H-NMR was successfully used in finding EEWs for ELO and TELO as well as tracking the transesterification reaction. The resulting epoxidized fatty acid methyl esters were used in the production of testing specimens. The EEW values were used in the blends prepared in this work.

Chapter 4 Screening of epoxy hardeners based on cashew nut shell liquid (CNSL)

4.1 Introduction

Epoxidized vegetable oils are effectively cured under UV-light with the employment of a photoinitiator [45], [46], [165]. Traditional composite and resin users benefit when a two-part system is available, as the use of UV-radiation requires specific installations. The lamps used for the curing can cause damage to unprotected skin. Epoxidized oil thermosets are obtained from bio-based hardeners [104], [111], [140], [142]–[146], [166] yet high temperatures are required. In this sense, commercial bio-based hardeners were investigated. These phenalkamines and phenalkamides are based on CNSL and used in conventional DGEBA epoxy systems, they enable cure at room temperature. This chapter will present the results found when the CNSL-based epoxy hardeners were tested against a conventional one. The conventional system comprises an epoxy resin and respective hardener obtained from the market and developed for resin infusion systems. All the hardeners used are based on amines and amides. These groups are very reactive and provide fast, room temperature curing [18]. Five different types of phenalkamine and phenalkamide hardeners were supplied by Cardolite Corporation. This screening was then performed to select one with properties closest to the properties given by the conventional hardener.

4.2 Experimental

4.2.1 Materials

A conventional epoxy infusion system was obtained from Gurit (resin PRIME 20LV and hardener FAST). The resin being based on DGEBA (2,2'-[(1-methylethylidene)bis(4,1-phenyleneoxymethylene)]bis) and hardener mainly based on 2-piperazin-1-ylethanamine. The phenalkamine and phenalkamide hardeners Ultra LITE 2009, LITE 3000, 3005, 3060 and 3100 were provided by Cardolite Corporation. The mixing ratios are given in Table 3.

Table 3 Properties of resin mixture components.

Hardener	Mix ratio resin:hardener (g)	Solids content (wt. %)	Final bio-based content (%)	Class	Hazards identification	Reference
Conventional	100:26	100	-	Cycloaliphatic, aliphatic and phenyl amines	Irritant, dangerous for the environment. R(36/38, 43, 51/53)	[167]
Ultra LITE 2009	100:55	≥ 97	24	Cycloaliphatic amine adduct and cardanol	Harmful. R20/22	[168]
LITE 3000	100:135	69 - 73	40	Phenalkamide	Harmful, irritant. R20/21, 38	[169]
LITE 3005	100:134	70	42	Phenalkamide	Harmful, irritant. R20/21, 38	[170]
LITE 3060	100:55	Solvent free	32	Polyamide and cardanol	Corrosive, irritant. R22, 34, 43, 37/38-41	[171]
LITE 3100	100:79	78 - 82	36	Polyamide adduct and cardanol	Flammable, corrosive, irritant. R20/21, 38, 34, 43, 36/38	[172]

4.2.2 Moulds preparation

In order to prepare tensile testing specimens, 3 mm polymethyl methacrylate (acrylic) sheets were laser cut to size based on specimen type 5 of ASTM D638-14 standard. Small type 5 specimens were chosen due to size and volume. They are also better suited for thermal and hygrothermal ageing [173]. Moulds were prepared with room temperature vulcanizing (RTV) silicone, purchased from EA silicones. The silicone was prepared as indicated by the supplier and degassed in a vacuum chamber to eliminate bubbles formed in the mixing process. It was then poured into a tray containing the type 5 acrylic specimens and left for 24 h at room temperature for curing. After curing, the solid silicone mould was taken from the tray and the acrylic specimens removed leaving hollow spaces for the resin. A picture of the mould is shown in Appendix A.

4.2.3 Samples preparation

The samples were prepared by thoroughly mixing the resin and the different hardeners according to the mixing ratios shown on Table 3. The mixtures were poured into the RTV silicone moulds and left to cure at room temperature for 24 h. Some samples were then post-cured in a fan-assisted oven at different times and temperatures (NPC: non post-cured, 16h60: 16 hours at 60 °C and 5h80: 5 hours at 80 °C). The conventional resin system supplier suggests post-curing at 50 ° for 16 h. Therefore, the post-curing temperatures were chosen so they would be closer to the initial glass transition temperature of the system (T_{g1} = 70 °C).

4.2.4 Hygrothermal ageing

The moisture absorption was evaluated based on ASTM D570 standard [174]. Five samples of each cured system, weighing 0.9 ± 0.1 g, were placed in distilled water at 40 °C for four weeks. Twice a week all the samples were removed from the water, dried with paper towel and weighed. The water uptake was measured by the weight change within the samples. The results were averaged and the standard deviation obtained. The Fickian water diffusion constant is obtained by finding the initial slope in the plot of percentage in weight change (%) in function of the square root of the immersion time (√ days).

4.2.5 Infrared spectroscopy

Infrared spectra were recorded in a Thermo Scientific Nicolet iS5 equipped with an iD7 device for attenuated total reflectance (ATR) spectroscopy. The ATR spectroscopy allows easy evaluation of solid and liquid samples. Each spectra is an average of 16 scans performed by the equipment from 680 cm^{-1} to 4000 cm^{-1}.

4.2.6 Gel content

The curing and post-curing processes in the epoxy systems allow the molecules to increase their crosslinking density, therefore enhancing the properties in the material and consequently their resistance to solvents [111]. Based on ASTM D 2765 standard [175], three samples of approximately 1 g were left in 15 mL of dichloromethane (DCM) for 7 days. The samples were separated from the solvent by filtration and rinsed with acetone. The remaining solid fraction was dried overnight in an oven at 65 °C. The solid fraction weight was measured in order to obtain the soluble fraction of the samples applying the following equation (8).

$$Gel\% = \left(1 - \frac{w_t - w_s}{w_s}\right) \times 100 \quad (8)$$

where w_t is the total weight of the sample before extractionand w_s is the weight of the remaining dry solids. Gel% values were averaged and the standard deviation obtained. The gel content is expected to be higher in cured and post-cured samples (samples with higher crosslinking density).

4.2.7 Density

The density of the cured samples was measured using Archimedes' principle, described in Hughes' work [176]. Five cured samples, described on item 4.2.3, were evaluated. The densities were obtained employing Equation (9).

$$d = {}^{w_s}/_{V_w} \quad (9)$$

where w_s is the sample's weight and V_w is the weight of the sample suspended in water, which denotes the water displaced and therefore the volume.

4.2.8 Viscosity

The viscosity of each system (resin + hardener) as well as each individual liquid component were assessed using a cone and plate viscometer (Brookfield CAP2000+) with a number 1 cone spindle, the temperature control set to 25.0 ± 0.1 °C. Three measurements were taken at different rotation speeds within 10 % to 90 % of the viscometer's measuring torque.

4.2.9 Mechanical testing

The elastic modulus or Young's Modulus (E) is defined by the deformation or strain a material suffers due to an applied stress, elaborated in the following Equation (10).

$$E = \frac{{}^{F}/_{A}}{{}^{\Delta L}/_{L_0}} \quad (10)$$

where F is the tensile load applied to the specimen, A is the undeformed cross section area of the specimen, ΔL is the variation in length (axial strain) of the specimen during the test and L_0 the initial length [8].

In order to compare the elastic modulus (stress/strain) of the specimens, as well as their strain at break, mechanical tensile tests were performed in an electromechanical testing machine (Instron 4204), where a tensile load was applied to the specimens until failure. In accordance with ASTM D638 standard [173], elastic modulus was calculated on axial strain range of 0.0005 to 0.0025 mm/mm. For the tests, all cross sections were measured individually. Extensometers or

strain gauges could not be used due to the specimen size; therefore, the strain was measured by the crosshead displacement.

4.2.10 Thermal analysis

Glass transition temperature (T_g) and the decomposition behaviour of the cured samples were obtained by Differential Scanning Calorimetry (DSC) and Thermogravimetric Analysis (TGA) respectively. DSC was recorded on a PerkinElmer DSC 6000 using closed aluminium pans under a 50 mL/min nitrogen flow. The samples were subject to heating from 0.0 °C to 90.0 °C, cooling from 90.0 °C to - 50.0 °C and heating again from - 50.0 °C to 90.0 °C. A rate of 20.0 °C/min was used for all three ramps. In order to obtain the T_g value, the derivative of the last curve was obtained and the peak centre was found. The software Origin 2017 (Academic) was used in the determinations. TGA was recorded in a thermal analyser TA Instruments Q600 SDT using an open alumina pan under a 50 mL/min airflow from room temperature to 650 °C at a rate of 20.0 °C/min.

4.3 Results and discussion

The blends made with hardeners LITE 3000 and LITE 3005 were not contemplated in the study because their initial curing time was much higher than 24 hours.

The results are presented as Non-aged and Aged samples. The aged samples were submitted to hygrothermal ageing as described on section 4.2.4. A representation of the samples used in this chapter is shown in Figure 33.

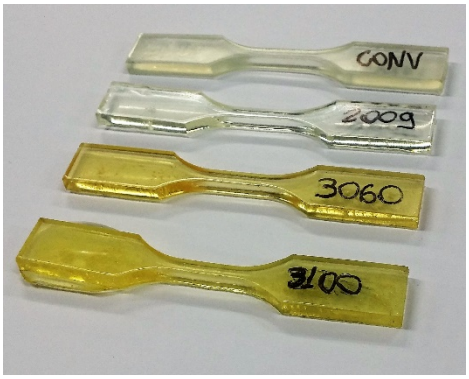

Figure 33 Epoxy blend samples based on ASTM D638-14 type 5 [173], cured by hardeners conventional, Ultra LITE 2009, LITE 3060 and 3100.

4.3.1 Hygrothermal ageing

The percentage of weight change recorded during the hygrothermal ageing is presented in Figure 34. Conventional hardener and LITE 3060 presented very similar behaviours for all the curing and post-curing conditions. Specimens cured with hardeners Ultra LITE 2009 and LITE 3100 performed differently. There was an initial water absorption but the material started to lose weight. Therefore, a different number of points were used to obtain absorption rate constants, seen on Table 4.

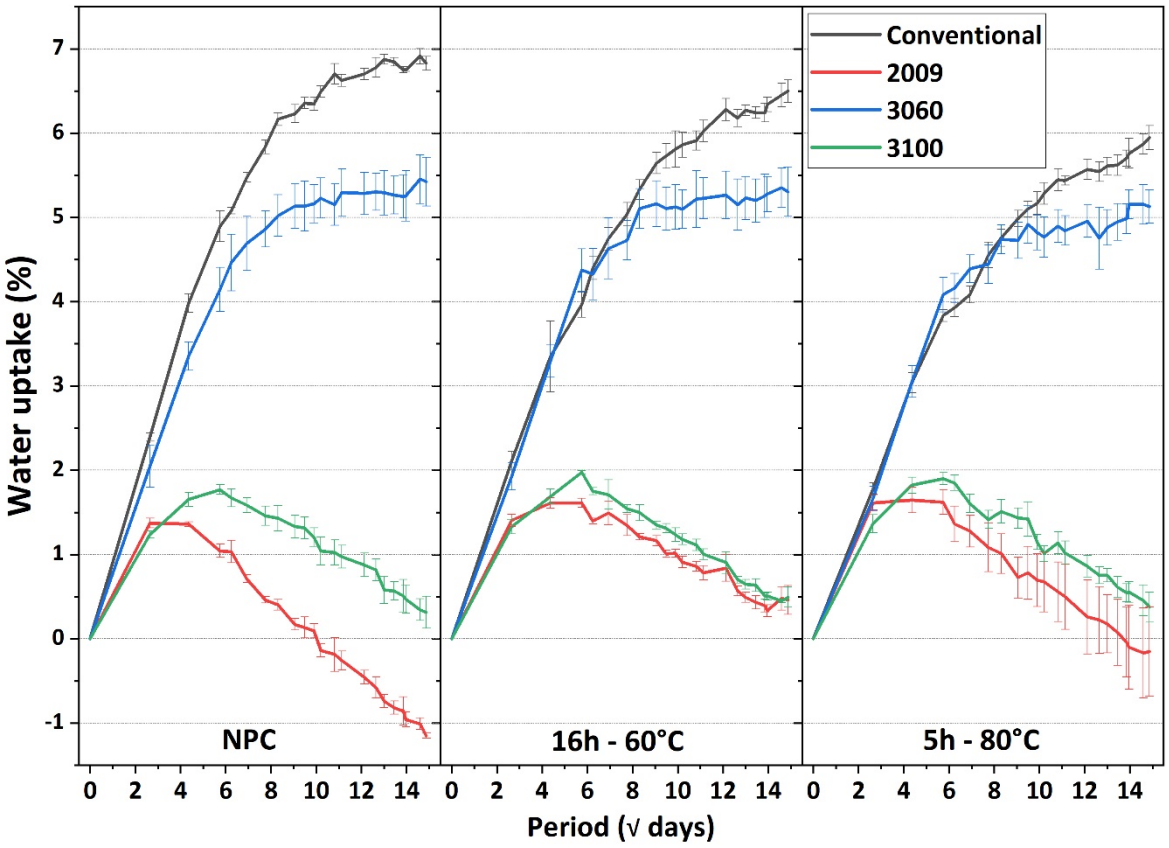

Figure 34 Mass percentage change over time (√ days).

Post-curing reduced the amount of water absorbed as well as the absorption rate for the samples cured with conventional hardener. With an exception for the specimens cured with hardener LITE 3060 (5h80), all the specimens had their absorption rate increased, indicating that the post-curing routines were detrimental to the CNSL-based hardeners.

Table 4 Diffusion constant (% weight change/ √ days) of water in samples cured by conventional and CNSL-based hardeners.

Hardener	Non-post-cured	R-square	16 h - 60 °C	R-square	5 h - 80 °C	R-square
Conventional[1]	0.8780	0.999	0.7280	0.996	0.6780	0.999
Ultra LITE 2009[2]	0.5190	1.000	0.5320	1.000	0.6100	1.000
LITE 3060[1]	0.7430	0.999	0.7560	1.000	0.6980	0.999

LITE 3100[3]	0.4030	0.991	0.4180	0.985	0.4450	0.990

Number of points in the linear fitting: [1] 4 points, [2] 2 points and [3] 3 points

Although some initial rates were higher than the ones provided by the conventional hardener, CNSL-based hardeners managed to reduce the overall water uptake. By taking the final point in the water uptake curves of conventional and LITE 3060 hardeners, the absolute reduction given by LITE 3060 for non-post-cured, 5h80 and 16h60 is respectively 1.40 %, 1.19 % and 0.82 %. The relative reduction being 20.5 %, 18.4 % and 13.7 %. These values show that both hardeners had similar water uptake reductions when post-cured for 5 h at 80 °C.

When the behaviour of these hardeners is taken into account amongst the different curing procedures, specimens cured with hardener 3060 were less susceptible to water uptake improvement. In the final data point of 3060's curves, there was an absolute reduction of 0.12 % and 0.30 % for post-cures 16h50 and 5h80 respectively. For the conventional hardener the absolute reduction was 0.33 % and 0.88 % respectively.

The cured resin obtained from the conventional hardener was highly cross-linked and required the extra heat provided by the post-curing to enable some molecular mobility and therefore curing of residual active groups. The samples cured by CNSL-based hardeners rely on the long aliphatic side chain featured in the cardanol moiety, which in turn is responsible for a more relaxed and more mobile structure, as well as natural hydrophobicity. CNSL-based hardeners did not need the post-curing process that the conventional one did to achieve low water uptake rates. Meaning that CNSL-hardeners can reduce the energy consumed in the post-curing of composites.

4.3.2 Infrared spectroscopy

In order to assess the curing state of the epoxy blends by FT-IR, spectra of liquid samples were obtained so the consumption of active groups during the curing could be tracked. These hardeners are found in the market and therefore not all their components are disclosed. Figure 35 presents the spectra from the liquid samples. Peak information are given in Table 5. Though this technique was not used in a quantitative manner, its use helps understanding the behaviour of the cured resin.

Table 5 Peaks of interest in the FT-IR of epoxy resins and hardeners [177].

Peak region	**Group**	**Intensity**	**Wavenumber (cm^{-1})**
1	Amines and amides	medium, weak	3250 - 3500
2	Amines and amides	strong, medium	1580 - 1700
3	Oxirane rings	medium	1200 - 1250
4	Oxirane rings	medium	810 - 960

Region 1 represents where medium and weak intensity peaks of amine groups are expected to appear; region 2, strong medium intensity peaks of amines and amides; region 3 and 4, medium intensity peaks of oxirane rings [177].

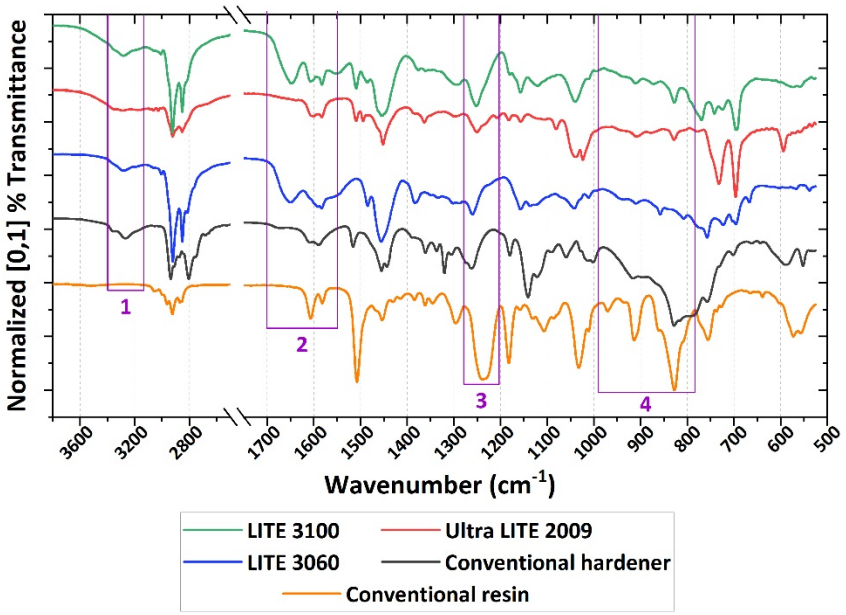

Figure 35 FT-IR spectra of liquid components used in the preparation of epoxy blends. Active groups are expected at regions: (1) and (2) for amines and amides, (3) and (4) for epoxides.

Peaks in region 1 represent primary and secondary amines and amides. When these groups become tertiary (fully cured epoxy) the signals disappear and are shown as medium (aliphatic) and strong (aromatic) peaks at around 1200 cm^{-1} and 1300 cm^{-1} respectively for amines. For amides, a strong peak appears at around 1700 cm^{-1}. Though peaks in regions 3 and 4 should not be expected for hardeners, these regions may also contain signals of aromatic groups, which are part of cardanol's structure or additives.

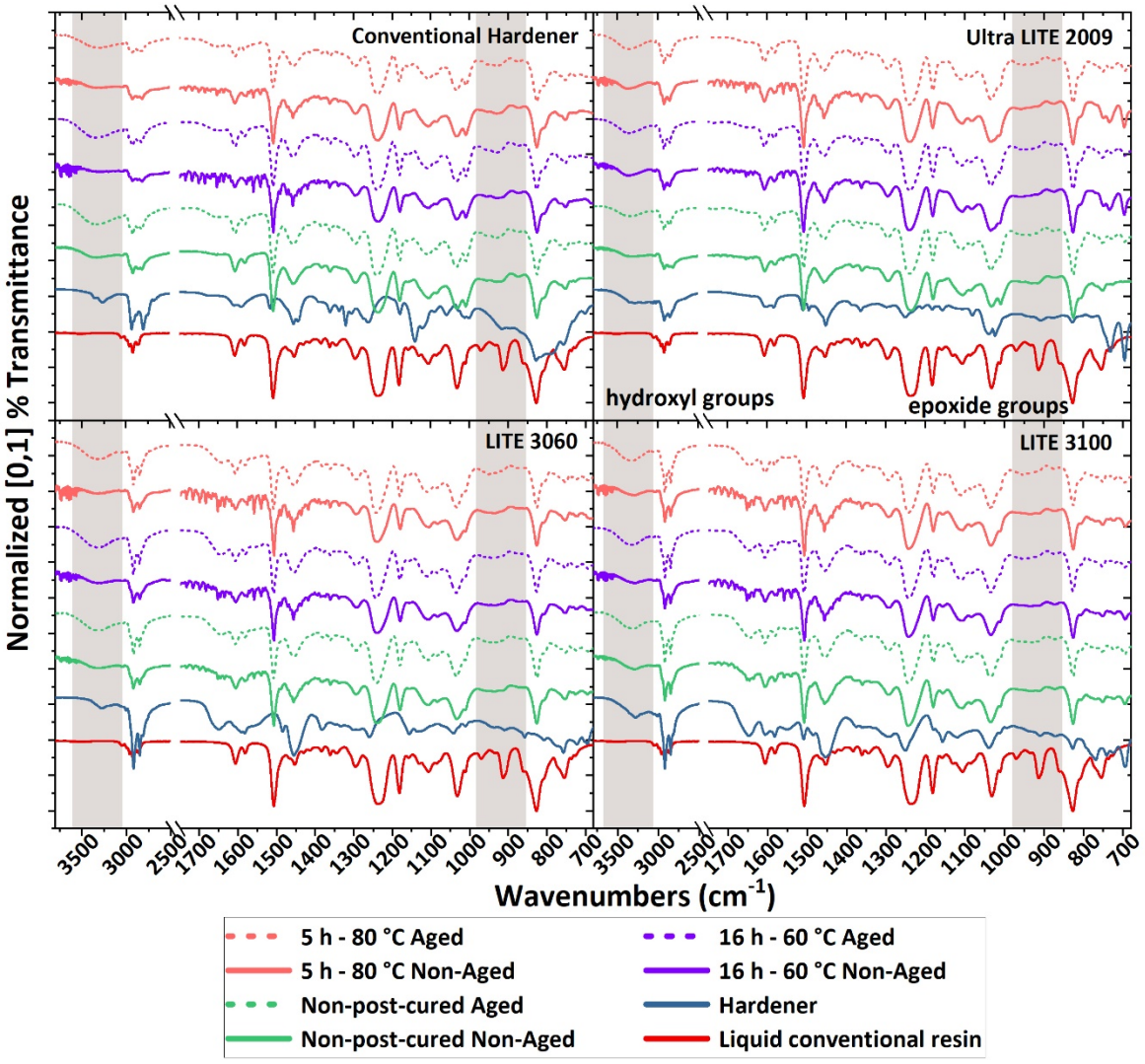

Figure 36 FT-IR spectra of cured and post-cured epoxy samples prepared with conventional and CNSL-based hardeners.

The epoxy ring-opening reaction caused during the curing process generated hydroxyl groups. Signals of these hydroxyl groups appeared as a strong and broad peak between 3100 cm^{-1} and 3500 cm^{-1}. Furthermore, the curing reaction consumed the oxirane rings, assessed by the disappearance of signals in region 3, which represents a high degree of curing.

4.3.3 Gel content

By calculating the loss in mass or the soluble content, it was possible to verify that post-curing improved the resistance to the solvent for Conventional hardener, as seen on Table 6. For the CNSL-based hardeners, due to a bigger standard deviation, it is not possible to infer that post-curing improved the resistance to the solvent.

Table 6 Gel content (solid content) of epoxy blends cured by conventional and CNSL-based hardeners.

Hardener	**Non-post-cured (%)**	**16 h - 60 °C (%)**	**5 h - 80 °C (%)**
Conventional	98.5 ± 1.16	99.8 ± 0.14	99.3 ± 0.76
2009	87.7 ± 1.02	89.5 ± 2.88	86.5 ± 1.96
3060	96.6 ± 1.86	95.9 ± 2.13	97.5 ± 2.14
3100	92.4 ± 1.39	90.6 ± 0.90	93.8 ± 1.58

The lower gel contents given by hardeners Ultra LITE 2009 and LITE 3100 are likely to be due to the washing out of the solvents/compatibilizing agent benzyl alcohol and xylene, present in the composition, see Table 7 on page 73. Hardener LITE 3060 also contains small amounts of salicylic acid that works as an accelerator [178] that is not part of the structure and can leach out.

4.3.4 Density

Density can be used as a way to assess the degree of curing. Once curing starts, the structure will shrink or expand as the molecules arrange themselves [179], [180]. Post-curing the solidified resins will eventually provide molecular mobility and allow the relaxation of the structure and further change in density by altering the overall volume. The values of density are shown in Figure 37.

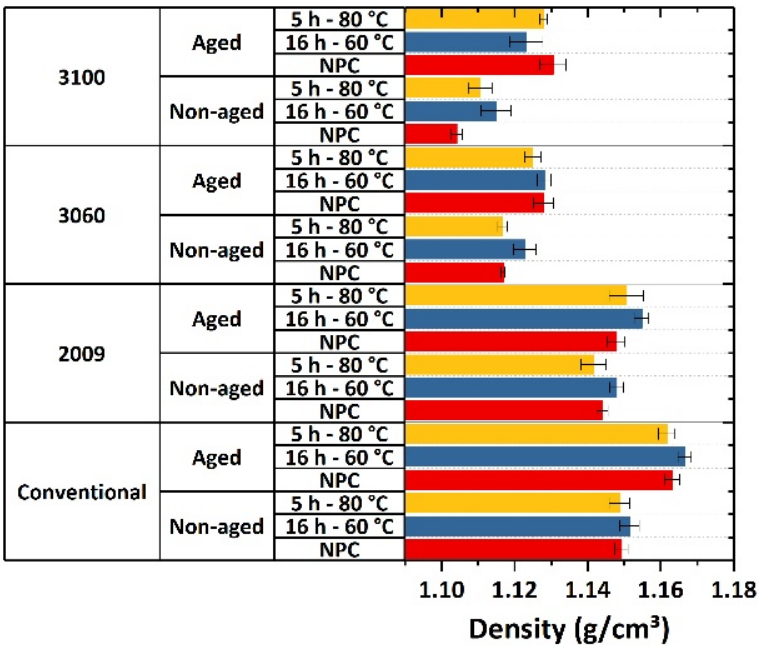

Figure 37 Density of cured and post-cured epoxy samples prepared with conventional and CNSL-based hardeners.

The aging process caused all the samples to absorb water and swell. CNSL-based hardeners are much bulkier than the conventional one because it carries the long cardanol structure within. It works by reducing the overall density by increasing the structure volume. That explains why conventional hardener resulted in a denser material. Hardener Ultra LITE 2009 is the one with the least amount of additives, which in turn contains heavier molecules that increase the system's mass.

4.3.5 Viscosity

Another important aspect on the curing of epoxy resins is the viscosity because it influences the molecular mobility and therefore low viscosity systems are not only likely to yield better materials because it allows a higher crosslinking density, they can better interact with the substrate where applied. Low viscosity epoxy resins can fill small imperfections and increase adhesiveness [18].

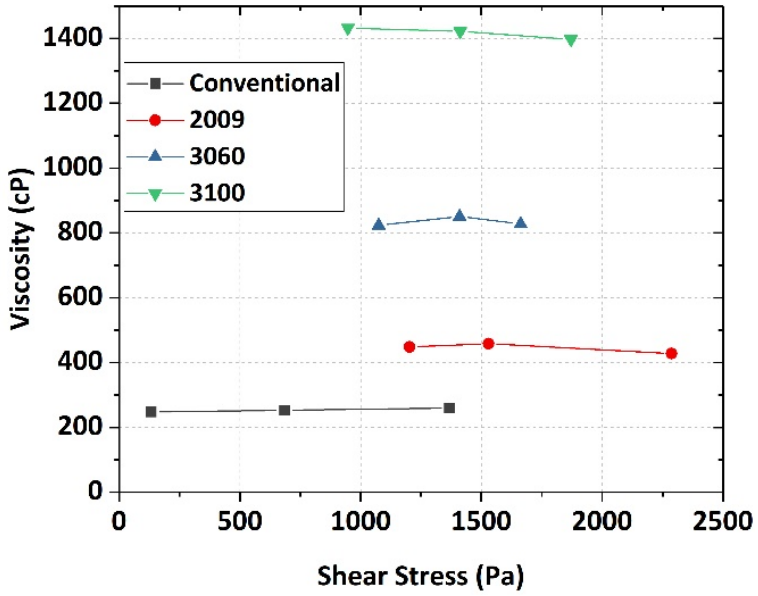

Figure 38 Viscosity of epoxy blends with conventional and CNSL-based hardeners.

According to Strong [41], viscosity is the single most important aspect of a resin system for infusion. It should range between 50 and 1000 cP. In that sense, hardener LITE 3100 would be over the infusion threshold. The viscosities found might be connected with the presence of additives in the composition of the hardeners. Hardener Ultra LITE 2009 has the largest amount of solvent/compatibilizing agent and therefore does not require additives to accelerate the curing reaction. As the viscosities increases, additives are added to accelerate curing speeds.

4.3.6 Mechanical testing

Stress versus strain curves of the aged and unaged samples are presented in Figure 39. Unaged samples cured by the conventional hardener managed to withstand similar loads regardless of the curing and post-curing processes used. The strain to failure was increased when post-curing was applied, giving a slightly less brittle material and decreasing the elastic modulus. Blends cured by hardeners Ultra LITE 2009 and LITE 3060 had their ultimate strength diminished when post-curing was employed, unlike LITE 3100, which had the ultimate strength almost doubled.

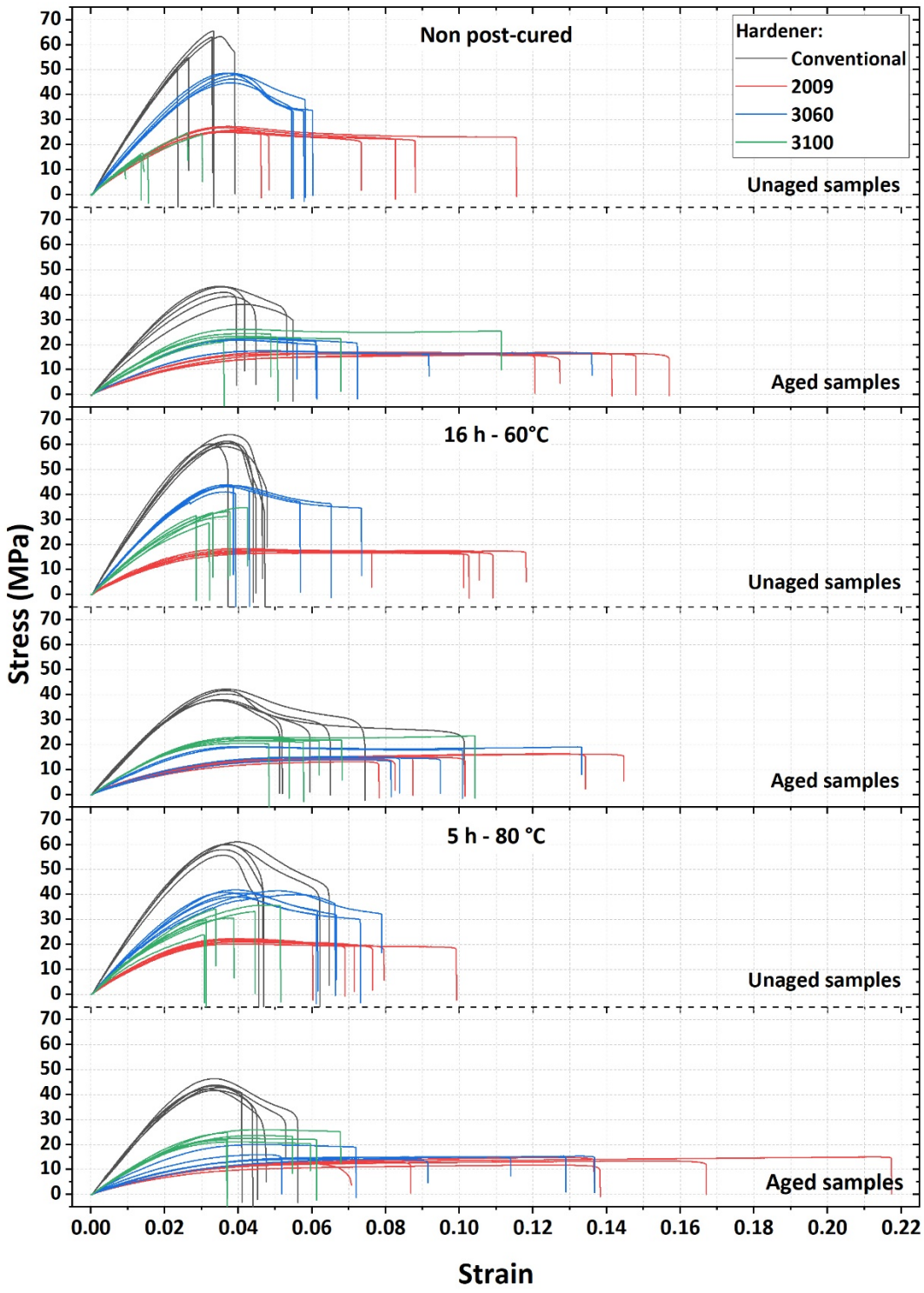

Figure 39 Stress vs Strain curves of aged and unaged epoxy blends.

Although the non-post-cured samples hardened by LITE 3100 improved their strengths after ageing, the extension at break was also increased which reduced the overall elastic modulus. Elastic moduli are shown in Figure 40.

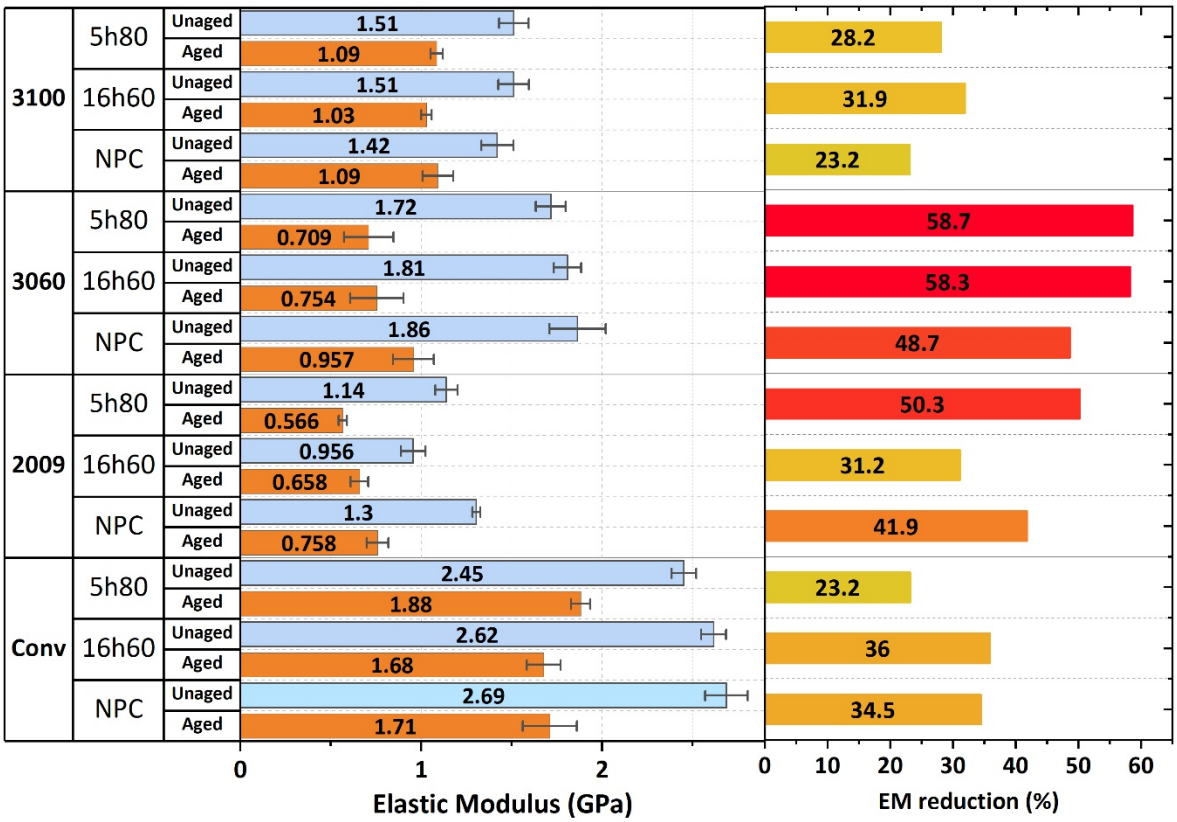

Figure 40 Elastic Modulus of aged and unaged epoxy/CNSL blends.

Aged samples cured by Ultra LITE 2009, LITE 3060 and 3100 also had their elongation at break increased. A great loss of mechanical properties is evidenced in terms of elastic modulus, particularly for hardener LITE 3060. According to the suppliers, hardeners Ultra LITE 2009 and LITE 3100 are adducts while LITE 3060 and Conventional are not. These types of hardeners are modified versions of amines or amides that preliminarily react with epoxide groups. Such modification is performed to increase the molecular weight of the hardeners, which reduces the volatility and increases the curing speed. Due to the addition of epoxide groups, the amine active groups are spread further apart, reducing the crosslinking density and increasing flexibility [18].

Nonetheless, the additives presented in each hardener composition might play an important role in the overall mechanical properties, mainly based on the types of amine present (primary, secondary and tertiary) [124], [126], listed in Table 7 on page 73.

Table 7 Types and proportions of additives in the hardeners.

Hardener	**Additives**[1]		**Proportion (%)**[1]
Conventional	2-piperazin-1-ylethylamine	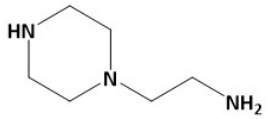	50 - 100
	4-tert-butylphenol	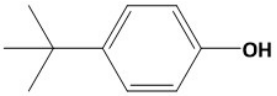	10 - 25
	m-phenylenebis(methylamine)	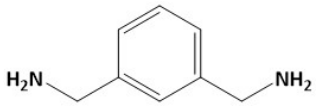	2.5 - 10
	trimethylhexane-1,6-diamine	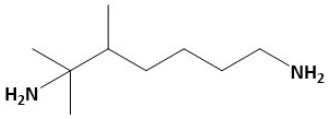	2.5 - 10
Ultra LITE 2009	benzyl alcohol	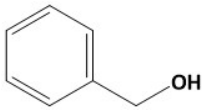	31 - 37
LITE 3060	1,3-cyclohexanedimethanamine	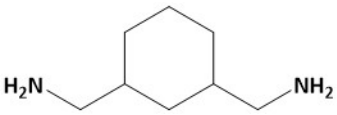	5 - 9
	3-aminopropyldimethylamine	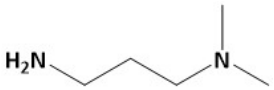	3 - 8
	salicylic acid	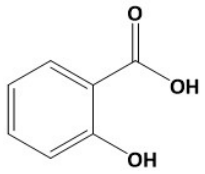	1 - 3
LITE 3100	xylene	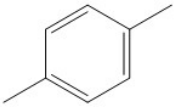	18 - 21
	m-phenylenebis(methylamine)	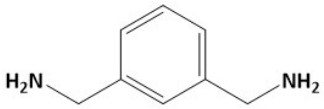	2 - 5
	2,4,6-tris(dimethylaminomethyl)phenol	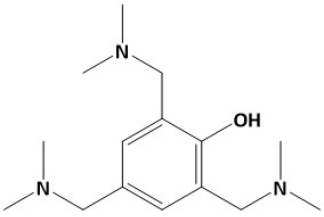	< 1.5

[1] According to information in the materials safety sheets.

Conventional hardener is a non-adduct that contains the highest amount of primary amines, which gives the systems a very high crosslinking density as well as resulting in a brittle material. Hardener LITE 3060 is not an adduct and has less primary amines than the conventional one, hence it has cardanol in its structure whose aliphatic side chain provides flexibility. Hardeners LITE

3100 and Ultra LITE 2009 are adducts and differ in the additives, the amine in LITE 3100 helps increase the crosslinking density and therefore the mechanical properties.

Overall, non-adducts performed better than adducts in terms of elastic modulus. The longer distance between amine active groups in the adducts combined with cardanol's long aliphatic side chains make these systems less resistant to high loads but it adds and/or increases the strain energy to failure. It creates a resisting and damage tolerant material, yet becoming too flexible.

4.3.7 Thermal analysis

4.3.7.1 Differential Scanning Calorimetry

Finding a polymer T_g is complicated because the thermal gradients used in the material's processing is stored within its structure. The amorphous/crystalline morphology of the polymer changes with temperature. Even with the routines of curing and post-curing, active groups are left unreacted and will be consumed further in the polymer's lifespan. Figure 41 shows the DSC curves of non-aged samples. On the first ramp, it is possible to see that along with a change in the heat capacity there are endothermic peaks. These peaks represent the absorption of heat by the polymer, which allow the polymer to relax and have its molecules rearrange in a crystalline way. Once the samples are cooled down (second ramp) and reheated (third ramp) these peaks disappear and only the change in heat capacity is shown. This change is then used to obtain the T_g temperatures.

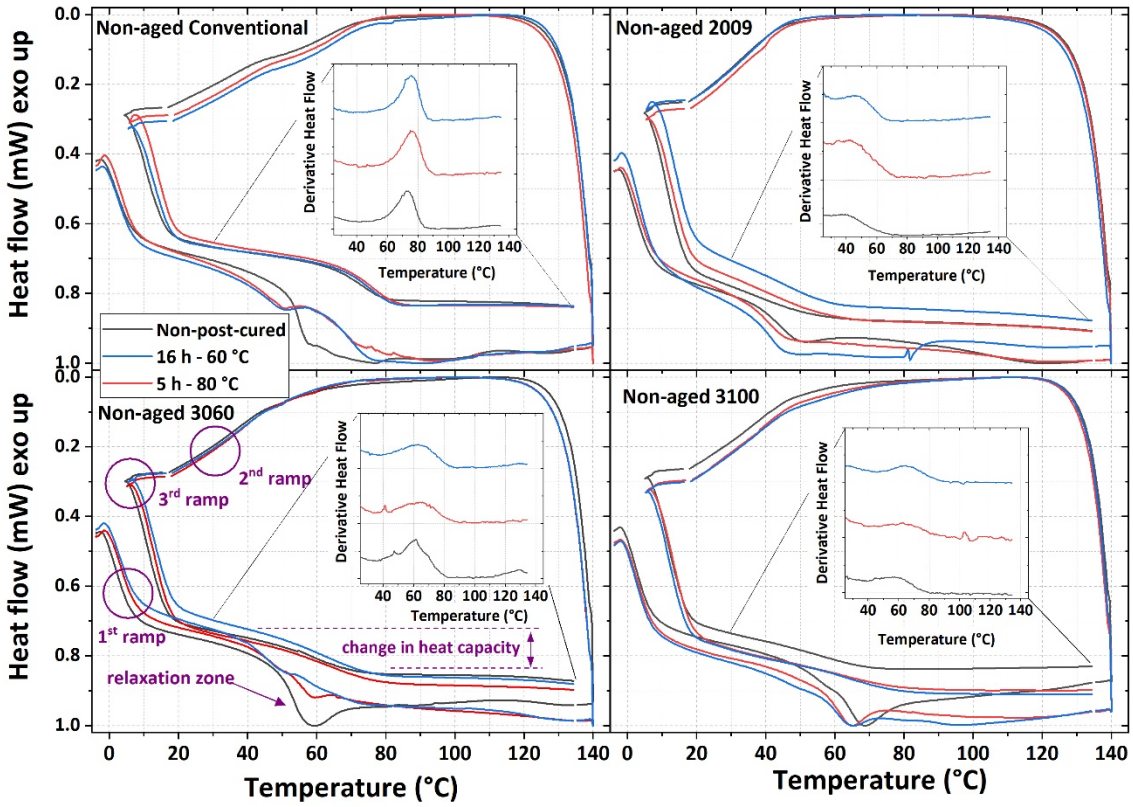

Figure 41 DSC curves of non-aged epoxy blends cured with conventional and CNSL-based hardeners.

The DSC curves for the aged samples are shown in Figure 42. There was a shift in the T_g peak temperature to a higher temperature. T_g is highly dependent not only on formulation but in the degree of curing of a certain polymer. Epoxy resins are thermosetting materials which, by their crosslinking nature, are less susceptible to glass transition [181]. During the curing process the molecular mobility is reduced, unreacted monomers left behind will cause molecular rearrangement when the polymer is reheated.

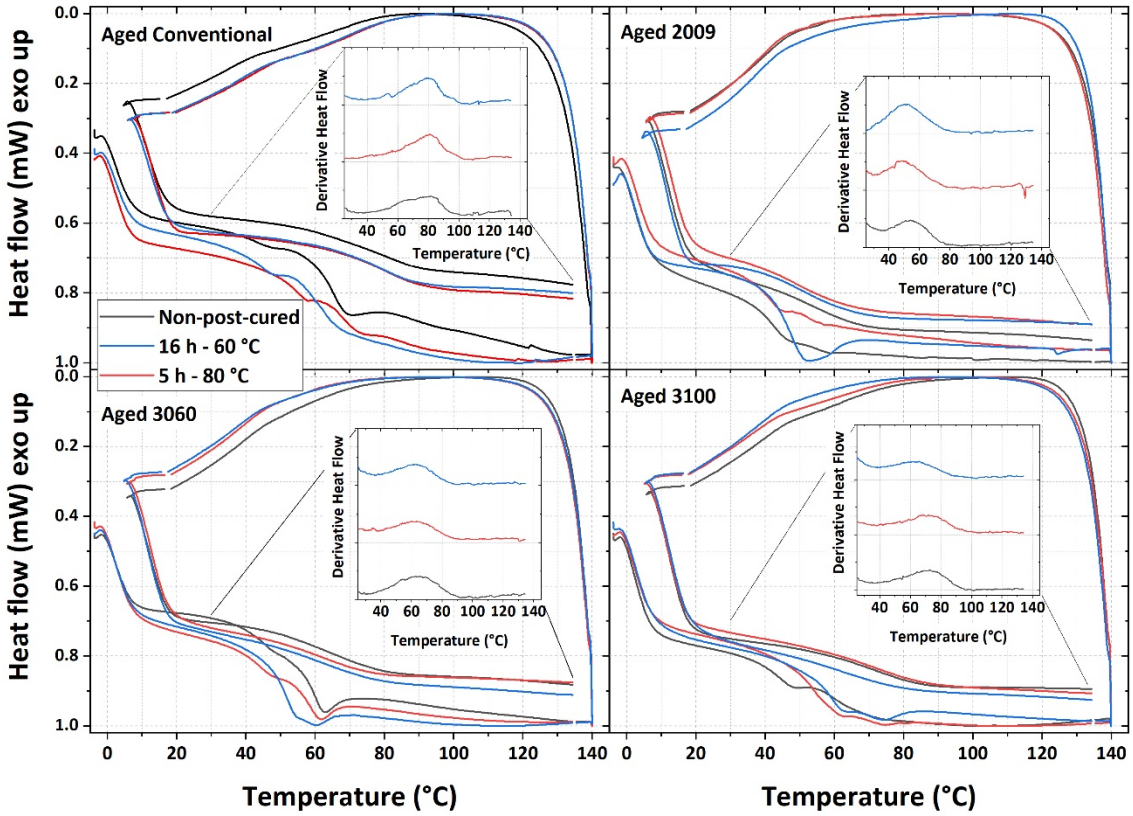

Figure 42 DSC curves of aged epoxy blends cured with conventional and CNSL-based hardeners.

In this work's scenario, the samples were aged at 40 °C for a period of 7 months. Apart from hardener LITE 3060, the ageing process improved all glass transition temperatures. The T_g temperatures are shown on Table 8

Table 8 Glass transition temperatures (T_g) of aged and non-aged epoxy blends cured with conventional and CNSL-based hardeners.

Hardener	Non-aged Non-post-cured (°C)	Aged Non-post-cured (°C)	Non-aged 16h60 (°C)	Aged 16h60 (°C)	Non-aged 5h80 (°C)	Aged 5h80 (°C)
Conventional	73.0	81.6	75.7	79.7	75.0	81.0
2009	37.3	54.0	44.3	52.0	42.3	49.0
3060	62.0	66.0	63.0	62.6	64.3	63.3
3100	57.0	73.0	64.7	66.0	62.6	68.0

From the T_g temperatures it is clear to see how the addition of extra primary amines improved the temperatures in the timeframe evaluated. Hardener Ultra LITE 2009 presented a very low T_g due to lack of additives and for the rubbery and flexible structure given by cardanol's aliphatic chain. Longer curing and post-curing times would eventually improve the T_g, for instance aged and non-post-cured 3100 samples achieved the same T_g as non-aged and non-post-cured conventional ones.

4.3.7.2 Thermogravimetric analysis

The thermal stability and degradation of the samples were evaluated by TGA. The loss of mass is shown in Figure 43. The samples presented different curves before ageing which tended to become similar with the aging process. Hardener Ultra LITE 2009 had an initial loss of mass that is also seen after ageing but in a smaller amount. Hardener LITE 3100 initially presented a higher degradation temperature that was reduced after ageing.

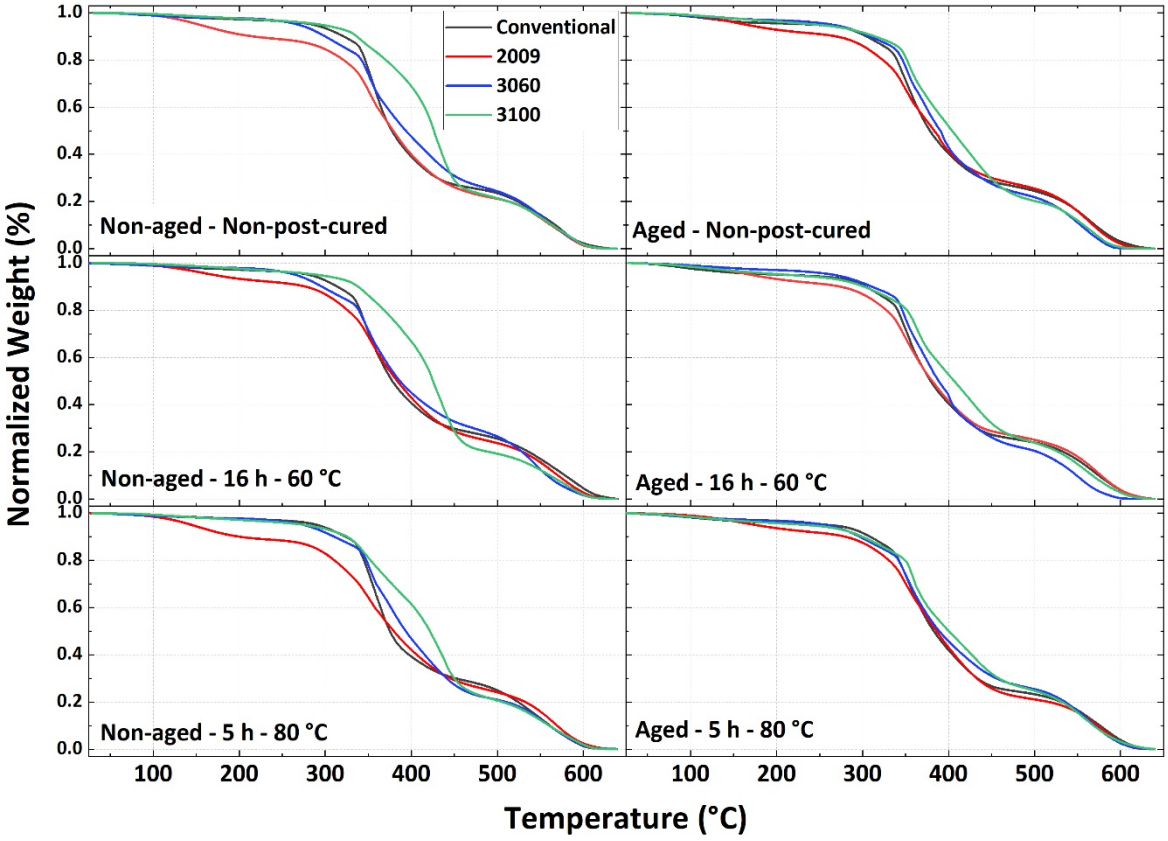

Figure 43 Thermal degradation curves of epoxy samples cured with conventional and CNSL-based hardeners.

Around 20 % of all samples were left as char that was finally degraded at final temperature. In order to assess the degradation temperatures, the derivative of the degradation curves was obtained, shown in Figure 44.

The initial mass loss shown by the specimens cured with hardener Ultra LITE 2009 is evidenced at around 160 °C. This hardener contains benzyl alcohol in the composition (boiling point 205.5 °C) [182]. Studies evaluated the atmospheric oxidation of benzyl alcohol but it happens under room temperature with the presence of radical OH or O_3 [183], [184]. Xylene in turn would be a solvent to evaporate at an approximate temperature (boiling point around 140 °C) [182], however there is no mention of it being part of this hardener's composition. Xylene is part of hardener LITE 3100 but its evaporation was not detected.

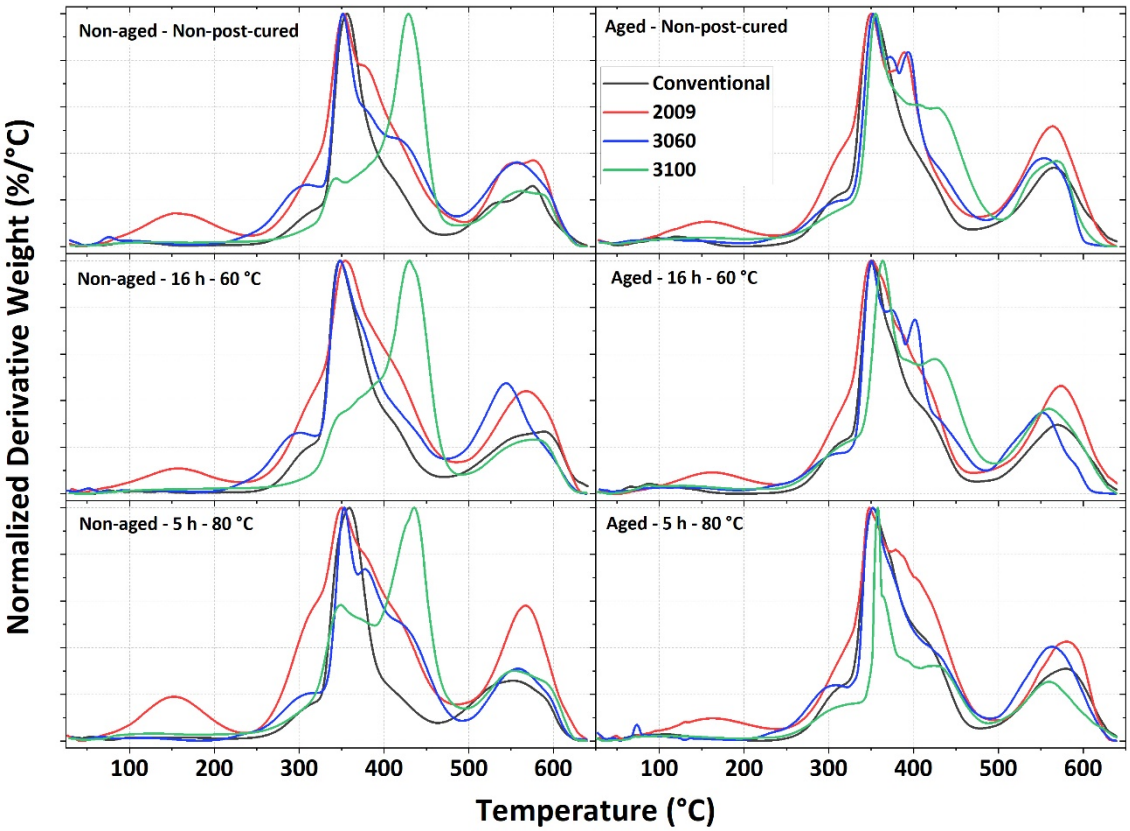

Figure 44 Derivative of degradation curves obtained from epoxy samples cured with conventional and CNSL-based hardeners.

Hardener LITE 3100 presented a change in the decomposition behaviour after ageing. The main decomposition peaks were shifted to lower temperatures, from around 430 °C to 358 °C. Such behaviour is specially noted for the aged sample post-cured for 5 h at 80 °C. There is a shoulder formation indicating this shift started in the non-aged samples and progressed further with higher post-curing temperatures. All hardeners also presented an extra shoulder at around 300 °C.

4.4 Summary

In the attempt to find the most comparable CNSL-based hardener to the conventional one, CNSL-based hardeners proved to be more resistant to water absorption when compared to the conventional one. Although LITE 3060 absorbed similar amounts of water to conventional, the amounts remained comparable and independent of the post-curing used. Unlike LITE 3060, conventional hardener needed post-curing to reach a reduction in water uptake. Hardeners Ultra LITE 2009 and LITE 3100 showed the best water uptake reduction, but there was mass loss tendency during the aging process.

Infrared spectroscopy showed a high and comparable degree of crosslinking amongst all samples due to the consumption of the oxirane rings in the epoxy systems. Furthermore, the differences in

gel content demonstrates that the curing and post-curing procedures were able to provide a highly cross-linked structure in the materials. The differences found are due to the nature of each hardener and do not imply that the material is under-cured.

In terms of density and viscosity, hardener Ultra LITE 2009 was closer to the conventional. The viscosity of hardener 3060 was high yet found to be within the infusion threshold. Notwithstanding, if the mechanical properties are taken into account, LITE 3060 properties are better than the other CNSL-based counterparts are. Even though there was a great loss in elastic modulus for 3060 after post-curing, the values were still higher than 2009. Hardener LITE 3100 showed good mechanical and T_g properties but its viscosity is over the infusion threshold and it would be impossible to obtain comparable composites specimens had they been done.

Considering these results, hardeners LITE 3060 was chosen for further study in the interaction with epoxidized linseed oil.

Chapter 5 Blends of epoxidized linseed oil cured by CNSL-based hardener.

5.1 Introduction

This section will present the findings from the preparation and analysis of epoxy blends, prepared epoxidized linseed oil and its transesterified version (fatty acid methyl esters). An attempt to cure ELO with CNSL-hardeners was performed and the results are found in Appendix B. The samples had to be cured in the oven at 220 °C to be able to get minimally hardened. Further to that, attempts using succinic acid as cross linker/acid catalyst were performed and found to be unsatisfactory, see Appendix D.

As discussed in section 3.2. The nature of the epoxide groups in ELO and TELO are less reactive than in conventional epoxy resins. In this sense, to be able to obtain solid samples feasible for tensile testing, conventional epoxy resin was employed in the blends. Hardener LITE 3060 was chosen based on the tests reported in 3.2.

5.2 Experimental

The epoxy blends were formulated by replacing 30 % of the epoxide content in the conventional resin by epoxide groups from ELO or TELO, shown on Table 9. Bio-based contents were estimated by the amount of ELO and TELO (as 100 % bio-based) added to the blend. The bio-based content present in hardener LITE 3060 was taken from its safety data sheet [171]. Conventional epoxy resin for vacuum infusion (ConvR) and hardener (ConvH) were provided by Gurit (EEW = 170, resin:hardener ratio = 100:26). The blends shown on Table 9 were calculated with EEW values obtained from ^{1}H NMR.

Table 9 Composition of resin blends for 100 g of conventional resin.

Sample	ELO (g)	TELO (g)	Conventional hardener (g)	LITE 3060 hardener (g)	Bio-based content (%)
ConvR - ConvH	-	-	27	-	0
ConvR - ELO - ConvH	44.8	-	32.5	-	25.3
ConvR - TELO - ConvH	-	53.8	32.5	-	28.9
ConvR - LITE 3060	-	-	-	55	32.3
ConvR - ELO - LITE 3060	44.8	-	-	68.8	48.5
ConvR - TELO - LITE 3060	-	53.8	-	68.8	50.6

All blends were thoroughly mixed and placed in a vacuum chamber to eliminate the bubbles formed during the manual stirring. Then they were poured onto RTV silicone moulds (ASTM D638 type 5 shape) comprising approximately 1.5 mL each. Samples were left for initial curing at room temperature for 24 h with following post-cure at 60 °C for 24 h in a fan-assisted oven.

5.2.1 Degree of cure - Fourier-Transform Infrared spectroscopy

Many works have used FT-IR for tracking the consumption of epoxide groups during the curing process of epoxy resins [101], [157], [185]–[187]. In FT-IR spectra of conventional epoxy resins, peaks at 1237 cm^{-1} and 1030 cm^{-1} can be used to assess the epoxide function. They are related to ether groups in general; hence, they can overlay oxirane ring signals. Peaks at 913 cm^{-1} and 863 cm^{-1} are less sensitive to this condition and are usually used to determine the presence of oxirane rings. Further, the broad region between 3550 - 3200 cm^{-1} is used to assess the presence of hydroxyl groups that are formed from the epoxide ring opening.

Spectra of liquid and cured samples were recorded in a Thermo Scientific Nicolet iS5 infrared equipped with an iD7 device for attenuated total reflectance (ATR) spectroscopy spectrometer. In order to avoid resin blends to cure in the spectrometer window, the spectra of all individual components were taken separately and the blend spectra was calculated proportionally to each component in the final blend, see Table 9 on page 81.

5.2.2 Viscosity

A Brookfield CAP 2000+ (spindle 1) was used to measure viscosity of all individual resins and hardeners as well as their blends, listed on Table 9, at 25.0 ± 0.1 °C. All measurements were taken at three different shear stresses (kPa) and the obtained viscosities (cP) were averaged. The three shear stress set values were not the same for all measurements; they were adjusted so the spindle spinning torque would fall between 10 % and 90 % of the equipment's limits.

5.2.3 Density

The density of the cured samples was measured using Archimedes' principle, described in Hughes' work [176]. Three cured samples, described on item 4.2.3, were evaluated. The densities were obtained employing Equation (11).

$$d = {}^{w_s}/_{V_w} \qquad (11)$$

Where w_s is the sample's weight and V_w is the weight of the sample suspended in water, which denotes the water displaced and therefore the volume.

5.2.4 Mechanical testing

Tensile testing was performed on an Instron 5569 tensometer based on ASTM D638 standard, using type 5 specimens [173] at a displacement speed of 1 mm/min. The stress/strain plots were obtained and the elastic modulus was calculated. Due to the small specimen size, extensometers were not used.

5.2.5 Thermal analysis

Differential Scanning Calorimetry (DSC) curves were recorded in a thermal analyser Discovery DSC from TA Instruments. Flakes of each sample were analysed using aluminium pans under a 50 mL/min nitrogen flow from 10 °C to 250 °C at a rate of 20 °C/min. Glass transition temperatures (T_g) were estimated from the DSC curves.

5.3 Results and discussion

5.3.1 Degree of cure

Spectra of liquid and solid samples are shown in Figure 45. The peaks at 913 cm^{-1} and 863 cm^{-1} regarded to the epoxide groups disappeared and there was a formation of a broad peak in the hydroxyl region, between 3550 cm^{-1} and 3200 cm^{-1}.

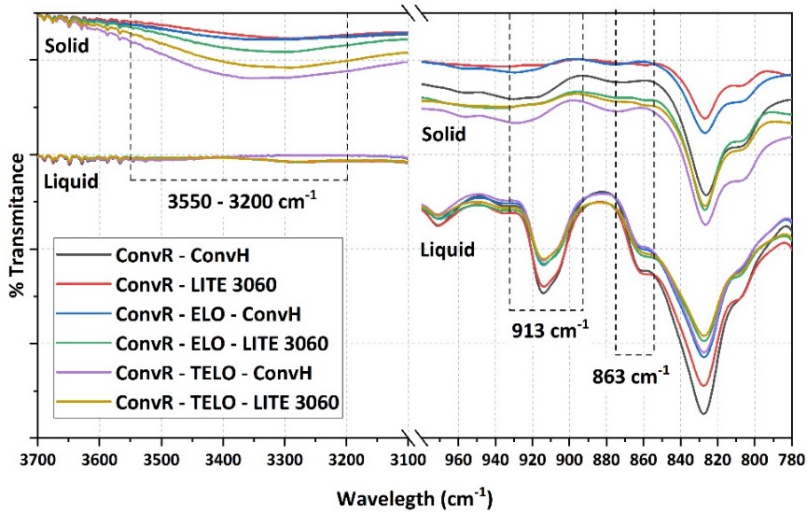

Figure 45 Normalized [0, 1] FT-IR spectra of liquid epoxy blends and respective solid cured samples.

The cure and post-cure cycles were sufficient for a full consumption of the epoxide groups in all samples, even with ELO and TELO in the composition, despite them being less reactive due to their internal epoxide positioning. Hardeners based on amines and amides (ConvH and LITE 3060)

can readily react with the terminal epoxides of ConvR but are not reactive enough for the internal ones in ELO and TELO, hence many works cited above used high temperatures. Internal epoxides are nonetheless prone to ring opening in acidic conditions, via cationic polymerization [46], [140]. Furthermore, according to Shechter *et al* [122], the presence of hydroxyl groups generated in the crosslinking, acts as a catalyst speeding up the reaction. The blends in this work had both types of epoxide groups (internal and external), and the curing reaction appears to have started in the highly reactive external epoxides. This generated hydroxyl groups that further enabled the crosslinking reaction to extend to the internal epoxides, depicted in Figure 46 and based on the findings of Shechter *et al* [122].

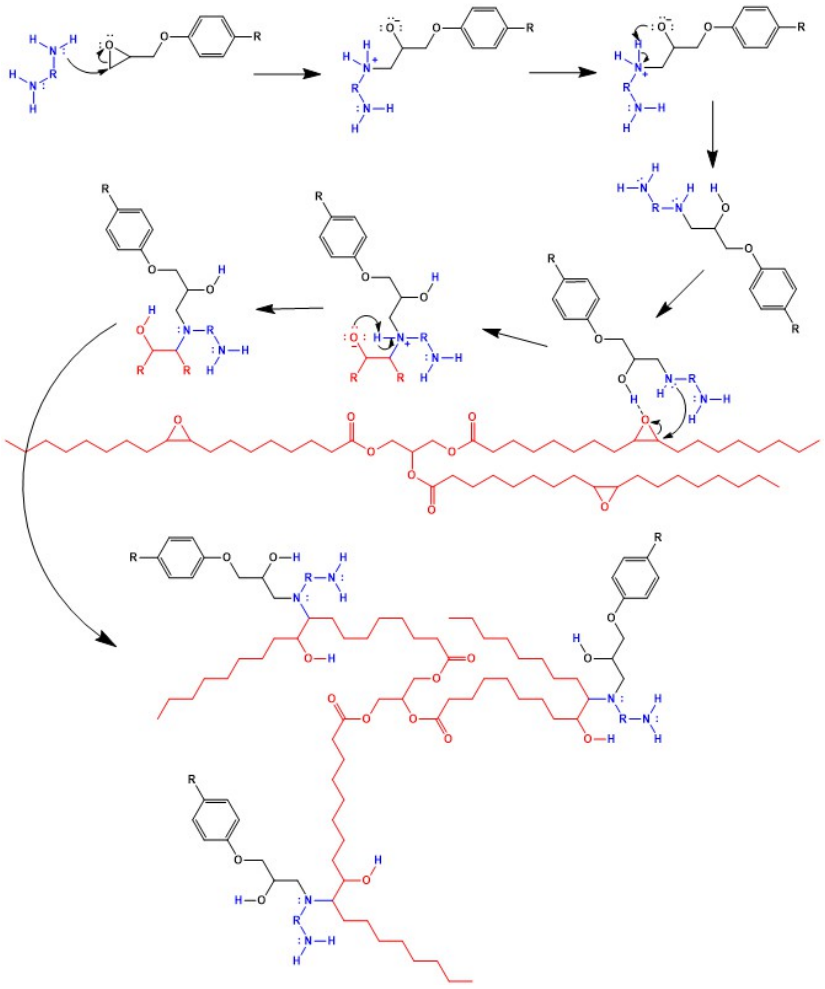

Figure 46 Proposed internal epoxide ring-opening by amines/amides facilitated by hydroxyl groups created in the reaction of terminal epoxides and amine/amide [122].

5.3.2 Viscosity measurements

Viscosity measurements of each independent component and respective mixtures are given in Figure 47. Conventional hardener has a lower viscosity than what the viscometer was able to measure in the used setup. ELO and hardener LITE 3060 have viscosities over the resin infusion

limit of 1000 cP [41], yet all the blends that contained them kept their viscosities within the threshold.

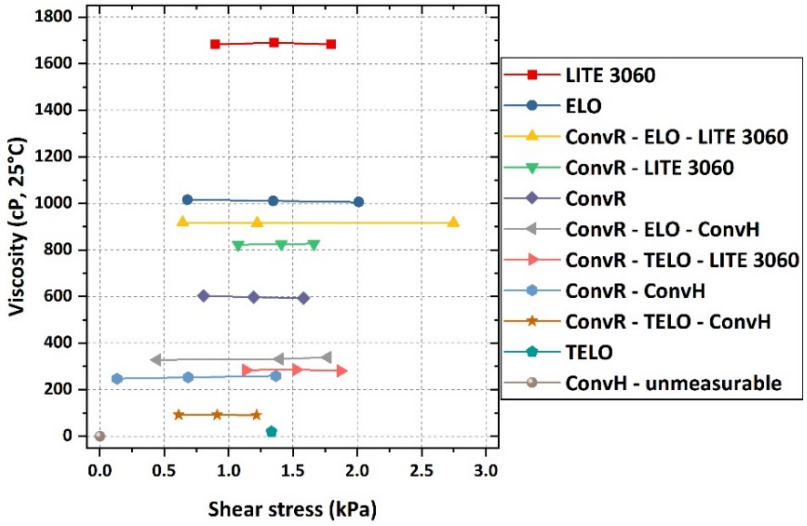

Figure 47 Viscosity measurements of individual components and mixtures.

TELO's viscosity was measured at the lowest torque limit (torque = 10.73 %), given its low viscosity, which is a characteristic of fatty acid methyl esters [188]. Both ConvH and TELO functioned as diluents, reducing viscosity when applied. Contrarily hardener LITE 3060 increased the system's viscosity in all the blends where it was employed.

5.3.3 Density

The density of the cured samples is shown in Figure 48. The conventional system is the one presenting the higher density, especially due to its degree of crosslinking and tight structure given by the small amine compounds in its composition.

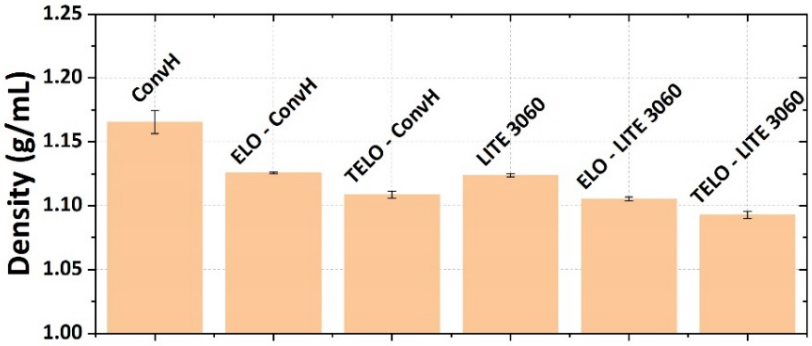

Figure 48 Density of epoxy and ELO/TELO samples, cured with CNSL-based and conventional hardeners.

Once bulkier molecules are added, such as ELO, TELO and LITE 3060, the density decreases. Dzielendziak *et al* [46] reported the formation of cavities in UV-curable epoxidized linseed oil specimens.

5.3.4 Mechanical testing

Best results were found when ConvH and LITE 3060 hardeners were employed solely with ConvR, with a loss of maximum tensile load for LITE 3060. ConvH comprises small molecules (Table 7) which allow a fast and highly cross-linked material. LITE 3060 is not only bulkier but also highly viscous, which in turn resulted in a material with higher extension at break. The same behaviour was evidenced in all of the other blends, shown in Figure 49. Hardener LITE 3060 increased extension at break when applied in conjunction with ELO and TELO. It has a long aliphatic side chain, a feature of cardanol-based materials [110], [113], that can decrease the crosslinking density, as well as increase extension at break.

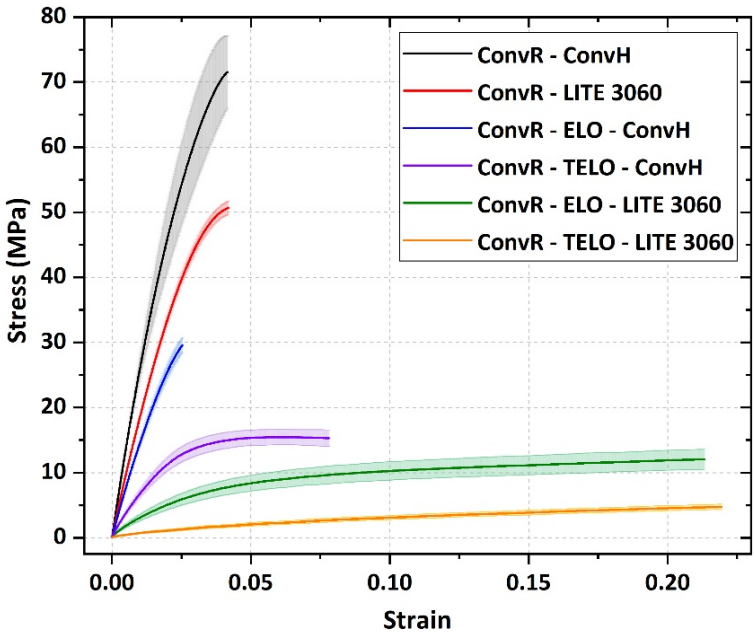

Figure 49 Averaged stress/strain curves for resin blends.

The elastic modulus, shown in Figure 50, was reduced in all applications in which a bio-based content was added, either from adding LITE 3060 or from replacing ConvR by ELO or TELO. Although hardener LITE 3060 did not yield the highest bio-based content and in fact, increased the viscosity, it had the highest elastic modulus amongst the samples with bio-based content.

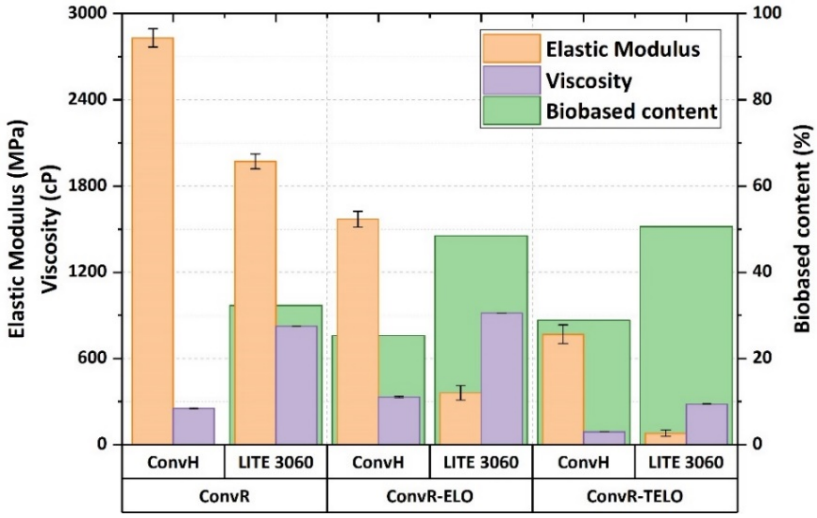

Figure 50 Elastic modulus, viscosity and bio-based content of epoxy resin blends containing bio-derived components (ELO, TELO and LITE 3060).

Unlike TELO, ELO increased viscosity in all applications. It also performed better regarding elastic modulus, which resulted in a more extension-resistant material. These results indicate that the bonding provided by the glycerol group within the triglyceride is responsible for a higher crosslinking degree, opposite to what happens with the loose mixture of fatty acid methyl esters in TELO.

5.3.5 Thermal analysis

T_g temperatures at around 40 °C are usually found in blends containing and/or fully developed with epoxidized vegetable oils [104], [157], [189], as a result of a decrease in the crosslinking density caused by the longer triglyceride and fatty acid chains. In DSC thermograms shown in Figure 51, the T_g temperatures were decreased when ELO and TELO were applied.

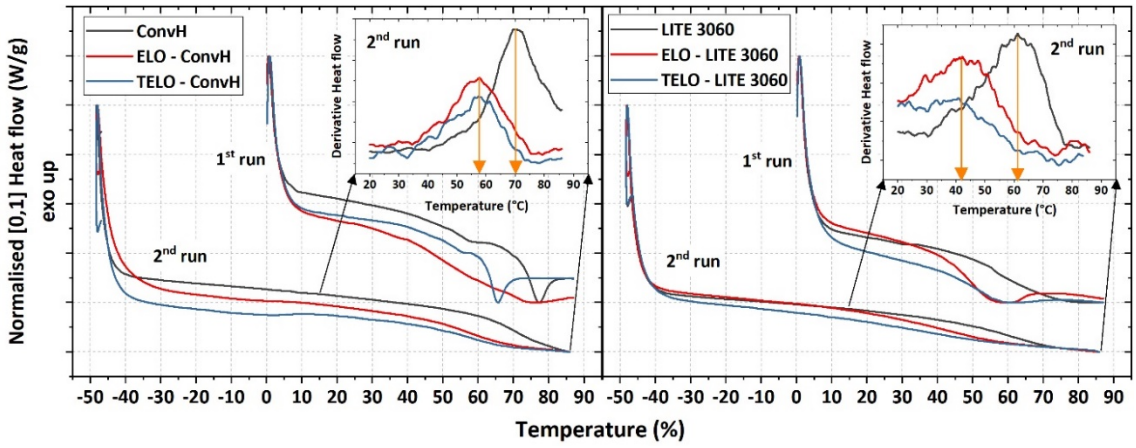

Figure 51 DSC curves of conventional epoxy resin blends containing bio-derived components (ELO, TELO and LITE 3060).

The T_g temperatures found for the samples not containing ELO or TELO are in accordance with a previous experiment whose results were reported on Table 8, on page 76. The first DSC run showed relaxation zones around the T_g temperature. These relaxation events were more intense when conventional hardener was used, except when triglycerides from ELO were in the structure. The relaxation zones were found to be less intense when LITE 3060 was applied and that is given by the long aliphatic side chain in cardanol's structure.

5.4 Summary

FT IR spectra showed that the testing specimens produced were fully cured with both internal and external epoxide groups being consumed in the process. LITE 3060 cured specimens had reduced elastic modules but had higher extension at break showing a better resistance to damage. ELO increased viscosity, however in some cases, due to its bulk molecules and thus lower crosslinking degree, it reduced the T_g. TELO functioned oppositely to ELO giving high crosslinking degree and very low viscosity, both increasing extension at break.

The blends containing the conventional hardener performed better in terms of mechanical properties but lacked in bio-based content. TELO managed to reduce the viscosity but the absence of the glycerol moiety that connects the three fatty acids reduced the mechanical properties.

Chapter 6 UV-curable epoxidized linseed oil

6.1 Introduction

This section will discuss the comparison between the mechanical properties given by ELO and TELO in mixtures containing different proportions of them. A UV-curable epoxidized linseed oil (UV-L) was chosen as base for the production of specimens. This way no photoinitiator needed to be sought.

6.2 Materials and method

UV-curable epoxidized linseed oil (UV-L) was supplied by Sustainable Composites Ltd. Epoxidized linseed oil (ELO) was purchased from Naturally Thinking. TELO was obtained from the transesterification of ELO (described in item 3.2 - Transesterification of epoxidized linseed oil). Test specimens were prepared by mixing UV-L and ELO or TELO in different weight proportions (5 %, 10 %, 20 %, 30 %, 40 % and 50 %). The mixtures were degassed in a vacuum chamber to eliminate bubbles and then poured into silicone moulds (see item 4.2.2 - Moulds preparation, page 60). A UV chamber was prepared to cure the test specimens comprising four UV lamps, pictures of the rig are shown in Appendix E. The silicone moulds containing the liquid mixtures were placed in the UV chamber and irradiated for 1 h. The samples were taken from the mould, flipped, placed on a grid and irradiated for another 30 minutes. Further to that, they were post-cured for 16 h at 35 °C in a fan-assisted oven.

6.2.1 Hygrothermal ageing

The moisture absorption was evaluated based on ASTM D570 standard [174]. Six samples of each cured system, weighing 0.9 ± 0.1 g, were placed in distilled water at 40 °C for four weeks. Twice a week all the samples were removed from the water, dried with a paper towel and weighed. The water uptake was measured by the weight change within the samples. The results were averaged and the standard deviation used as upper and lower limits. The water diffusion constant is obtained by finding the initial slope in the plot of weight change as a function of the square root of the immersion time (√ days).

6.2.2 Infrared spectroscopy

Infrared spectra were recorded in a Thermo Scientific Nicolet iS5 equipped with an iD7 device for attenuated total reflectance (ATR) spectroscopy. The ATR spectroscopy allows easy evaluation of solid and liquid samples. Each spectrum is an average of 16 scans from 680 cm^{-1} to 4000 cm^{-1} wavenumbers.

6.2.3 Gel content

The curing and post-curing processes in the epoxy systems allow the molecules to increase their crosslinking density, therefore enhancing the properties in the material and consequently their resistance to solvents [111]. Based on ASTM D 2765 standard [175], three samples of approximately 1 g were left in 15 mL of dichloromethane (DCM) for 7 days. The samples were separated from the solvent by filtration and rinsed with acetone. The remaining solid fraction was dried overnight in an oven at 65 °C. The solid fraction weight was measured in order to obtain the soluble fraction of the samples applying the following Equation:

$$\mathrm{Gel}\% = \left(1 - \frac{w_t - w_s}{w_s}\right) \times 100 \quad (12)$$

Where w_t is the total weight of the sample before extraction, w_s is the weight of the remaining dry solids. Gel% values were averaged and the standard deviation obtained. The gel content is expected to be higher in better, cured and post-cured samples (those with higher crosslinking density).

6.2.4 Density

The density of the cured samples was measured using Archimedes' principle, described in Hughes [176]. Five cured samples were evaluated. The densities were obtained employing Equation (13).

$$d = {}^{w_s}/_{V_w} \quad (13)$$

where w_s is the sample's weight and V_w is the weight of the sample suspended in water, which denotes the water displaced and therefore the volume. The samples were hung by a thin wire whose density was subtracted off.

6.2.5 Viscosity

The viscosity of each system (resin + hardener) as well as each individual liquid component were assessed in a viscometer Brookfield CAP2000+ with a number 1 cone spindle, the temperature

control set to 25.0 ± 0.1 °C. Three measurements were taken at different rotation speeds within 10 % to 90 % of the viscometer's measuring torque.

6.2.6 Mechanical testing

The Elastic Modulus or Young's Modulus (E) is defined by the deformation or strain a material suffers due to an applied stress, elaborated in the following Equation (14).

$$E = \frac{F/A}{\Delta L/L_0} \quad (14)$$

where F is the pulling load applied to the specimen, A is the cross section area of the specimen, ΔL is the variation in length (axial strain) of the specimen during the test and L_0 the initial length [8].

In order to compare the elastic modulus (stress/strain) of the specimens, as well as their strain at break, mechanical tensile tests were performed in an electromechanical testing machine Instron 4204, where a pulling load was applied to the specimens until failure. In accordance with ASTM D638 standard [173], elastic modulus were calculated on axial strain range of 0.0005 to 0.0025 mm/mm. For the tests, all cross sections were measured individually. Extensometers or strain gauges could not be used due to the small size of the specimen.

6.2.7 Thermal analysis

Glass transition temperature (T_g) and the decomposition behaviour of the cured samples were obtained by Differential Scanning Calorimetry (DSC) and Thermogravimetric Analysis (TGA) respectively. DSC was recorded on a PerkinElmer DSC 6000 using closed aluminium pans under a 50 mL/min nitrogen flow. The samples were subject to heating from 0.0 °C to 90.0 °C, cooling from 90.0 °C to - 50.0 °C and heating again from - 50.0 °C to 90.0 °C. A rate of 20.0 °C/min was used for all three ramps. In order to obtain the T_g value, the derivative of the last curve was obtained and the peak centre was found. The software Origin 2017 (Academic) was used in the determinations. TGA was recorded in a thermal analyser TA Instruments Q600 SDT using an open alumina pan under a 50 mL/min airflow from room temperature to 650 °C at a rate of 20 °C/min.

6.3 Results and discussion

6.3.1 Hygrothermal ageing

The mass gain over time is presented in Figure 52. The samples containing ELO performed similarly unlike the ones containing TELO. With higher amounts of TELO, the water uptake was reduced.

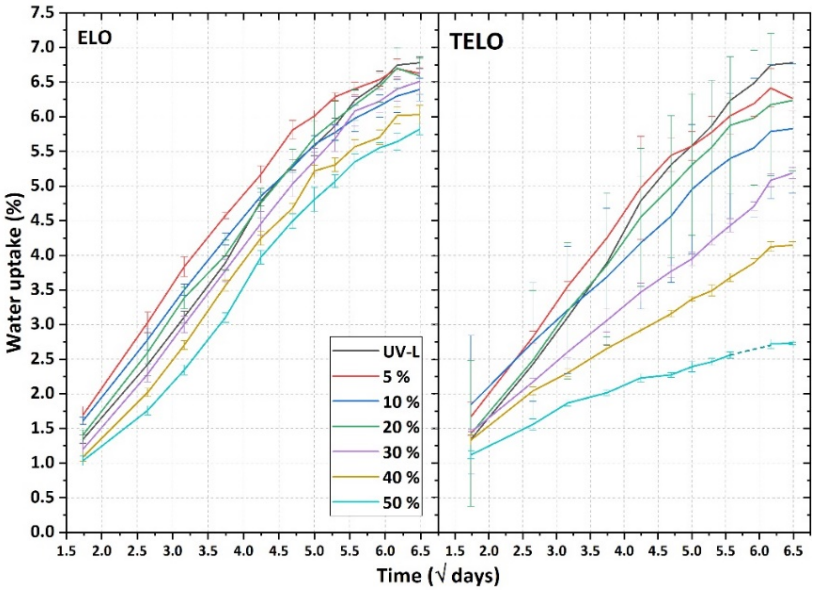

Figure 52 Water uptake of UV-L with added amounts of ELO and TELO.

The five initial data points were linearly fitted and the slopes recorded as water diffusion constant rates, shown in Figure 53. Because UV-L has a photoinitiator in it, even when stored away from light, there were moments when it was exposed and the crosslinking reaction started, which makes the polymer chains grow. For this reason, UV-L is more viscous than ELO so the more ELO is added the less viscous the mixture gets and a better degree of crosslinking is achieved due to a higher molecular mobility.

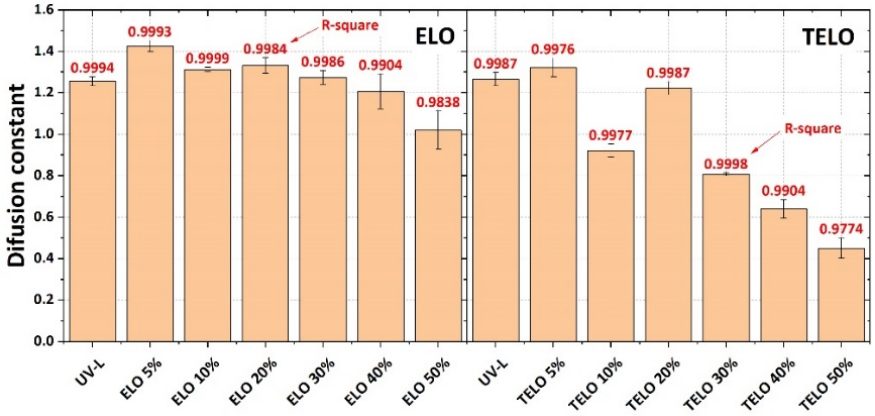

Figure 53 Diffusion constant rates of UV-L samples with added amount of ELO and TELO.

6.3.2 Infrared spectroscopy

The spectra of all the mixtures containing ELO and TELO were averaged, shown in Figure 54. The spectra of cured UV-L and of the averaged samples containing ELO and TELO are very similar, indicating that all samples are at the same stage of curing for further comparison.

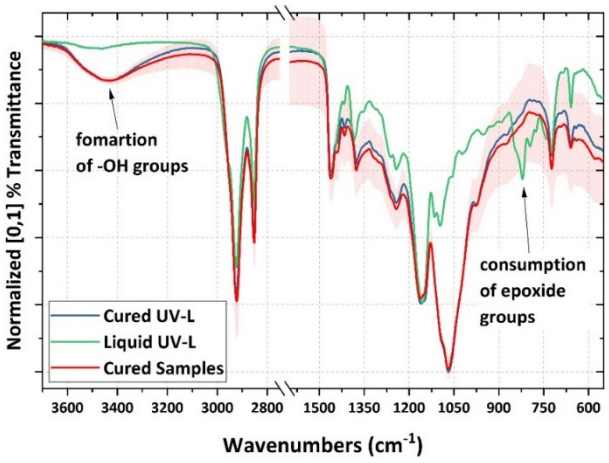

Figure 54 FT-IR spectra of liquid and cured UV-L with added amounts of ELO and TELO.

The peak corresponding to the epoxide groups in the liquid UV-L spectra was fully consumed and a broad peak of hydroxyl groups (-OH) was created. The hydroxyl groups are a result of the crosslinking reaction. The FT-IR results indicates all the samples have a high degree of curing.

6.3.3 Gel content

The solid content is shown in Figure 55. The addition of ELO improved the resistance to DCM and oppositely, the addition of TELO decreased it. Although ELO and UV-L have the same composition in terms of triglycerides, UV-L has a much higher molecular weight because even when kept away from light, crosslinking reactions are slowly happening.

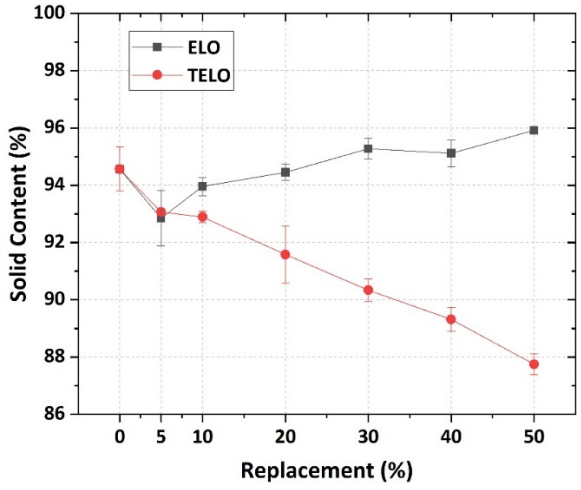

Figure 55 Solid content of UV-L cured samples with added amounts of ELO and TELO.

The addition of no cross-linked ELO decreased the viscosity and allowed a higher molecular mobility, which in turn promoted a tighter cured structure and was therefore more resistant to the solvent. The absence of the glycerol moiety in TELO makes the structure looser and more prone to the solvent attack.

6.3.4 Density

The densities of UV-L specimens cured with ELO and TELO are shown in Figure 56. The samples containing from 30 % replacement had the non-aged density very similar to the aged samples. The densities diminished in all cases and it was due to the swelling ratio of the specimens. There was a gain in mass from the absorption of water but the gain in volume by swelling was higher.

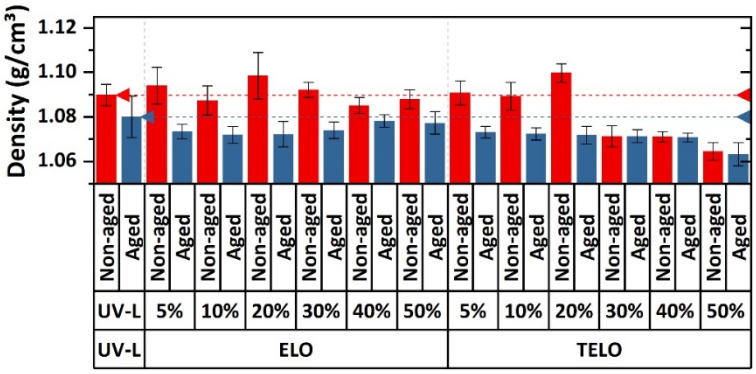

Figure 56 Density of aged and non-aged samples of UV-L cured with ELO and TELO.

The variation in volume and mass is given in Appendix G. Further to that. The swelling caused cracks in the specimens, shown in Figure 57.

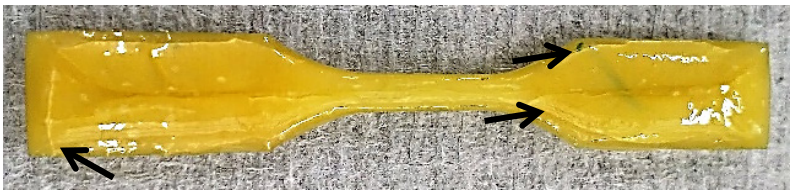

Figure 57 Crack formation in a UV-L aged sample.

6.3.5 Viscosity

The viscosity of the UV-L replacement mixtures is given in Figure 58. The addition of TELO decreased the viscosity values drastically. ELO has a viscosity close to the infusion threshold and the same chemical structure of UV-L (triglyceride). Hence, the reduction in viscosity is smaller.

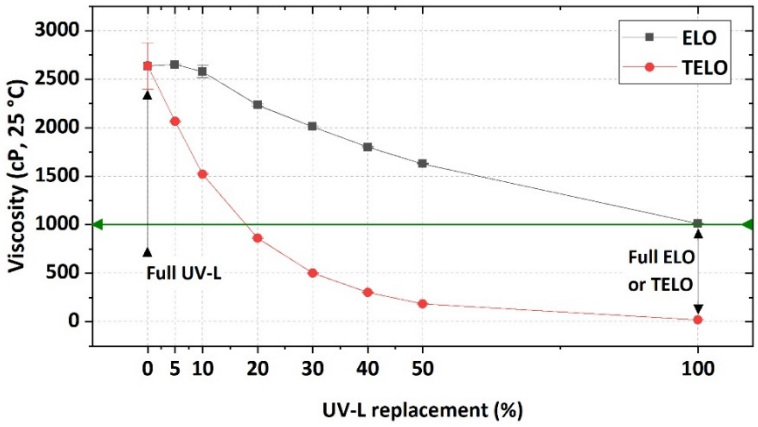

Figure 58 Viscosity of UV-L with replacements by ELO and TELO.

6.3.6 Mechanical properties

The stress *vs* strain curves of samples containing different amounts of ELO and TELO are shown in Figure 59. The blends containing ELO mantained the mechanical properties closer to UV-L. The increase of ELO amounts initially reduced the elastic modulus but increased again from 40 % UV-L replacement. The elastic modulus values are shown in Figure 60.

After the hygrothermal ageing process the majority of the samples had their elastic modulus reduced. The very low elastic modulus of samples containing the highest amounts of TELO showed the smallest changes.

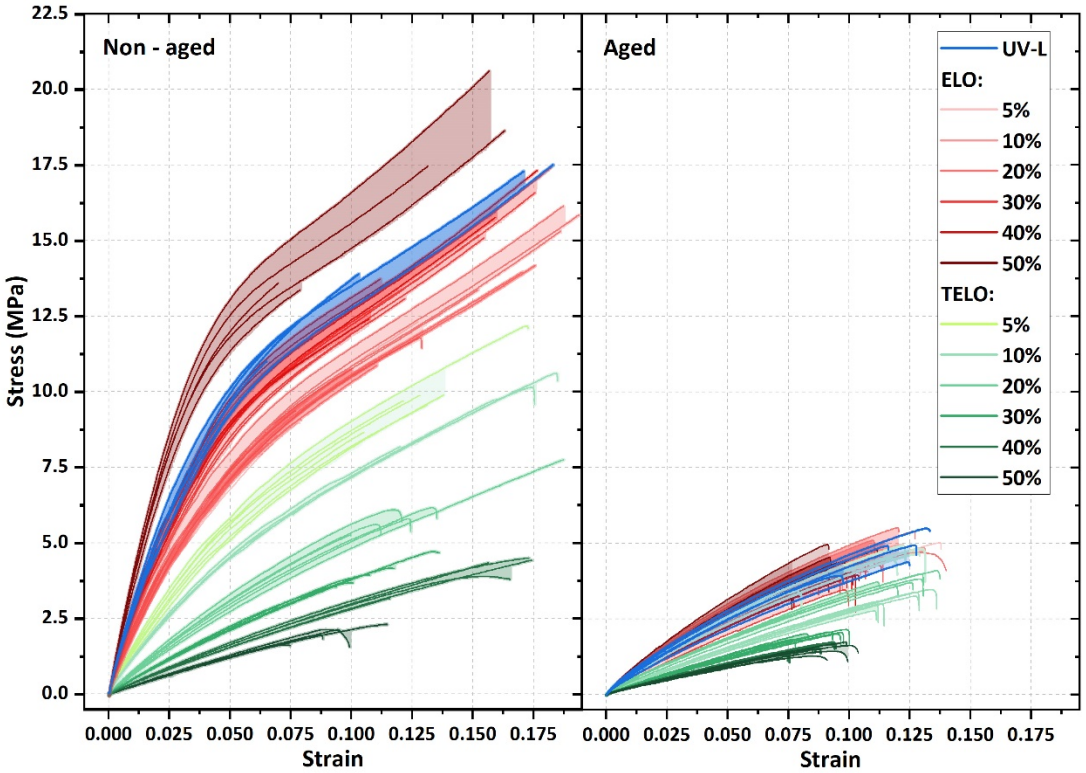

Figure 59 Stress vs Strain curves of samples prepared with different amounts of ELO or TELO.

Unlike ELO, TELO proportionally decreased the elastic modulus in all applications. Though TELO is capable of crosslinking and has a very low viscosity that enhances molecular mobility (reactive diluent), the lack of the glycerol group connecting the FAME molecules decreased the mechanical properties. UV-L has a large molecular weight that increases the viscosity throughout its lifespan. The addition of diluents, such as ELO and TELO, helps improving the crosslinking but the nature of the diluent changes the final properties.

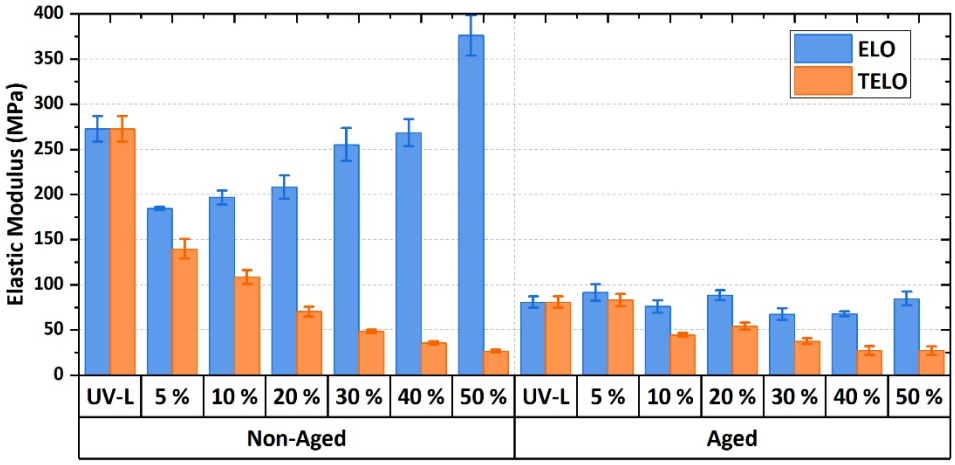

Figure 60 Elastic modulus of UV-L samples prepared with different amounts of ELO and TELO.

The glycerol moiety is connected to the FAMEs by ester groups that can spontaneously be hydrolysed (water-catalysed hydrolysis) [21], [190]. Such hydrolysis is dependent on the medium pH, it can be acid or alkali catalysed, as depicted in Figure 61.

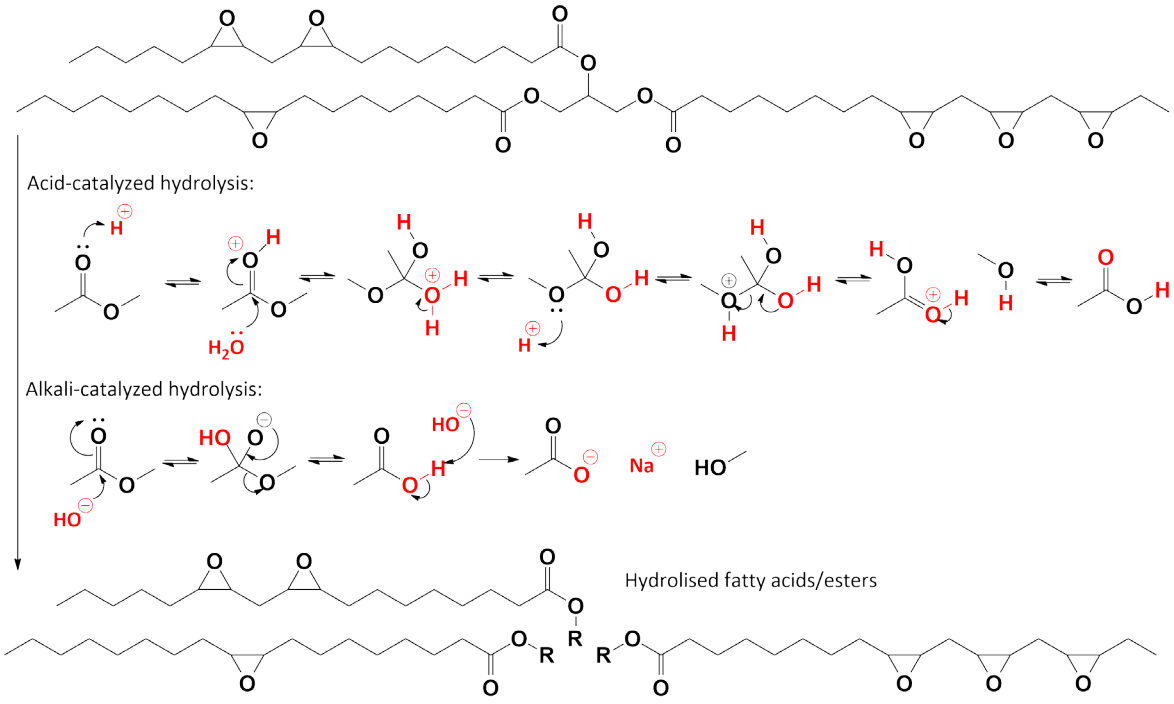

Figure 61 Acid and alkali catalysed hydrolysis of esters [50].

The results after the hygrothermal ageing show that the ester bonds in ELO were hydrolysed and the FAMEs became loose, which is the same as the structure in TELO that does not have the esters being part of the cross-linked structure. After the ageing process, the only remaining crosslinking bonds are the ones created in the curing procedure. Ageing in warm distilled water made the structure of cured ELO turn into the structure found in TELO. The cured molecular structures of ELO and TELO are shown in Appendix F.

6.3.7 Thermal analysis

Dzielendziak *et al* [46] reported the T_g temperature for UV-L between 40 °C and 46 °C. These values coincide with the relaxation zones found in the first DSC run of the samples, shown in Figure 62. However, in the second run this value disappears, even when the derivative graph is obtained, the T_g region is difficult to identify.

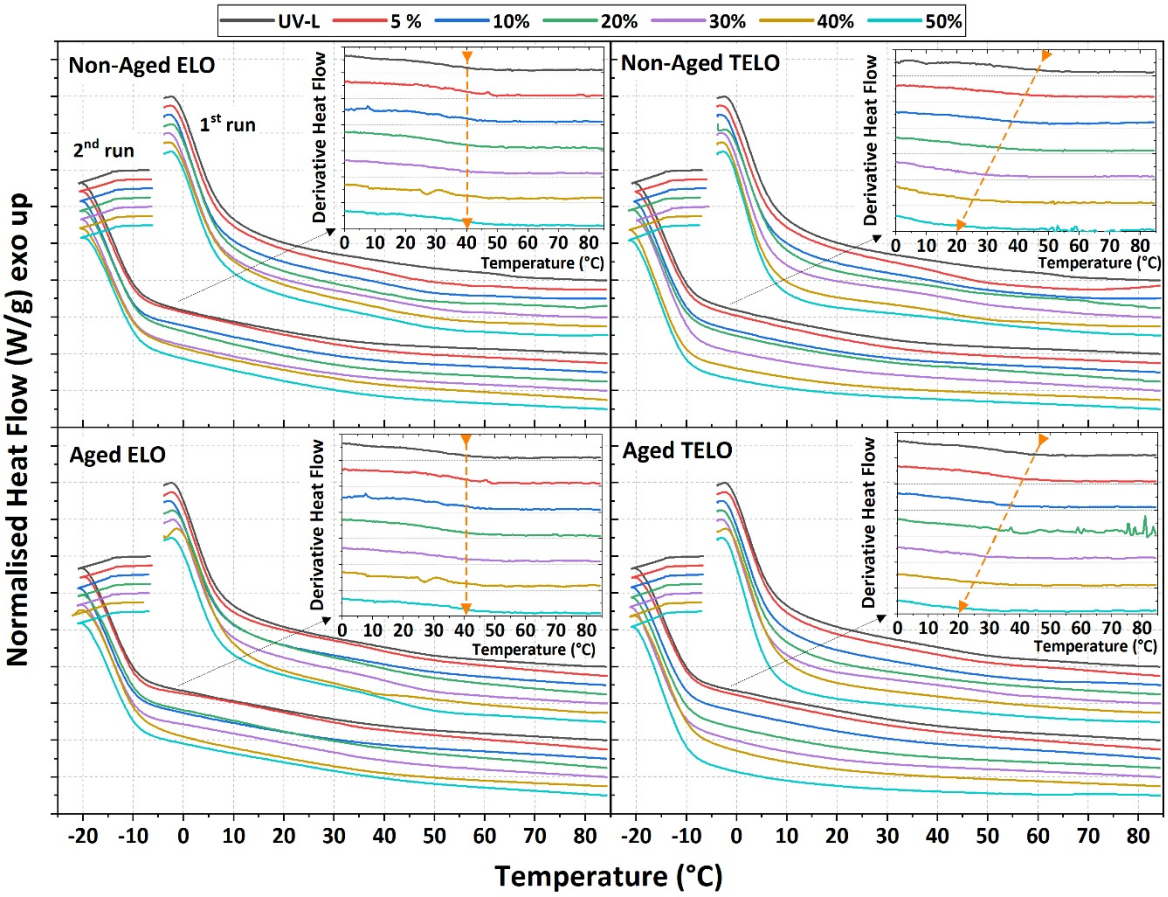

Figure 62 DSC curves of UV-L samples prepared with different amounts of ELO and TELO.

Taking the derivative of the second DSC run into consideration, the UV-L curves (in black) reach a plateau at around 40 °C, regardless of the aging process applied. Following the same behaviour, the samples containing ELO had similar curves throughout the different formulations. In the

samples containing TELO, these plateau regions were diminished with the increasing amounts of TELO in the composition.

UV-L and ELO have the same triglyceride composition, but in different stages of crosslinking densities and molecular weight. TELO comprises a mixture of fatty acid methyl esters that work as a reactive diluent, which in turn reduced the T_g temperature. The addition of diluents might not only reduce the T_g temperature, but the mechanical strength and modulus [22].

The degradation curves are shown in Figure 63. Even though the addition of TELO decreased the T_g, the curves followed the same pattern and the main decomposition temperature, between 415 °C and 420 °C, did not change amongst compositions and ageing processes.

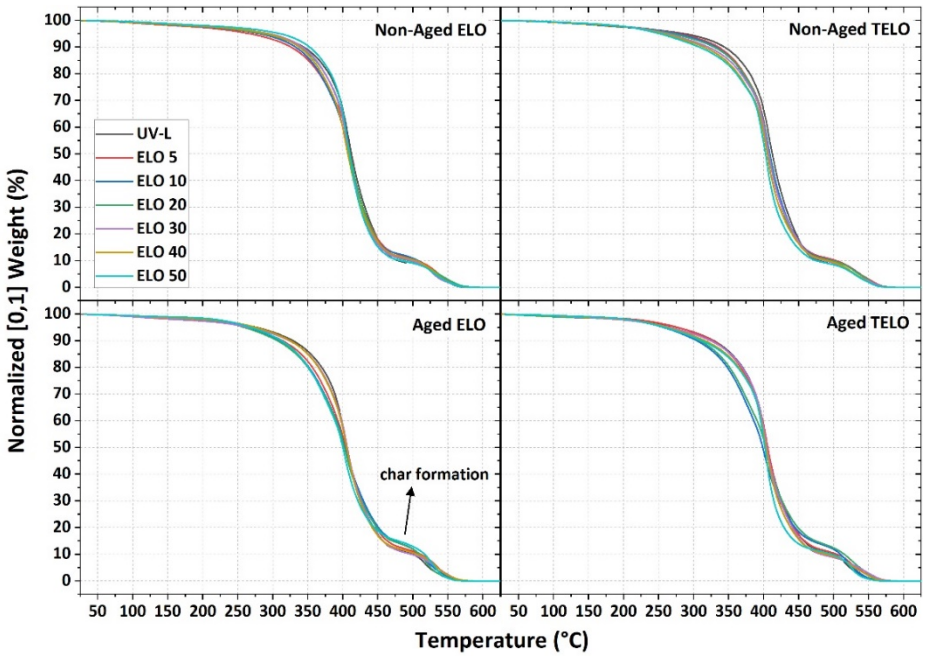

Figure 63 Thermal decomposition of UV-L samples prepared with different amounts of ELO and TELO.

The decomposition curve derivatives are shown in Figure 64. UV-L and samples prepared with the addition of ELO present a degradation peak at just above 450 °C. This peak tends to shift to higher temperatures with increased amounts of UV-L replacement by both ELO and TELO. After ageing, the peaks are highly reduced and only a second large peak for char degradation remains.

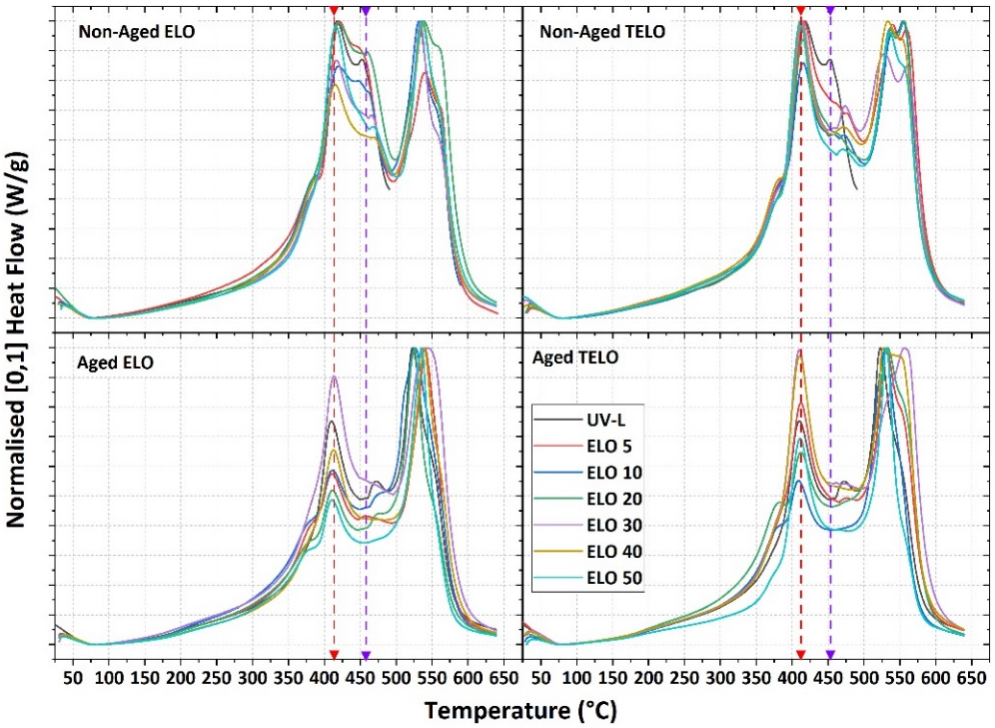

Figure 64 Derivative curves (DTGA) of the thermal decomposition of UV-L samples prepared with different amounts of ELO and TELO.

6.3.8 Summary

The use of UV radiation curing allowed a high consumption of epoxide groups and therefore a highly cross-linked structure. Further, the addition of reactive diluents such as ELO and TELO decreased UV-L's viscosity. TELO was able to reduce the viscosity to a much higher extent than ELO. Its addition also reduced density and water uptake in comparison to ELO. Though TELO-based blends were much less viscous than those prepared with ELO, tensile strength and elastic moduli diminished drastically.

According to the tests to assess the degree of curing, all the epoxide groups were consumed; therefore, all samples tested reached a high curing state. The deviations in the properties of the blends found in the tests were due to the polymeric structure, rather the unreacted monomers.

The internal and unbiased epoxide groups within the epoxidized oils are less reactive than terminal ones in conventional DGEBA epoxy resin. Initial curing attempts of ELO and TELO performed with phenalkamines, phenalkamides and succinic acid did not result in solid polymers; see Appendix B and Appendix D.

Both ELO and TELO showed a plasticizing effect reducing tensile strength and elastic modulus; it also reduced the brittleness of the final materials, which enhanced the resistance to damage and failure under their supported loads. TELO was also able to reduce the water uptake most likely by

filling the voids inside the structure. These voids, according to Dzielendziak *et al* [46], are filled in by water. The glycerol moiety that connects the fatty acids is crucial for retaining these mechanical properties, but the ester groups in it are hydrolysed. This behaviour is seen in other resins containing ester groups, such as polyester and vinyl ester [190].

Chapter 7 Final considerations, conclusion and future work

The search for sustainable materials is challenging yet necessary. Such materials can drastically change the way human activities affect the planet. Vegetable oils can provide long aliphatic chains, lignin and cardanol aromatics. The biofuel industry also benefits from plant sugars and oils. All these compounds can be used in the synthesis of new materials and decrease the current crude oil dependency.

The synthesis of a low viscosity epoxy resin derived from linseed oil was initially planned using heterogeneous catalysts. The epoxidation of the FAMEs reached much higher yields than that of ELO over TS-1 did, but the transesterification was not successful in the parameters tested. Further investigation of the catalysis was not carried out due to the small amounts of resin produced, instead a homogeneous approach was adopted. The transesterification of ELO reduced the viscosity and allowed its use in composite production with vacuum and infusion systems. Lighter and more water resistant materials were produced with the EFAMEs, yet with very poor tensile and thermal properties.

In spite of the fact that methyl linolenate, the major FAME in linseed oil compositions, has three unsaturated bonds that are able to be epoxidized these groups were unable to provide a highly cross-linked network. These bonds are near each other and are not able to reach other monomers and growing chains that could create a tight polymer network. The epoxidized triglycerides (ELO) however, are able to create more crosslinks due to the size of the molecule. The structure of the cross-linked ELO is not as tight as in a DGEBA system. The long aliphatic chains in ELO make the structure loose, functioning as a plasticizer. This reduces the tensile strength, elastic modulus and glass transition temperature.

CNSL-based hardeners are a great alternative to conventional hardeners. They can provide comparable mechanical properties to the conventional ones with an added bio-based content. Further to that, the cardanol moiety can receive different amines and amides to create tailored hardeners, depending on the application of the resin system applied. The aliphatic side chains in cardanol have unsaturations where amine and amide groups can be added.

In systems formulated only with epoxidized oils as monomers, suitable curing procedures were the employment of a hardener and high curing temperature, or the addition of a photoinitiator and exposure to UV-light. Each of these methods hasbenefits and drawbacks. The cure with hardeners and heat is suitable for thick composites but the process can be slow. The UV curing

process is fast but requires thin materials. The fibres in the structure create shadowed regions that will not initially cure. These UV systems are able to cure without the UV source once the reaction is started but the process is slow and is affected by the viscosity of the material.

7.1 Conclusions

The suitability of linseed oil based epoxy resins for maritime application was evaluated. Other types of oils apart from linseed oil are suitable for the production of epoxy resins. However, the degree of unsaturation in each fatty acid has to be taken into account. A high degree of unsaturation will result in a higher epoxide content but also in a high viscosity. The vegetable oil based resins are less reactive then their common synthetic counterparts. The epoxide groups located in the fatty acids of the vegetable oils are internal and symmetrical, hence the curing reactions must be more energetic, such as with application of heat or radiation (UV-light). The lower reactivity hinders the use not only of traditional epoxy curing agents but also those derived from natural feedstock, such as phenalkamides and phenalkamines.

TELO showed a great capacity for reducing the resins' viscosity, functioning as a reactive diluent. The synthesis of TELO eliminates the glycerol moiety from the original triglyceride. Glycerol is responsible for linking the fatty acid molecules together, it was proven to be a great influencer of the mechanical properties, because it strengthens the material. The bond between the glycerol and the fatty acids are ester linkages. These bonds, similarly to those in polyester and vinyl ester resins, are susceptible to hydrolysis, in both acid and alkaline conditions. Therefore, it can be concluded that the maritime environment can be very detrimental to the epoxy resins derived from triglycerides (vegetable oils), limiting their applications in this area.

7.2 Future works

Although the resins developed from epoxidized vegetable oils did not perform as well as the DGEBA resin, many applications can still be explored, such as materials that do not require high stiffness and strength. Therefore, as well as carrying out further research in the material's properties knowledge gathered must be disseminated so that these products can be available to other markets.

The hydrolysis of ester bonds in the triglyceride was responsible for the loss of mechanical properties when the resins were exposed to hygrothermal ageing, therefore further work should be carried out to investigate how the reaction occurs, especially in the area of how the water molecules diffuse through the cured material and propagate the hydrolysis. The use of molecular

modelling is a great tool in that sense. Dzielendziak *et at* [46] carried out modelling simulations to investigate the diffusion of water in epoxidized linseed oil resins. The work showed that the cured structure contains voids through which water penetrates. Furthermore, the cure of epoxide groups generates hydroxyl groups that also attract water molecules. The knowledge around these diffusion and hydrolysis mechanisms would help in the development of modifications that could protect the resin structure, or make the molecules more highly organized and therefore tighter, reducing water diffusion.

TELO is a version of the resin that does not have ester groups in the composition, and is thus not affected by hydrolysis. However, the absence of the glycerol moiety reduced the mechanical properties. A different approach would be the decarboxylation of fatty acids, substituting the ester by a group that is able to crosslink via a different functional group or bond. In a recent work by Sun *et al* [191], the carbonyl group in carboxylic acids was substituted by a double-bond, producing an α-olefin. This extra double bond in the already unsaturated long chain from the fatty acid can also be functionalized with an epoxide group. Though this could be a promising monomer for cross-linked resins, the cost of the photocatalyst used was considered very high for the application [191]. The synthesis of these monomers could be improved by heterogeneous catalysis and this presents an opportunity for further work.

Additionally, the development of heterogeneous catalysis for the decarboxylation and/or transesterification of vegetable oils would highly benefit the biofuel industry. Biodiesel derived from vegetable oils is the product of a transesterification reaction of the triglyceride in the oil. The parameters used for heterogeneous catalysis in this work were limited to the extent of what heterogeneous catalysts can achieve.

Some aspects of the present work did not consider the twelve principles of green chemistry [4]. The epoxidation reactions over TS-1 and Ti-SiO_2 were carried out in acetonitrile as solvent, which is harsh and toxic. The choice of using it came from the work of Wilde *et al* [93], as although other solvents were analysed in their work, acetonitrile showed the best reaction yields. There is an opportunity to further develop the reaction in solvents that are more sustainable, tuning the reaction parameters in order to achieve higher yields.

Still in the area of sustainability, CNSL-based hardeners are not the ultimate replacement for the conventional ones, but the bio-based content given by them is a claim for lower environmental impact. Nonetheless, these phenalkamines and phenalkamides have amines and amides in the composition, which in case of a fire in a marine vessel, would generate toxic fumes. Cardanol can be used for the production of epoxy resin monomers. The aliphatic side chain has unsaturations that can be functionalized (epoxidized/acrylated).

The UV curing used is limited by the material's transparency, thickness and any fillers in the structure. To overcome these limitations, photosensitizers can be employed in conjunction with the photoinitiators to help the curing process. Further to that, electron bean curing could also be studied because it can penetrate deeper into the material and does not require photoinitiators.

This work was carried out so that a final resin derived from linseed oil with some environmental benefits, could be evaluated,. A whole Lifecycle Assessment needs to be carried out, evaluating all the steps in the process of production, usage and disposal of the resin, in order to assess its full environmental impact. Linseed oil is not readily available all around the globe, other oils will have different fatty acid profiles and their employment might not be feasible, due to differing unsaturation content. The lifecycle assessment methodology developed will then be able to identify if such alternative materials really are sustainable for the application they will be proposed for.

Appendix A RTV silicone moulds for preparation of test specimens

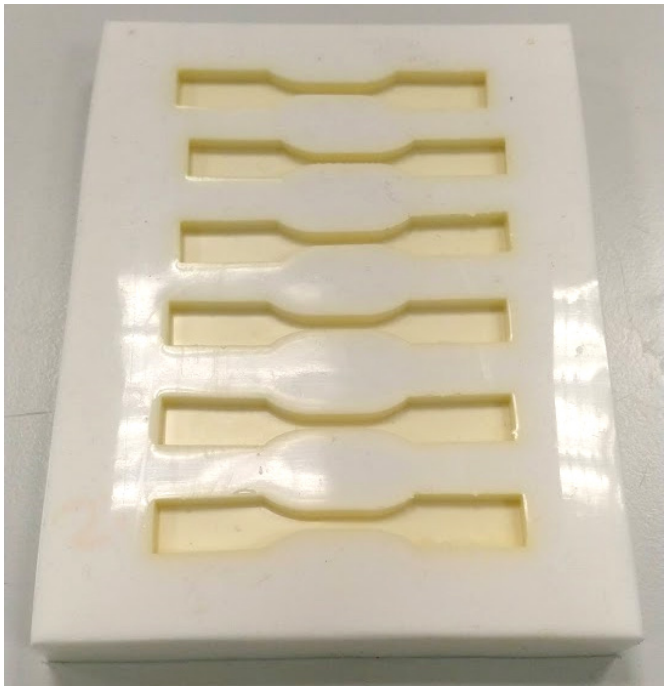

Appendix B Properties of commercial thermosetting resins for maritime application.

Commercial name	Type	Description	Viscosity (cP at 25 °C)	Cured density (g/cm³)	Water uptake (%) [a]	Tg (°C)	Elastic Modulus (GPa)	Reference
Prime 20LV	Epoxy	Designed for infusion systems	NA	1.153	NA	DMTA: 82.8	3.2	[192][192]
Prime 27	Epoxy	Designed for infusion systems	260 - 280	1.13	NA	HDT: 64.0	3.2	[193]
Crystic 701PAX	Polyester	Low viscosity, isophthalic	160	1.19	“10 mg”	HDT: 75.0	3.58	[194]
EC - IP2	Polyester	Designed for infusion systems	160	1.19	“10 mg”	HDT: 75.0	3.58	[195]
Hydrex 100HF	Vinyl ester	Designed for infusion systems	175	NA	0.16	HDT: 123.0	3.79	[196]
Crystic VE 671-03	Vinyl ester	Bisphenol A based resin	150 - 200	NA	“35 mg”	HDT: 95 - 100	3.4	[197]

NA: Not available values. [a] water absorption after “24 h at 23 °C”, according to data sheet. DMTA: Dynamic mechanical thermal analysis. HDT: Heat distortion temperature.

Appendix C ELO and CNSL-based hardeners

					
ELO:FAST	8.7:1.3	ELO:2009	7.7:2.3	ELO:3000	5.8:4.2
					
ELO:3005	5.8:4.2	ELO:3060	7.7:2.3	ELO:3100	7.0:3.0

- 3 initial hours for 220°C in fan-assisted oven. Samples containing hardeners 3000, 3005 and 3060 presented a non-sticky film formation on the surface of the resin.
- Samples containing hardener 3100 presented bumps/bubbles on the surface, they were left in the oven for 5h. There was a resulting non-sticky part as well as liquid remaining, which became non-sticky with time after oven.
- Samples made with ELO and hardeners FAST/2009 had a rugged film on the surface after 5h.

Appendix D ELO and succinic acid 10 wt.%

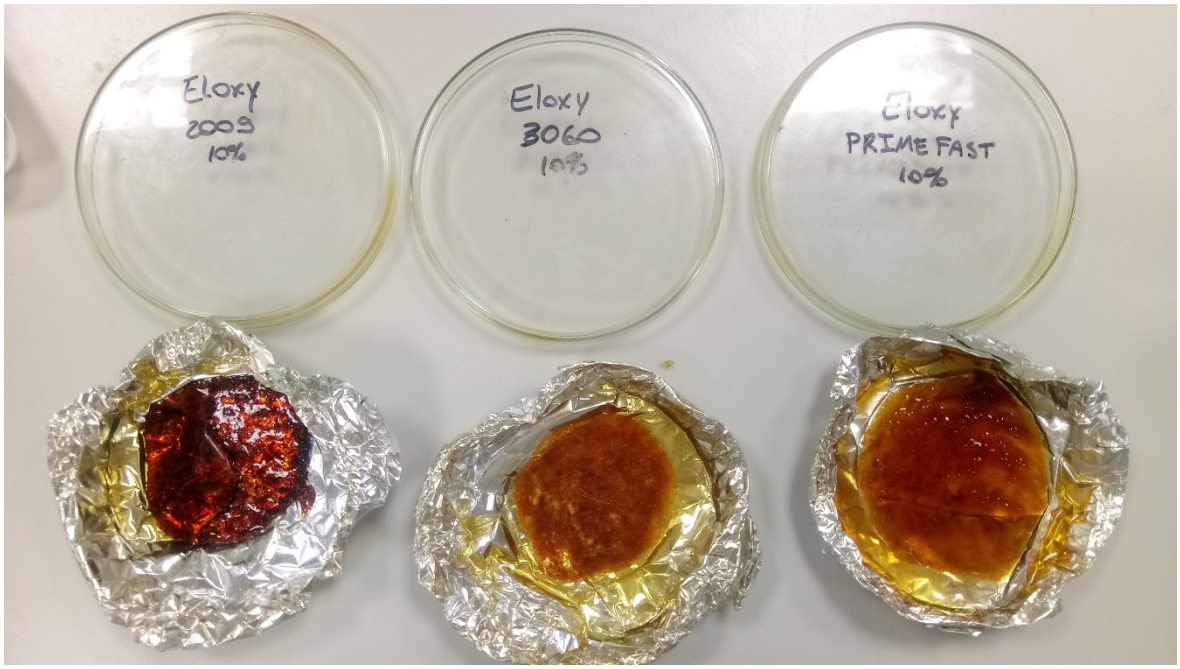

Appendix E UV rig for resin curing

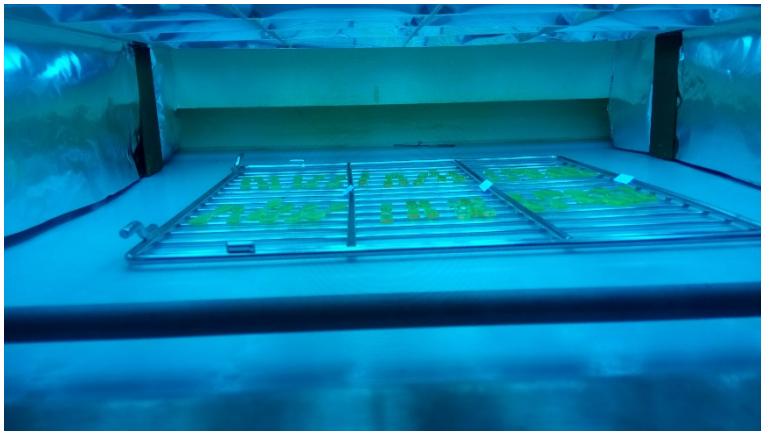

4 Cosmedico cosmopower s 50/58w ballasts.

4 Philips Cleo 40W-R UV lamps

Appendix F Cured ELO and TELO

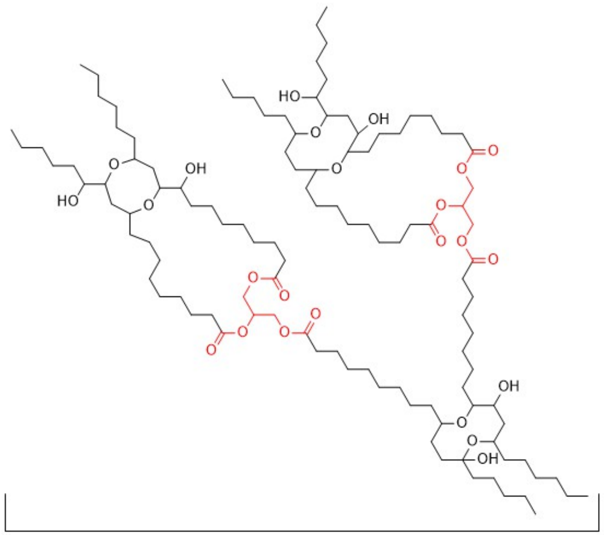

Representation of ELO

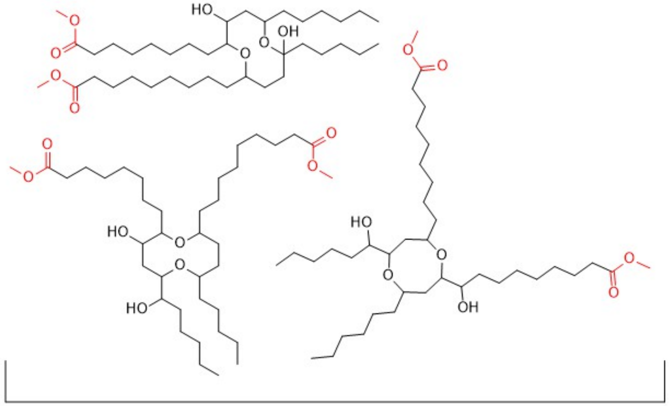

Representation of TELO

Appendix G Increase in Volume and Mass of aged UV-L cured samples

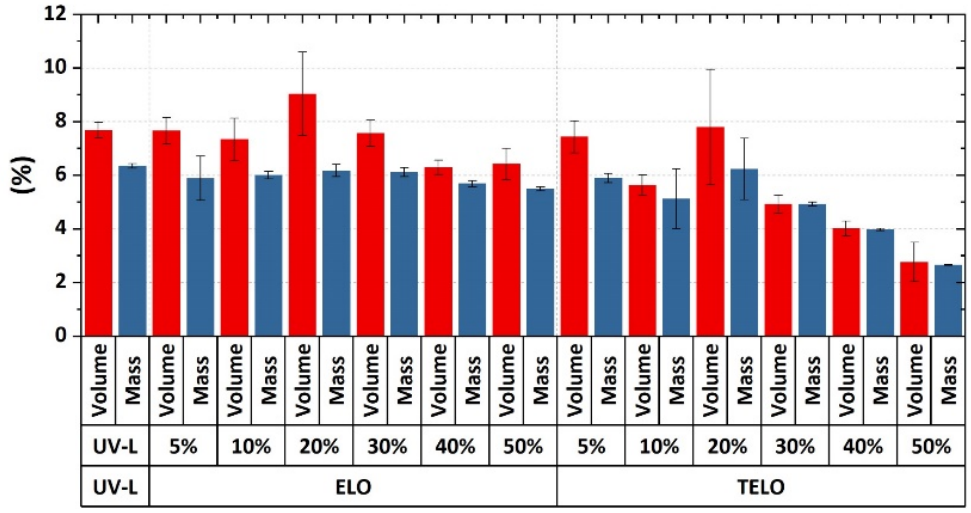

List of References

[1] World Commission on Environment and Development, *Our Common Future*. Oxford University Press, 1987.

[2] R. Geyer, J. R. Jambeck, and K. L. Law, "Production, use, and fate of all plastics ever made," *Sci. Adv.*, vol. 3, no. 7, p. e1700782, Jul. 2017.

[3] R. Verma, K. S. Vinoda, M. Papireddy, and A. N. S. Gowda, "Toxic Pollutants from Plastic Waste- A Review," *Procedia Environ. Sci.*, vol. 35, no. 8, pp. 701–708, Jan. 2016.

[4] P. T. Anastas and J. C. Warner, *Green Chemistry: Theory and Practice*. Oxford University Press, 1998.

[5] A. Azapagic, A. Emsley, and I. Hamerton, *Polymers: The Environment and Sustainable Development*. Wiley, 2003.

[6] C. R. Álvarez-Chávez, S. Edwards, R. Moure-Eraso, and K. Geiser, "Sustainability of bio-based plastics: general comparative analysis and recommendations for improvement," *J. Clean. Prod.*, vol. 23, no. 1, pp. 47–56, Mar. 2012.

[7] A. L. Andrady and M. A. Neal, "Applications and societal benefits of plastics.," *Philos. Trans. R. Soc. Lond. B. Biol. Sci.*, vol. 364, no. 1526, pp. 1977–84, Jul. 2009.

[8] W. Callister and D. Rethwisch, *Materials science and engineering: an introduction*, vol. 94. John Wiley & Sons, 2007.

[9] A. K. Kaw, *Mechanics of Composite Materials*, vol. 34. Dordrecht: Springer Netherlands, 1994.

[10] G. F. Hays, "Now is the time," *The World Corrosion Organization*. [Online]. Available: http://corrosion.org/Corrosion+Resources/Publications.html. [Accessed: 20-Mar-2019].

[11] "Composites 2019: A multitude of markets : CompositesWorld." [Online]. Available: https://www.compositesworld.com/articles/composites-2019-a-multitude-of-markets. [Accessed: 20-Mar-2019].

[12] A. O'Donnell, M. . Dweib, and R. . Wool, "Natural fiber composites with plant oil-based resin," *Compos. Sci. Technol.*, vol. 64, no. 9, pp. 1135–1145, Jul. 2004.

[13] Eric Greene Associates., *Marine Composites*. Eric Greene Associates, 1999.

[14] Markets and Markets, “Composites Market worth 115.43 Billion USD by 2022,” *Markets and Markets*, 2017. [Online]. Available: www.marketsandmarkets.com/PressReleases/composite.asp. [Accessed: 19-Mar-2019].

[15] “Boeing: 787 By Design: By Design: Advanced Composite Use.” [Online]. Available: https://www.boeing.com/commercial/787/by-design/#/advanced-composite-use. [Accessed: 19-Mar-2019].

[16] S. C. Das and E. H. Nizam, “Applications of Fibber Reinforced Polymer Composites (FRP) in Civil Engineering,” *Int. J. Adv. Struct. Geothacnical Eng.*, vol. 03, no. 03, 2014.

[17] M. Mukhopadhyay, *Mechanics of composite materials and structures*. Universities Press, 2004.

[18] E. M. Petrie, *Epoxy Adhesive Formulations*, 1st ed. Mexico: McGraw-Hill Professional, 2005.

[19] M. N. Balgacem and A. Gandini, Eds., *Monomers, Polymers and Composites from Renewable Resources*. Elsevier, 2011.

[20] C. S. Brazel, S. L. Rosen, and S. L. Rosen, *Fundamental principles of polymeric materials, third edition*. Wiley, 2012.

[21] J. F. Mata-Segreda, “Spontaneous hydrolysis of ethyl formate: Isobaric activation parameters,” *Int. J. Chem. Kinet.*, vol. 32, no. 1, pp. 67–71, 2000.

[22] D. Ratna, *Handbook of Thermoset Resins*. Smithers Rapra, 2009.

[23] E. Asmatulu, M. M. Rahman, A. Alonayni, and M. Alamir, “Sustainability of fiber reinforced laminate and honeycomb composites in manufacturing industries,” in *Behavior and Mechanics of Multifunctional Materials and Composites XII*, 2018, vol. 10596, p. 69.

[24] N. Vijay, V. Rajkumara, and P. Bhattacharjee, “Assessment of Composite Waste Disposal in Aerospace Industries,” *Procedia Environ. Sci.*, vol. 35, pp. 563–570, Jan. 2016.

[25] A. J. Sobey, J. I. R. Blake, and R. A. Shenoi, “Monte Carlo reliability analysis of tophat stiffened composite plate structures under out of plane loading,” *Reliab. Eng. Syst. Saf.*, vol. 110, pp. 41–49, Feb. 2013.

[26] W. Thielemans, E. Can, S. S. Morye, and R. P. Wool, “Novel applications of lignin in composite materials,” *J. Appl. Polym. Sci.*, vol. 83, no. 2, pp. 323–331, 2002.

[27] G. Koronis, A. Silva, and M. Fontul, “Green composites: A review of adequate materials for

automotive applications," *Composites Part B: Engineering*, vol. 44, no. 1. pp. 120–127, 2013.

[28] R. Ayerza, "Oil content and fatty acid composition of chia (Salvia hispanica L.) from five northwestern locations in Argentina," *J. Am. Oil Chem. Soc.*, vol. 72, no. 9, pp. 1079–1081, Sep. 1995.

[29] J. M. F. A. Blanchard, A. J. Sobey, and J. I. R. Blake, "Multi-scale investigation into the mechanical behaviour of flax in yarn, cloth and laminate form," *Compos. Part B Eng.*, vol. 84, pp. 228–235, 2016.

[30] M. J. A. den van Oever, H. L. Bos, and M. J. J. M. van Kemenade, "Influence of the Physical Structure of Flax Fibres on the Mechanical Properties of Flax Fibre Reinforced Polypropylene Composites," *Appl. Compos. Mater.*, vol. 7, no. 5/6, pp. 387–402, 2000.

[31] G. Hou, G. R. Ablett, K. P. Pauls, and I. Rajcan, "Environmental effects on fatty acid levels in soybean seed oil," *J. Am. Oil Chem. Soc.*, vol. 83, no. 9, pp. 759–763, Sep. 2006.

[32] H. Ozer, T. Polat, and E. Ozturk, "Response of irrigated sunflower (Helianthus annuus L.) hybrids to nitrogen fertilization: growth, yield and yield components," *Plant Soil Environ.*, vol. 50, no. 5, pp. 205–211, 2004.

[33] V. Dubois, S. Breton, M. Linder, J. Fanni, and M. Parmentier, "Fatty acid profiles of 80 vegetable oils with regard to their nutritional potential," *Eur. J. Lipid Sci. Technol.*, vol. 109, no. 7, pp. 710–732, Jul. 2007.

[34] V. Sharma and P. P. Kundu, "Addition polymers from natural oils—A review," *Prog. Polym. Sci.*, vol. 31, no. 11, pp. 983–1008, Nov. 2006.

[35] Z. S. Petrović, A. Guo, I. Javni, and W. Zhang, "Plastics and Composites from Soybean Oil," in *Natural Fibers, Plastics and Composites*, Boston, MA: Springer US, 2004, pp. 167–192.

[36] U. Biermann *et al.*, "New Syntheses with Oils and Fats as Renewable Raw Materials for the Chemical Industry.," *Angew. Chem. Int. Ed. Engl.*, vol. 39, no. 13, pp. 2206–2224, Jul. 2000.

[37] T. Saurabh, M. Patnaik, S. L. Bhagt, and V. C. Renge, "Epoxidation of vegetable oils: a review," *Int. J. Adv. Eng. Technol.*, vol. 2, no. 4, pp. 491–501, 2011.

[38] S. M. Danov, V. L. Krasnov, A. V. Sulimov, and A. V. Ovcharova, "Mechanism of olefin epoxidation in the presence of a titanium-containing zeolite," *Russ. J. Phys. Chem. A*, vol. 87, no. 11, pp. 1809–1812, Oct. 2013.

[39] Statista, “Global vegetable oil consumption,” *The Statistics Portal*, 2017. [Online]. Available: https://www.statista.com/statistics/263937/vegetable-oils-global-consumption/. [Accessed: 10-Jan-2019].

[40] P. Muturi, D. Wang, and S. Dirlikov, “Epoxidized vegetable oils as reactive diluents I. Comparison of vernonia, epoxidized soybean and epoxidized linseed oils,” *Prog. Org. Coatings*, vol. 25, no. 1, pp. 85–94, Oct. 1994.

[41] A. B. Strong, *Fundamentals of Composites Manufacturing, Second Edition: Materials, Methods and Applications*. Society of Manufacturing Engineers, 2008.

[42] J. L. Clarke, *Structural Design of Polymer Composites: Eurocomp Design Code and Background Document*. Taylor & Francis, 2003.

[43] S.-C. Chua, X. Xu, and Z. Guo, “Emerging sustainable technology for epoxidation directed toward plant oil-based plasticizers,” *Process Biochem.*, vol. 47, no. 10, pp. 1439–1451, Oct. 2012.

[44] T. F. Parreira, M. M. C. Ferreira, H. J. S. Sales, and W. B. de Almeida, “Quantitative Determination of Epoxidized Soybean Oil Using Near-Infrared Spectroscopy and Multivariate Calibration,” *Appl. Spectrosc.*, vol. 56, no. 12, pp. 1607–1614, Dec. 2002.

[45] M. Malmstein, A. R. Chambers, and J. I. R. Blake, “Hygrothermal ageing of plant oil based marine composites,” *Compos. Struct.*, vol. 101, pp. 138–143, Jul. 2013.

[46] A. S. Dzielendziak *et al.*, “Spectroscopic chemical insights leading to the design of versatile sustainable composites for enhanced marine application,” *RSC Adv.*, vol. 5, no. 122, pp. 101221–101231, Nov. 2015.

[47] G. L. Téllez, E. Vigueras-Santiago, and S. Hernández-López, “Characterization of linseed oil epoxidized at different percentages,” *Superf. y vacío*, vol. 22, no. 1, pp. 5–10, 2009.

[48] H. Baumann, M. Bühler, H. Fochem, F. Hirsinger, H. Zoebelein, and J. Falbe, “Natural Fats and Oils—Renewable Raw Materials for the Chemical Industry,” *Angew. Chemie Int. Ed. English*, vol. 27, no. 1, pp. 41–62, Jan. 1988.

[49] N. Prileschajew, “Oxydation ungesättigter Verbindungen mittels organischer Superoxyde,” *Berichte der Dtsch. Chem. Gesellschaft*, vol. 42, no. 4, pp. 4811–4815, Nov. 1909.

[50] J. J. Clayden, N. Greeves, S. Warren, and P. Wothers, *Organic Chemistry*, vol. 40. 2001.

[51] J.-Y. Kim *et al.*, “Catalytic pyrolysis of lignin over HZSM-5 catalysts: Effect of various

parameters on the production of aromatic hydrocarbon," *J. Anal. Appl. Pyrolysis*, vol. 114, pp. 273–280, Jun. 2015.

[52] M. S. F. Lie Ken Jie and M. K. Pasha, "Epoxidation reactions of unsaturated fatty esters with potassium peroxomonosulfate," *Lipids*, vol. 33, no. 6, pp. 633–637, Jun. 1998.

[53] S. T. Oyama, *Mechanisms in Homogeneous and Heterogeneous Epoxidation Catalysis*. Elsevier Science, 2008.

[54] B. Mudhaffar, J. Salimon, B. M. Abdullah, and J. Salimon, "Epoxidation of Vegetable Oils and Fatty Acids: Catalysts, Methods and Advantages," *J. Appl. Sci.*, vol. 10, no. 15, pp. 1545–1553, Dec. 2010.

[55] S. Dinda, A. V Patwardhan, V. V Goud, and N. C. Pradhan, "Epoxidation of cottonseed oil by aqueous hydrogen peroxide catalysed by liquid inorganic acids.," *Bioresour. Technol.*, vol. 99, no. 9, pp. 3737–44, Jun. 2008.

[56] S. Bonollo, D. Lanari, and L. Vaccaro, "Ring-Opening of Epoxides in Water," *European J. Org. Chem.*, vol. 2011, no. 14, pp. 2587–2598, May 2011.

[57] C. Cai *et al.*, "Studies on the kinetics of in situ epoxidation of vegetable oils," *Eur. J. Lipid Sci. Technol.*, vol. 110, no. 4, pp. 341–346, Apr. 2008.

[58] V. V. Goud, A. V. Patwardhan, and N. C. Pradhan, "Studies on the epoxidation of mahua oil (Madhumica indica) by hydrogen peroxide," *Bioresour. Technol.*, vol. 97, no. 12, pp. 1365–1371, 2006.

[59] P. Meyer, N. Techaphattana, S. Manundawee, S. Sangkeaw, W. Junlakan, and C. Tongurai, "Epoxidation of Soybean Oil and Jatropha Oil," *Thammasat Int. J. Sci. Technol.*, vol. 13, p. 5, 2008.

[60] R. Mungroo, N. C. Pradhan, V. V. Goud, and A. K. Dalai, "Epoxidation of Canola Oil with Hydrogen Peroxide Catalyzed by Acidic Ion Exchange Resin," *J. Am. Oil Chem. Soc.*, vol. 85, no. 9, pp. 887–896, Aug. 2008.

[61] U. Törnvall, C. Orellana-Coca, R. Hatti-Kaul, and D. Adlercreutz, "Stability of immobilized Candida antarctica lipase B during chemo-enzymatic epoxidation of fatty acids," *Enzyme Microb. Technol.*, vol. 40, no. 3, pp. 447–451, Feb. 2007.

[62] C. Orellana-Coca, S. Camocho, D. Adlercreutz, B. Mattiasson, and R. Hatti-Kaul, "Chemo-enzymatic epoxidation of linoleic acid: Parameters influencing the reaction," *Eur. J. Lipid*

Sci. Technol., vol. 107, no. 12, pp. 864–870, Dec. 2005.

[63] S. Sun *et al.*, "Enzymatic epoxidation of Sapindus mukorossi seed oil by perstearic acid optimized using response surface methodology," *Ind. Crops Prod.*, vol. 33, no. 3, pp. 676–682, May 2011.

[64] M. Rüsch gen. Klaas and S. Warwel, "Complete and partial epoxidation of plant oils by lipase-catalyzed perhydrolysis," *Ind. Crops Prod.*, vol. 9, no. 2, pp. 125–132, Jan. 1999.

[65] M. R. gen Klaas and S. Warwel, "Chemoenzymatic epoxidation of unsaturated fatty acid esters and plant oils," *J. Am. Oil Chem. Soc.*, vol. 73, no. 11, pp. 1453–1457, Nov. 1996.

[66] A. Campanella and M. A. Baltanás, "Degradation of the oxirane ring of epoxidized vegetable oils with solvated acetic acid using cation-exchange resins," *Eur. J. Lipid Sci. Technol.*, vol. 106, no. 8, pp. 524–530, Aug. 2004.

[67] B. Rangarajan, A. Havey, E. A. Grulke, and P. D. Culnan, "Kinetic parameters of a two-phase model for *in situ* epoxidation of soybean oil," *J. Am. Oil Chem. Soc.*, vol. 72, no. 10, pp. 1161–1169, Oct. 1995.

[68] V. V. Goud, A. V. Patwardhan, S. Dinda, and N. C. Pradhan, "Epoxidation of karanja (Pongamia glabra) oil catalysed by acidic ion exchange resin," *Eur. J. Lipid Sci. Technol.*, vol. 109, no. 6, pp. 575–584, Jun. 2007.

[69] S. Dinda, V. V Goud, A. V Patwardhan, and N. C. Pradhan, "Selective epoxidation of natural triglycerides using acidic ion exchange resin as catalyst," *Asia-Pacific J. Chem. Eng.*, vol. 6, no. 6, pp. 870–878, Nov. 2011.

[70] S. Sinadinović-Fišer, M. Janković, and Z. S. Petrović, "Kinetics of in situ epoxidation of soybean oil in bulk catalyzed by ion exchange resin," *J. Am. Oil Chem. Soc.*, vol. 78, no. 7, pp. 725–731, Jul. 2001.

[71] A. F. Aguilera *et al.*, "Epoxidation of Fatty Acids and Vegetable Oils Assisted by Microwaves Catalyzed by a Cation Exchange Resin," *Ind. Eng. Chem. Res.*, vol. 57, no. 11, pp. 3876–3886, Mar. 2018.

[72] B. Notari, "Titanium silicalites," *Catal. Today*, vol. 18, no. 2, pp. 163–172, 1993.

[73] R. A. Sheldon, M. Wallau, I. W. C. E. Arends, and U. Schuchardt, "Heterogeneous catalysts for liquid-phase oxidations: Philosophers' stones or Trojan horses?," *Acc. Chem. Res.*, vol. 31, no. 8, pp. 485–493, 1998.

[74] J. Kollar, “Catalytic epoxidation of an olefinically unsaturated compound using an organic hydroperoxide as an epoxidizing agent.” Google Patents, 31-Oct-1967.

[75] M. N. Sheng and J. G. Zajacek, “Hydroperoxide Oxidations Catalyzed by Metals,” 1968, pp. 418–432.

[76] R. A. Sheldon, J. A. Van Doorn, C. W. A. Schram, and A. J. De Jong, “Metal-catalyzed epoxidation of olefins with organic hydroperoxides: II. The effect of solvent and hydroperoxide structure,” *J. Catal.*, vol. 31, no. 3, pp. 438–443, 1973.

[77] F. Bigi *et al.*, “Molybdenum-MCM-41 silica as heterogeneous catalyst for olefin epoxidation,” *J. Mol. Catal. A Chem.*, vol. 386, pp. 108–113, 2014.

[78] J. C. van der Waal and H. van Bekkum, “Zeolite titanium beta: A versatile epoxidation catalyst. Solvent effects,” *J. Mol. Catal. A Chem.*, vol. 124, no. 2–3, pp. 137–146, Oct. 1997.

[79] M. Clerici, “Epoxidation of Lower Olefins with Hydrogen Peroxide and Titanium Silicalite,” *J. Catal.*, vol. 140, no. 1, pp. 71–83, Mar. 1993.

[80] X. Huali *et al.*, “A review on heterogeneous solid catalysts and related catalytic mechanisms for epoxidation of olefins with H2O2,” *Chem. Biochem. Eng. Q.*, vol. 22, no. 1, pp. 25–39, Mar. 2008.

[81] D. R. C. Huybrechts, P. L. Buskens, and P. A. Jacobs, “Physicochemical and catalytic properties of titanium silicalites,” *J. Mol. Catal.*, vol. 71, no. 1, pp. 129–147, Jan. 1992.

[82] S. C. Laha and R. Kumar, “Highly Selective Epoxidation of Olefinic Compounds over TS-1 and TS-2 Redox Molecular Sieves Using Anhydrous Urea–Hydrogen Peroxide as Oxidizing Agent,” *J. Catal.*, vol. 208, no. 2, pp. 339–344, Jun. 2002.

[83] M. Neurock and L. E. Manzer, “Theoretical insights on the mechanism of alkene epoxidation by H2O2 with titanium silicalite,” *Chem. Commun.*, no. 10, p. 1133, Jan. 1996.

[84] W. Panyaburapa, T. Nanok, and J. Limtrakul, “Epoxidation Reaction of Unsaturated Hydrocarbons with H 2 O 2 over Defect TS-1 Investigated by ONIOM Method: Formation of Active Sites and Reaction Mechanisms,” *J. Phys. Chem. C*, vol. 111, no. 8, pp. 3433–3441, Mar. 2007.

[85] G. N. Vayssilov and R. A. van Santen, “Catalytic Activity of Titanium Silicalites—a DFT Study,” *J. Catal.*, vol. 175, no. 2, pp. 170–174, Apr. 1998.

[86] G. Bellussi, “Reactions of titanium silicalite with protic molecules and hydrogen peroxide,”

J. Catal., vol. 133, no. 1, pp. 220–230, Jan. 1992.

[87] M. G. Clerici, “Oxidation of saturated hydrocarbons with hydrogen peroxide, catalysed by titanium silicalite,” *Appl. Catal.*, vol. 68, no. 1, pp. 249–261, Jan. 1991.

[88] E. Karlsen and K. Schöffel, “Titanium - Silicalite catalyzed epoxidation of ethylene with hydrogen peroxide a theoretical study,” *Catal. Today*, vol. 32, no. 1–4, pp. 107–114, Dec. 1996.

[89] I. V. Yudanov, P. Gisdakis, C. Di Valentin, and N. Rösch, “Activity of peroxo and hydroperoxo complexes of Ti(IV) in olefin epoxidation: A density functional model study of energetics and mechanism,” *Eur. J. Inorg. Chem.*, vol. 1999, no. 12, pp. 2135–2145, Dec. 1999.

[90] M. Guidotti, N. Ravasio, R. Psaro, E. Gianotti, L. Marchese, and S. Coluccia, “Heterogeneous catalytic epoxidation of fatty acid methyl esters on titanium-grafted silicas,” *Green Chem.*, vol. 5, no. 4, p. 421, Aug. 2003.

[91] A. Campanella, M. A. Baltanas, M. C. Capel-Sanchez, J. M. Campos-Martin, and J. L. G. Fierro, “Soybean oil epoxidation with hydrogen peroxide using an amorphous Ti/SiO2 catalyst,” *Green Chem.*, vol. 6, no. 7, p. 330, Jul. 2004.

[92] M. Guidotti, N. Ravasio, R. PSARO, E. GIANOTTI, S. COLUCCIA, and L. Marchese, “Epoxidation of unsaturated FAMEs obtained from vegetable source over Ti(IV)-grafted silica catalysts: A comparison between ordered and non-ordered mesoporous materials,” *J. Mol. Catal. A Chem.*, vol. 250, no. 1–2, pp. 218–225, May 2006.

[93] N. Wilde, C. Worch, W. Suprun, and R. Gläser, “Epoxidation of biodiesel with hydrogen peroxide over Ti-containing silicate catalysts,” *Microporous Mesoporous Mater.*, vol. 164, pp. 182–189, Dec. 2012.

[94] N. Wilde, M. Pelz, S. G. Gebhardt, and R. Gläser, “Highly efficient nano-sized TS-1 with micro-/mesoporosity from desilication and recrystallization for the epoxidation of biodiesel with H 2 O 2,” *Green Chem.*, vol. 17, no. 6, pp. 3378–3389, Jun. 2015.

[95] M. L. A. von Holleben, P. R. Livotto, and C. M. Schuch, “Experimental and theoretical study on the reactivity of the R-CN/H2O2 system in the epoxidation of unfunctionalized olefins,” *J. Braz. Chem. Soc.*, vol. 12, no. 1, pp. 42–46, 2001.

[96] M. Guidotti *et al.*, “The use of H2O2 over titanium-grafted mesoporous silica catalysts: a step further towards sustainable epoxidation,” *Green Chem.*, vol. 11, no. 9, p. 1421, 2009.

[97] M. Guidotti, E. Gavrilova, A. Galarneau, B. Coq, R. Psaro, and N. Ravasio, “Epoxidation of methyl oleate with hydrogen peroxide. The use of Ti-containing silica solids as efficient heterogeneous catalysts,” *Green Chem.*, vol. 13, no. 7, p. 1806, 2011.

[98] G. B. Payne and P. H. Williams, “Reactions of Hydrogen Peroxide. VI. Alkaline Epoxidation of Acrylonitrile,” *J. Org. Chem.*, vol. 26, no. 3, pp. 651–659, Mar. 1961.

[99] G. B. Payne, P. H. Deming, and P. H. Williams, “Reactions of Hydrogen Peroxide. VII. Alkali-Catalyzed Epoxidation and Oxidation Using a Nitrile as Co-reactant,” *J. Org. Chem.*, vol. 26, no. 3, pp. 659–663, Mar. 1961.

[100] G. B. Payne, “Reactions of Hydrogen Peroxide. VIII. Oxidation of Isopropylidenemalononitrile and Ethyl Isopropylidenecyanoacetate,” *J. Org. Chem.*, vol. 26, no. 3, pp. 663–668, Mar. 1961.

[101] C. Ding, P. S. Shuttleworth, S. Makin, J. H. Clark, and A. S. Matharu, “New insights into the curing of epoxidized linseed oil with dicarboxylic acids,” *Green Chem.*, vol. 17, no. 7, pp. 4000–4008, 2015.

[102] C. S. Kovash, E. Pavlacky, S. Selvakumar, M. P. Sibi, and D. C. Webster, “Thermoset Coatings from Epoxidized Sucrose Soyate and Blocked, Bio-Based Dicarboxylic Acids,” *ChemSusChem*, vol. 7, no. 8, pp. 2289–2294, Aug. 2014.

[103] Q. B. Reiznautt, I. T. S. Garcia, and D. Samios, “Oligoesters and polyesters produced by the curing of sunflower oil epoxidized biodiesel with cis-cyclohexane dicarboxylic anhydride: Synthesis and characterization,” *Mater. Sci. Eng. C*, vol. 29, no. 7, pp. 2302–2311, 2009.

[104] J. M. España, L. Sánchez-Nacher, T. Boronat, V. Fombuena, and R. Balart, “Properties of biobased epoxy resins from epoxidized soybean oil (ESBO) cured with maleic anhydride (MA),” *JAOCS, J. Am. Oil Chem. Soc.*, vol. 89, no. 11, pp. 2067–2075, Nov. 2012.

[105] C. N. Kuncho, D. F. Schmidt, and E. Reynaud, “Effects of Catalyst Content, Anhydride Blending, and Nanofiller Addition on Anhydride-Cured Epoxidized Linseed Oil-Based Thermosets,” *Ind. Eng. Chem. Res.*, vol. 56, no. 10, pp. 2658–2666, Mar. 2017.

[106] D. dos S. Martini, B. A. Braga, and D. Samios, “On the curing of linseed oil epoxidized methyl esters with different cyclic dicarboxylic anhydrides,” *Polymer (Guildf).*, vol. 50, no. 13, pp. 2919–2925, 2009.

[107] J.-L. Dallons, “High performance in a nutshell,” *Eur. Coatings J.*, no. 6, pp. 34–41, 2005.

[108] F. Jaillet, E. Darroman, A. Ratsimihety, B. Boutevin, and S. Caillol, “Synthesis of cardanol oil building blocks for polymer synthesis,” *Green Mater.*, vol. 3, no. 3, pp. 59–70, Sep. 2015.

[109] P. Anilkumar, *Cashew Nut Shell Liquid*. Cham: Springer International Publishing, 2017.

[110] Z. Dai, A. Constantinescu, A. Dalal, and C. Ford, “Phenalkamine Multipurpose Epoxy Resin Curing Agents,” 1994.

[111] C. Ding and A. S. Matharu, “Recent Developments on Biobased Curing Agents: A Review of Their Preparation and Use,” *ACS Sustain. Chem. Eng.*, vol. 2, no. 10, pp. 2217–2236, Oct. 2014.

[112] M. Kathalewar and A. Sabnis, “Effect of molecular weight of phenalkamines on the curing, mechanical, thermal and anticorrosive properties of epoxy based coatings,” *Prog. Org. Coatings*, vol. 84, no. 0, pp. 79–88, Jul. 2015.

[113] P. Anilkumar, *Cashew Nut Shell Liquid: A Goldfield for Functional Materials.* Springer, 2017.

[114] C. Voirin, S. Caillol, N. V. Sadavarte, B. V. Tawade, B. Boutevin, and P. P. Wadgaonkar, “Functionalization of cardanol: towards biobased polymers and additives,” *Polym. Chem.*, vol. 5, no. 9, pp. 3142–3162, 2014.

[115] C.-W. F. Cheng, A. Bender, and H. T. Wang, “Phenalkamine curing agents and epoxy resin compositions containing the same,” US6262148, 1999.

[116] S. Sato, C. Shah, Shailesh, C. Bueno, Ramiro, M. Moon, Robert, and A. Ferreira, “Phenalkamine and salted amine blends as curing agents for epoxy resins,” WO2009080209, 03-Jul-2008.

[117] S. K. Pathak and B. S. Rao, “Structural effect of phenalkamines on adhesive viscoelastic and thermal properties of epoxy networks,” *J. Appl. Polym. Sci.*, vol. 102, no. 5, pp. 4741–4748, Dec. 2006.

[118] K. Ghosh, P. Garcia, and E. Galgoci, “Recent advances in epoxy curing agent technology for low temperature cure coatings,” *Anti-Corrosion Methods Mater.*, vol. 46, no. 2, pp. 100–110, Apr. 1999.

[119] B. S. Rao and S. K. Pathak, “Thermal and viscoelastic properties of sequentially polymerized networks composed of benzoxazine, epoxy, and phenalkamine curing agents,” *J. Appl. Polym. Sci.*, vol. 100, no. 5, pp. 3956–3965, Jun. 2006.

[120] K. Huang *et al.*, “Preparation of biobased epoxies using tung oil fatty acid-derived C21

diacid and C22 triacid and study of epoxy properties," *Green Chem.*, vol. 15, no. 9, p. 2466, 2013.

[121] K. Huang, Y. Zhang, M. Li, J. Lian, X. Yang, and J. Xia, "Preparation of a light color cardanol-based curing agent and epoxy resin composite: Cure-induced phase separation and its effect on properties," *Prog. Org. Coatings*, vol. 74, no. 1, pp. 240–247, May 2012.

[122] L. Shechter, J. Wynstra, and R. P. Kurkjy, "Glycidyl Ether Reactions with Amines," *Ind. Eng. Chem.*, vol. 48, no. 1, pp. 94–97, Jan. 1956.

[123] Y. Liu, J. Wang, and S. Xu, "Synthesis and curing kinetics of cardanol-based curing agents for epoxy resin by in situ depolymerization of paraformaldehyde," *J. Polym. Sci. Part A Polym. Chem.*, vol. 52, no. 4, pp. 472–480, Feb. 2014.

[124] E. Darroman, L. Bonnot, R. Auvergne, B. Boutevin, and S. Caillol, "New aromatic amine based on cardanol giving new biobased epoxy networks with cardanol," *Eur. J. Lipid Sci. Technol.*, vol. 117, no. 2, pp. 178–189, Feb. 2015.

[125] Z. Ma, B. Liao, K. Wang, Y. Dai, J. Huang, and H. Pang, "Synthesis, curing kinetics, mechanical and thermal properties of novel cardanol-based curing agents with thiourea," *RSC Adv.*, vol. 6, no. 107, pp. 105744–105754, Nov. 2016.

[126] J. Zhang and S. Xu, "Curing kinetics of epoxy cured by cardanol-based phenalkamines synthesized from different polyethylenepolyamines by Mannich reaction," *Iran. Polym. J.*, vol. 26, no. 7, pp. 499–509, Jul. 2017.

[127] D. Balgude, A. Sabnis, and S. K. Ghosh, "Synthesis and characterization of cardanol based reactive polyamide for epoxy coating application," *Prog. Org. Coatings*, vol. 104, pp. 250–262, Mar. 2017.

[128] S. K. Sahoo, V. Khandelwal, and G. Manik, "Development of toughened bio-based epoxy with epoxidized linseed oil as reactive diluent and cured with bio-renewable crosslinker," *Polym. Adv. Technol.*, vol. 29, no. 1, pp. 565–574, Jan. 2018.

[129] F. M. White, *Fluid Mechanichs, 7th Edition*. 2011.

[130] S. K. Sahoo, V. Khandelwal, and G. Manik, "Renewable Approach To Synthesize Highly Toughened Bioepoxy from Castor Oil Derivative–Epoxy Methyl Ricinoleate and Cured with Biorenewable Phenalkamine," *Ind. Eng. Chem. Res.*, vol. 57, no. 33, pp. 11323–11334, Aug. 2018.

[131] S. E. Denmark, *Organic Reactions*, no. v. 84. Wiley, 2014.

[132] G. Maerker and E. T. Haeberer, “Direct cleavage of internal epoxides with periodic acid,” *J. Am. Oil Chem. Soc.*, vol. 43, no. 2, pp. 97–100, 1966.

[133] D. Radojčić *et al.*, “Study on the reaction of amines with internal epoxides,” *Eur. J. Lipid Sci. Technol.*, vol. 118, no. 10, pp. 1507–1511, Oct. 2016.

[134] N. S. Allen, “Photoinitiators for UV and visible curing of coatings: Mechanisms and properties,” *J. Photochem. Photobiol. A Chem.*, vol. 100, no. 1–3, pp. 101–107, Oct. 1996.

[135] J. V. CRIVELLO and J. H. W. LAM, “The Photoinitiated Cationic Polymerization of Epoxy Resins,” in *Epoxy Resin Chemistry*, vol. 114, no. 114, AMERICAN CHEMICAL SOCIETY, 1979, pp. 1–16.

[136] C. Decker, T. Nguyen Thi Viet, and H. Pham Thi, “Photoinitiated cationic polymerization of epoxides,” *Polym. Int.*, vol. 50, no. 9, pp. 986–997, Sep. 2001.

[137] W. A. Green, *Industrial Photoinitiators: A Technical Guide*. CRC Press, 2010.

[138] N. S. Allen, *Photochemistry and Photophysics Of Polymer Materials*. 2010.

[139] V. R. Patel, G. G. Dumancas, L. C. Kasi Viswanath, R. Maples, and B. J. J. Subong, “Castor Oil: Properties, Uses, and Optimization of Processing Parameters in Commercial Production.,” *Lipid Insights*, vol. 9, pp. 1–12, 2016.

[140] S.-J. Park, F.-L. Jin, J.-R. Lee, and J.-S. Shin, “Cationic polymerization and physicochemical properties of a biobased epoxy resin initiated by thermally latent catalysts,” *Eur. Polym. J.*, vol. 41, no. 2, pp. 231–237, Feb. 2005.

[141] J. D. Espinoza-Perez, B. A. Nerenz, D. M. Haagenson, Z. Chen, C. A. Ulven, and D. P. Wiesenborn, “Comparison of curing agents for epoxidized vegetable oils applied to composites,” *Polym. Compos.*, vol. 32, no. 11, pp. 1806–1816, Nov. 2011.

[142] M. D. Samper, V. Fombuena, T. Boronat, D. García-Sanoguera, and R. Balart, “Thermal and mechanical characterization of epoxy resins (ELO and ESO) cured with anhydrides,” *JAOCS, J. Am. Oil Chem. Soc.*, vol. 89, no. 8, pp. 1521–1528, Feb. 2012.

[143] S. Kumar, S. K. Samal, S. Mohanty, and S. K. Nayak, “Epoxidized soybean oil based epoxy blend cured with Anhydride based crosslinker: Thermal and Mechanical Characterization,” *Ind. Eng. Chem. Res.*, vol. 56, no. 3, p. acs.iecr.6b03879, Jan. 2016.

[144] X.-Y. Jian, Y. He, Y.-D. Li, M. Wang, and J.-B. Zeng, “Curing of epoxidized soybean oil with crystalline oligomeric poly(butylene succinate) towards high performance and sustainable epoxy resins,” *Chem. Eng. J.*, vol. 326, pp. 875–885, Oct. 2017.

[145] R.-T. Zeng, Y. Wu, Y.-D. Li, M. Wang, and J.-B. Zeng, “Curing behavior of epoxidized soybean oil with biobased dicarboxylic acids,” *Polym. Test.*, vol. 57, pp. 281–287, Feb. 2017.

[146] M. Qi, Y.-J. Xu, W.-H. Rao, X. Luo, L. Chen, and Y.-Z. Wang, “Epoxidized soybean oil cured with tannic acid for fully bio-based epoxy resin,” *RSC Adv.*, vol. 8, no. 47, pp. 26948–26958, Jul. 2018.

[147] M. A. G. Benega, R. Raja, and J. I. R. Blake, “A preliminary evaluation of bio-based epoxy resin hardeners for maritime application,” *Procedia Eng.*, vol. 200, pp. 186–192, 2017.

[148] J. Van Gerpen, “Biodiesel processing and production,” *Fuel Process. Technol.*, vol. 86, no. 10, pp. 1097–1107, 2005.

[149] T. de O. Macedo, R. G. Pereira, J. M. Pardal, A. S. Soares, and V. deJ. Lameira, “Viscosity of Vegetable Oils and Biodiesel and Energy Generation,” *World Acad. Sci. Eng. Technol. Int. J. Chem. Mol. Nucl. Mater. Metall. Eng.*, vol. 7, no. 5, pp. 251–256, 2013.

[150] R. A. Holser, “Transesterification of epoxidized soybean oil to prepare epoxy methyl esters,” *Ind. Crops Prod.*, vol. 27, no. 1, pp. 130–132, Jan. 2008.

[151] J. García-Aguilar *et al.*, “Enhanced ammonia-borane decomposition by synergistic catalysis using CoPd nanoparticles supported on titano-silicates,” *RSC Adv.*, vol. 6, no. 94, pp. 91768–91772, 2016.

[152] G. Knothe, “Rapid monitoring of transesterification and assessing biodiesel fuel quality by near-infrared spectroscopy using a fiber-optic probe,” *J. Am. Oil Chem. Soc.*, vol. 76, no. 7, pp. 795–800, Jul. 1999.

[153] G. Knothe and J. A. Kenar, “Determination of the fatty acid profile by1H-NMR spectroscopy,” *Eur. J. Lipid Sci. Technol.*, vol. 106, no. 2, pp. 88–96, Feb. 2004.

[154] R. Popescu, D. Costinel, O. R. Dinca, A. Marinescu, I. Stefanescu, and R. E. Ionete, “Discrimination of vegetable oils using NMR spectroscopy and chemometrics,” *Food Control*, vol. 48, pp. 84–90, Feb. 2015.

[155] W. Xia, S. M. Budge, and M. D. Lumsden, “New ^{1}H NMR-Based Technique To Determine

Epoxide Concentrations in Oxidized Oil.," *J. Agric. Food Chem.*, vol. 63, no. 24, pp. 5780–6, Jun. 2015.

[156] C. Jo, K. Cho, J. Kim, and R. Ryoo, "MFI zeolite nanosponges possessing uniform mesopores generated by bulk crystal seeding in the hierarchical surfactant-directed synthesis," *Chem. Commun.*, vol. 50, no. 32, pp. 4175–4177, Mar. 2014.

[157] F. C. Fernandes, K. Kirwan, D. Lehane, and S. R. Coles, "Epoxy resin blends and composites from waste vegetable oil," *Eur. Polym. J.*, vol. 89, pp. 449–460, Apr. 2017.

[158] E. D. Hernandez, A. W. Bassett, J. M. Sadler, J. J. La Scala, and J. F. Stanzione, "Synthesis and Characterization of Bio-based Epoxy Resins Derived from Vanillyl Alcohol," *ACS Sustain. Chem. Eng.*, vol. 4, no. 8, pp. 4328–4339, Aug. 2016.

[159] A. S. Sarpal *et al.*, "Direct Method for the Determination of the Iodine Value of Biodiesel by Quantitative Nuclear Magnetic Resonance (q ^{1}H NMR) Spectroscopy," *Energy & Fuels*, vol. 29, no. 12, pp. 7956–7968, Dec. 2015.

[160] J. G. Dorsey, G. F. Dorsey, A. C. Rutenberg, and L. A. Green, "Determination of the Epoxide Equivalent Weight of Glycidyl Ethers by Proton Magnetic Resonance Spectrometry," *Anal. Chem.*, vol. 49, no. 8, pp. 1144–1145, 1977.

[161] A. Adomenas, K. Curran, and M. Falconer-Flint, "Epoxy Resins and Curing Agents," *Surf. Coatings*, no. May, p. 179, 1993.

[162] L. M. Meng, Y. C. Yuan, M. Z. Rong, and M. Q. Zhang, "A dual mechanism single-component self-healing strategy for polymers," *J. Mater. Chem.*, vol. 20, no. 29, p. 6030, Jul. 2010.

[163] A. Patel, A. Maiorana, L. Yue, R. A. Gross, and I. Manas-Zloczower, "Curing Kinetics of Biobased Epoxies for Tailored Applications," *Macromolecules*, vol. 49, no. 15, pp. 5315–5324, Aug. 2016.

[164] G. Vigli, A. Philippidis, A. Spyros, and P. Dais, "Classification of edible oils by employing 31P and 1H NMR spectroscopy in combination with multivariate statistical analysis. A proposal for the detection of seed oil adulteration in virgin olive oils," *J. Agric. Food Chem.*, vol. 51, no. 19, pp. 5715–5722, 2003.

[165] C. Decker, F. Morel, and D. Decker, "UV-radiation curing of vinyl ether-based coatings," *JOCCA - Surf. Coatings Int.*, vol. 83, no. 4, pp. 173–180, Apr. 2000.

[166] J. D. Espinoza-Perez, B. A. Nerenz, D. M. Haagenson, Z. Chen, C. A. Ulven, and D. P.

Wiesenborn, “Comparison of curing agents for epoxidized vegetable oils applied to composites,” *Polym. Compos.*, vol. 32, no. 11, pp. 1806–1816, Nov. 2011.

[167] Gurit™, “Prime FAST Hardener.” [Online]. Available: https://www.gurit.com/-/media/Gurit/Datasheets/prime-20lv.pdf. [Accessed: 07-Oct-2019].

[168] Cardolite Corporation, “Ultra LITE 2009.” [Online]. Available: https://www.cardolite.com/wp-content/uploads/2017/09/Ultra-LITE-2009-TDS-EN.pdf. [Accessed: 07-Oct-2019].

[169] Cardolite Corporation, “LITE 3000.” [Online]. Available: https://www.cardolite.com/wp-content/uploads/2017/09/LITE-3000-TDS-EN.pdf. [Accessed: 07-Oct-2019].

[170] Cardolite Corporation, “LITE 3005.” [Online]. Available: https://www.cardolite.com/wp-content/uploads/2017/09/LITE-3005-TDS-EN.pdf. [Accessed: 07-Oct-2019].

[171] Cardolite Corporation, “LITE 3060.” [Online]. Available: https://www.cardolite.com/wp-content/uploads/2017/09/LITE-3060-TDS-EN.pdf.

[172] Cardolite Corporation, “LITE 3100.” [Online]. Available: https://www.cardolite.com/wp-content/uploads/2017/09/LITE-3100-TDS-EN.pdf. [Accessed: 07-Oct-2019].

[173] ASTM D638-14, “Standard Test Method for Tensile Properties of Plastics,” *ASTM International*, 2014. .

[174] “ASTM D 570 – 98 – Standard Test Method for Water Absorption of Plastics,” *ASTM Stand.*, vol. 16, pp. 1–4, 1985.

[175] ASTM D2765-16, “Standard Test Methods for Determination of Gel Content and Swell Ratio of Crosslinked Ethylene Plastics,” *ASTM International*, 2016. [Online]. Available: www.astm.org. [Accessed: 09-Feb-2017].

[176] S. W. Hughes, “Archimedes revisited: a faster, better, cheaper method of accurately measuring the volume of small objects,” *Phys. Educ.*, vol. 40, no. 5, pp. 468–474, Sep. 2005.

[177] R. M. Silverstein, F. X. Webster, and D. J. Kiemle, “Spectrometric identification of organic compounds 7ed 2005 - Silverstein, Webster & Kiemle.pdf,” *Microchemical Journal*, vol. 21. p. 496, 2005.

[178] A. M. Partansky, “A Study of Accelerators for Epoxy-Amine Condensation Reaction,” in *Advances in Chemistry*, vol. 92, 1970, pp. 29–47.

[179] V. B. Gupta, L. T. Drzal, C. Y.-C. Lee, and M. J. Rich, “The temperature-dependence of some mechanical properties of a cured epoxy resin system,” *Polym. Eng. Sci.*, vol. 25, no. 13, pp. 812–823, Sep. 1985.

[180] Y. G. Won, J. Galy, J. P. Pascault, and J. Verdu, “Volumetric properties of epoxy networks cured by cycloaliphatic mono- and diamines,” *Polymer (Guildf).*, vol. 32, no. 1, pp. 79–83, Jan. 1991.

[181] M. Sharifi, C. W. Jang, C. F. Abrams, and G. R. Palmese, “Toughened epoxy polymers via rearrangement of network topology,” *J. Mater. Chem. A*, vol. 2, no. 38, pp. 16071–16082, Sep. 2014.

[182] A. I. Vogel, *A text-book of practical organic chemistry, including qualitative organic analysis*. London,: Longmans, 1974.

[183] L. Wang, “The Atmospheric Oxidation Mechanism of Benzyl Alcohol Initiated by OH Radicals: The Addition Channels,” *ChemPhysChem*, vol. 16, no. 7, pp. 1542–1550, May 2015.

[184] F. Bernard *et al.*, “Atmospheric Chemistry of Benzyl Alcohol: Kinetics and Mechanism of Reaction with OH Radicals,” *Environ. Sci. Technol.*, vol. 47, no. 7, pp. 3182–3189, Apr. 2013.

[185] J. Cañavate, X. Colom, P. Pagès, and F. Carrasco, “Study of the curing process of an epoxy resin by FTIR spectroscopy,” *Polym. Plast. Technol. Eng.*, vol. 39, no. 5, pp. 937–943, Nov. 2000.

[186] R. A. Chowdhury *et al.*, “Self-healing epoxy composites: Preparation, characterization and healing performance,” *J. Mater. Res. Technol.*, vol. 4, no. 1, pp. 33–43, Jan. 2015.

[187] M. G. González, J. C. Cabanelas, and J. Baselga, “Applications of FTIR on Epoxy Resins - Identification, Monitoring the Curing Process, Phase Separation and Water Uptake,” in *Infrared Spectroscopy - Materials Science, Engineering and Technology*, InTech, 2012.

[188] S. K. Hoekman, A. Broch, C. Robbins, E. Ceniceros, and M. Natarajan, “Review of biodiesel composition, properties, and specifications,” *Renew. Sustain. Energy Rev.*, vol. 16, no. 1, pp. 143–169, Jan. 2012.

[189] S. G. Tan and W. S. Chow, “Biobased Epoxidized Vegetable Oils and Its Greener Epoxy Blends: A Review,” *Polym. Plast. Technol. Eng.*, vol. 49, no. 15, pp. 1581–1590, Nov. 2010.

[190] R. Pemberton, J. Summerscales, and J. Graham-Jones, *Marine Composites: Design and*

Performance. Elsevier Science, 2018.

[191] X. Sun, J. Chen, and T. Ritter, “Catalytic dehydrogenative decarboxyolefination of carboxylic acids,” *Nat. Chem.*, vol. 10, no. 12, pp. 1229–1233, Dec. 2018.

[192] Gurit™, “PRIME™ 20LV.” [Online]. Available: https://www.gurit.com/-/media/Gurit/Datasheets/prime-20lv.pdf. [Accessed: 17-Feb-2017].

[193] Gurit™, “PRIME™ 27.” [Online]. Available: https://www.gurit.com/-/media/Gurit/Datasheets/prime-27.pdf. [Accessed: 25-Jul-2019].

[194] S. Bader, “Crystic® Polyester Resin 701PAX – Scott Bader.” [Online]. Available: https://www.scottbader.com/business/composites/crystic-resin-701pa/. [Accessed: 25-Jul-2019].

[195] Easy Composites, “IP2 Isophthalic Polyester Infusion Resin - Easy Composites.” [Online]. Available: https://www.easycomposites.co.uk/#!/resin-gel-silicone-adhesive/polyester-and-vinylester/ip2-polyester-infusion-resin.html. [Accessed: 25-Jul-2019].

[196] Aurora Composites, “Hydrex 100 Infusion.” [Online]. Available: https://www.auroracomposites.com/wp-content/uploads/2016/04/HYDREX-100-33375.pdf. [Accessed: 28-Jul-2019].

[197] Scott Bader, “Crystic® Vinyl Ester Resin VE671-03.” [Online]. Available: https://www.scottbader.com/wp-content/uploads/1141_crystic-ve671-03-resin-en-feb13.pdf. [Accessed: 28-Jul-2019].